

URSI Commission F Microwave Signatures 2013

Specialist Symposium on Microwave Remote Sensing of the
Earth, Oceans, and Atmosphere

28-31 October 2013 in Espoo, Finland

Jaan Praks, Martti Hallikainen, Juha
Kainulainen, Matti Vaaja, Jaakko Seppänen
(editors)



Aalto University



Aalto University

SCIENCE +
TECHNOLOGY

REPORT

URSI Commission F Microwave Signatures 2013

Specialist Symposium on Microwave Remote
Sensing of the Earth, Oceans, and Atmosphere

28-31 October 2013 in Espoo, Finland

**Jaan Praks, Martti Hallikainen, Juha Kainulainen,
Matti Vaaja, Jaakko Seppänen (editors)**

Aalto University publication series
SCIENCE + TECHNOLOGY 23/2013

© Jaan Praks, Martti Hallikainen, Juha Kainulainen, Matti Vaaja,
Jaakko Seppänen (editors), and the authors of the individual articles

ISBN 978-952-60-5400-1
ISBN 978-952-60-5399-8 (pdf)
ISSN-L 1799-4896
ISSN 1799-4896 (printed)
ISSN 1799-490X (pdf)
<http://urn.fi/URN:ISBN:978-952-60-5399-8>

Unigrafia Oy
Helsinki 2013

Finland



441 697
Printed matter

Foreword

The URSI Commission F Microwave Signatures 2013 Symposium is the 11th of a series of meetings held in Berne, Switzerland (1974), Lawrence, Kansas (1981 and 1994), Toulouse, France (1984), Göteborg, Sweden (1987), Hyannis, Massachusetts (1990), Igls, Austria (1992), Boulder, Colorado (2001), Ispra, Italy (2005), and Florence, Italy (2010). The meeting series is intended for specialists working with theoretical, experimental or application aspects of active and passive microwave remote sensing of the Earth, Oceans, Ice and Atmosphere.

Microwave Signatures 2013 provides an international forum for reporting and discussing recent achievements in microwave remote sensing instrumentation, methodology, and applications. The meeting has attracted professionals from around the world and consists of a serial sequence of oral and poster sessions.

We would like to thank all members of the International Steering Committee for their work for a successful symposium. Thanks are also due to the organizers of the invited sessions: GNSS Reflectometry, L-band Active/Passive Land Surface Retrievals and SMAP, and Microwave Propagation in Vegetated and Snow Covered Soils.

We also wish to thank sponsors of the Symposium. Three Commissions of the International Union of Radio Science (URSI) support the Symposium: Commission F (mode B, including travel support) and Commissions B and E (mode A, technical support). Other sponsors include the Institute of Electrical and Electronics Engineers (IEEE) Geoscience and Remote Sensing Society (GRSS) (technical support), Aalto University, and the City of Espoo.

We sincerely hope that you enjoy the Symposium and your stay in Finland.

On behalf of the Local Organizing Committee

Martti Hallikainen
Jaan Praks
Juha Kainulainen
Jaakko Seppänen
Matti Vaaja

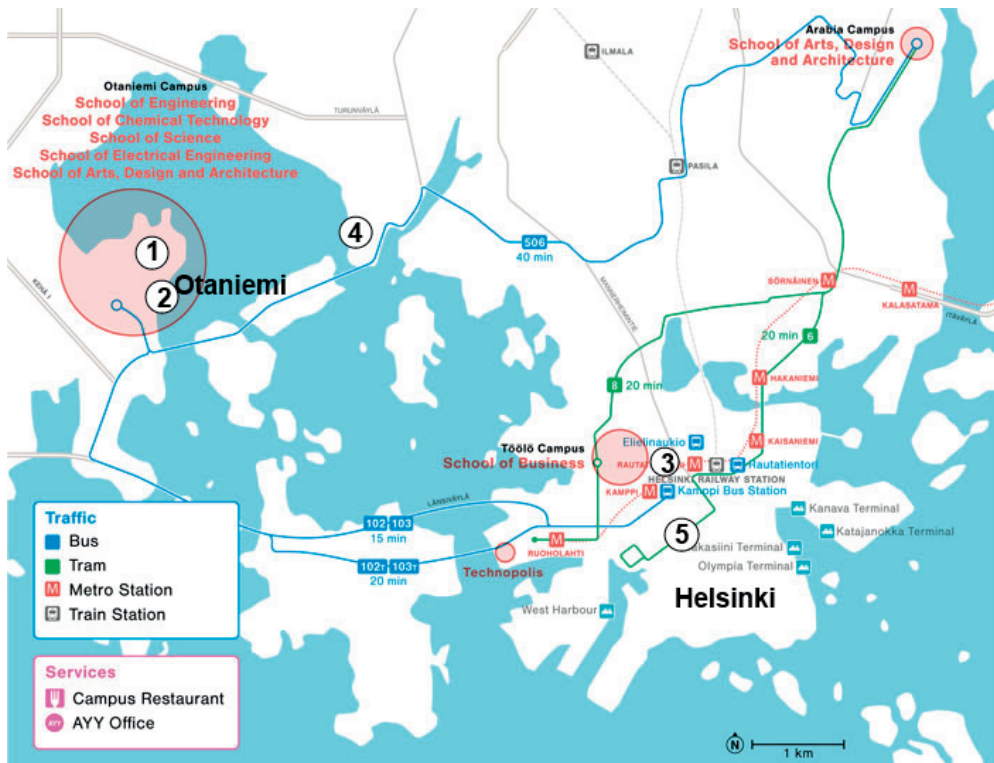
Steering Committee

Meeting Chairs

- Martti Hallikainen, Aalto University, Finland
- Jaan Praks, Aalto University, Finland
- Juha Kainulainen, Aalto University, Finland

Committee Members

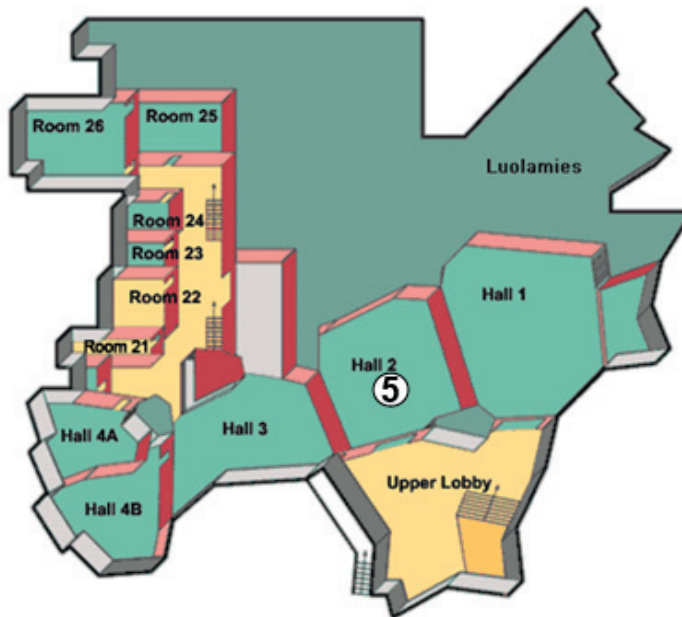
- Adriano Camps, UPC, Spain
- V. Chandrasekar, Colorado State University, USA
- Andreas Colliander, Jet Propulsion Laboratory, USA
- Torbjørn Eltoft, University of Tromsø, Norway
- Laurence Eymard, LOCEAN, France
- Jordi Font, SCIC, Spain
- Irena Hajsek, DLR, Germany
- Tuomas Häme, VTT, Finland
- Tom Jackson, ARS/USDA, USA
- Yann Kerr, CESBIO, France
- Jarkko Koskinen, Finnish Geodetic Institute
- Janne Lahtinen, Harp Technologies, Finland
- Roger Lang, George Washington University, USA
- Thuy Le Toan, CESBIO, France
- David Le Vine, NASA GSFC, USA
- Manuel Martín-Neira, ESA/ESTEC, Netherlands
- Simonetta Paloscia, IFAC-CNR, Italy
- Paolo Pampaloni, IFAC-CNR, Italy
- Jouni Pulliainen, Finnish Meteorological Institute
- Helmut Rott, University of Innsbruck, Austria
- Jiancheng Shi, University of California, USA
- Ari Sihvola, Aalto University, Finland
- Niels Skou, Technical University of Denmark
- Leung Tsang, University of Washington, USA
- Lars Ulander, Swedish Defence Research Agency
- Urs Wegmüller, Gamma Remote Sensing, Switzerland
- David Weissman, Hofstra University, USA
- Simon Yueh, Jet Propulsion Laboratory, USA



Map 1: Symposium venue in Aalto University Otaniemi Campus with major public transport lines. ① Dipoli Congress Centre, ② Radisson Blu Hotel Espoo, ③ Presidentti Hotel, ④ Hilton Kalastajatorppa Hotel, ⑤ Other Symposium hotels. Bus lines from Helsinki (Kamppi Bus Station) to Dipoli Congress Centre: 102, 102T, 103, 103T.



Map 2: Aalto University Otaniemi Campus; ① Aalto University main building, ⑱ Dipoli Congress Centre, ④ School of Electrical Engineering, ⑮ Aalto University Library, ⑳ Shopping Centre, ④② Radisson Blu Hotel Espoo.



Map 3: Dipoli Congress Centre: Level 1(top) and Level 2 (bottom). (1) Symposium Auditorium, (2) Coffee and Poster Lobby, (3) Symposium Reception Desk, (4) Cloak-room, (5) Symposium Lunch hall.

Monday		Tuesday		Wednesday		Thursday	
October 28		October 29		October 30		October 31	
		08:20	Sensors and Calibration	08:20	Microwave Propagation in Vegetated and Snow Covered Soils	08:20	Remote Sensing of Precipitation
		10:00	Coffee break	10:00	Coffee break	10:00	Coffee break
10:30	Registration	10:30	RFI in Remote Sensing	10:30	Remote Sensing of Snow	10:30	Remote Sensing of Precipitation and Atmosphere
12:30	Lunch	12:10	Lunch	12:10	Lunch	12:10	Closing Remarks
13:20	Opening	13:10	Remote Sensing of Land	13:10	Remote Sensing of Snow and Ice		
13:30	GNSS Reflectometry I						
15:10	Coffee break	15:10	Coffee break	14:50	Coffee break		
15:40	GNSS Reflectometry II	15:10	Poster Session I	14:50	Poster Session II		
		15:40	L-band Active/Passive Land Surface Retrievals and SMAP	15:20	Remote Sensing of Forest and Vegetation		
17:30	Welcome Reception			19:30	Symposium Dinner		

Monday, October 28

GNSS Reflectometry I

Session Chairs: Manuel Martín-Neira and Jens Wickert

13:30	The NASA Cyclone Global Navigation Satellite System (CYGNSS) Mission <i>M.P. Clarizia, S. Gleason, J. Johnson, A. O'Brien, A. Ridley, C.S. Ruf, Y. Yi, V. Zavorotny</i> 19
13:50	GEROS-ISS - GNSS Reflectometry, Radio Occultation and Scatterometry onboard the International Space Station <i>J. Wickert, G. Beyerle, E. Cardellach, C. Förste, T. Gruber, A. Helm, M.P. Hess, P. Hoeg, N. Jakowski, M. Kern, O. Montenbruck, A. Rius, M. Rothacher, C.K. Shum, C. Zuffada</i> 20
14:10	PARIS In-Orbit Demonstration Mission: First End-to-End Breadboard Test Results <i>M. Martín-Neira, J. Benito, M. Segarra, J. Herrero, A. Rius, A. Camps, A. Andres-Beivide, A. Olea, P. Saameño, X. Ballesteros, R. Vilaseca, A. Navarro, J. Garriga, S. Ribo, H. Park</i> 21
14:30	System Performance Simulation of Spaceborne GNSS-R Altimeters <i>H. Park, A. Camps, D. Pascual, H. Carreno-Luengo, A. Alonso-Arroyo, F. Martín, R. Onrubia</i> 22
14:50	TIGRIS Experiment: Characterizing a Typhoon with GNSS Reflectometry <i>F. Fabra, W. Li, M. Martín-Neira, A. Rius, Y. Dongkai</i> 24

GNSS Reflectometry II

Session Chairs: Manuel Martín-Neira and Serge Reboul

15:40	GNSS-R Experiments and Simulations for Soil and Vegetation Monitoring <i>L. Guerriero, N. Pierdicca, A. Egido, M. Caparrini, S. Paloscia, E. Santi, N. Floury</i> 27
16:00	GNSS Reflectometry for Permittivity Retrieval of Wet Soil <i>Y. Pei, R. Notarpietro, P. Savi, M. Pini</i> 28
16:20	Normalized GNSS Interference Pattern Technique <i>S. Reboul, C. Botteron, M.A. Ribot, G. Stienne, J. Leclère, J.B. Choquel, M. Benjelloun, P.A. Farine</i> 29
16:40	MIR: the Microwave Interferometric Reflectometer, a New Airborne Sensor to Experiment Different GNSS-R Techniques <i>R. Onrubia, D. Pascual, A. Camps, A. Alonso-Arroyo, H. Park</i> 30
17:00	3Cat-2: A Novel Approach to Space-borne GNSS-R Ocean Altimetry Using CubeSats <i>H. Carreno-Luengo, A. Camps, I. Perez-Ramos, G. Forte, R. Onrubia, R. Diez, R. Jove</i> 31

Tuesday, October 29

Sensors and Calibration

Session Chairs: Yann Kerr and Paolo Pampaloni

08:20	The SMOS Mission After Almost 4 Years into Orbit: Main Results and Achievements <i>Y.H. Kerr, P. Richaume, P. Waldteufel, J.-P. Wigneron, A. Al Bitar, F. Cabot, O. Merlin, A. Mialon, N. Reul, J. Boutin, J. Font, S. Mecklenburg</i> 35
08:40	Performance of the Noise injection Radiometers Onboard SMOS <i>J. Kainulainen, A. Colliander, M. Martín-Neira, M. Hallikainen</i> 36
09:00	Three Frequency Precipitation Profiling Radar in Helsinki <i>W. Schmidt, K. Rautiainen, A.-M. Harri</i> 37
09:20	Microwave Spectroradiometric Complex for Remote Sounding of the Earth Surface <i>A.A. Shvetsov, V.G. Ryskin, L.M. Kukin, L.I. Fedoseev, A.M. Shchitov, V.M. Demkin</i> 38
09:40	Microwave Sensor and Nanosatellite Research at Aalto University <i>M. Hallikainen, J. Kainulainen, J. Praks, M. Vaaja</i> 39

RFI in Remote Sensing

Session Chairs: Niels Skou and Janne Lahtinen

10:30	Detection of Spread Spectrum RFI Signals <i>J. Lahtinen, J. Uusitalo, T. Ruokokoski, J. Ruoskanen</i> 43
10:50	Active/Passive RFI Environment at L-Band <i>D.M. Le Vine, P. de Matthaeis</i> 44
11:10	SMOS, L Band and RFI: Where are we? <i>Y.H. Kerr, P. Richaume, Y. Soldo, J. Pla, R. Oliva Balager, E. Daganzo, S. Nieto</i> 45
11:30	Protection of the 1.4 GHz Passive Frequency Band from Radio Interferences <i>P. Jokela</i> 46
11:50	Radio Frequency Interference Maps to Locate Their Sources from a Fixed Location <i>G. Forte, A. Camps, M. Vall-llossera</i> 47

Tuesday, October 29

Remote Sensing of Land

Session Chairs: Kyle McDonald and Urs Wegmüller

13:10	Towards a Long-term Dataset of ELBARA-II Measurements in Support of SMOS Level-3 Product and Algorithm Validation at the Valencia Anchor Station (MELBEX Experiment 2010-2013) <i>R. Fernández-Morán, J.-P. Wigneron, A. Coll Pajaron, Y. Kerr, M. Miernecki, P. Salgado-Hernanz, M. Schwank, E. Lopez-Baeza</i> 51
13:30	Global Soil Frost Detection Using SMOS <i>K. Rautiainen, J. Pulliainen, J. Lemmetyinen, A. Kontu, C.B. Menard, J. Ikonen, M. Schwank, C. Mätzler, A. Wiesmann</i> 53
13:50	The Light Airborne Reflectometer for GNSS-R Observations (LARGO) Instrument: Towards Soil Moisture Retrievals <i>A. Alonso-Arroyo, G. Forte, A. Camps, H. Park, D. Pascual, R. Onrubia</i> 54
14:10	Soil Moisture Monitoring with SAR Time Series <i>U. Wegmüller, M. Santoro, C. Werner</i> 55
14:30	Flood Detection Using SAR Data: Key Radar Signatures and Possible Ambiguities <i>N. Pierdicca, L. Pulvirenti, M. Chini, L. Guerriero</i> 56
14:50	Statistical Modeling and Fusion of Multifrequency PolSAR Features for Improved Rural Area Land Cover Classification <i>N. Gökhan Kasapoglu, T. Eltoft</i> 57

L-band Active/Passive Land Surface Retrievals and SMAP

Session Chairs: Thomas Jackson and Andreas Colliander

15:40	SMAP Status and Calibration/Validation Activities <i>T.J. Jackson, E. Njoku, D. Entekhabi, P. O'Neill, A. Colliander</i> 61
16:00	Estimation of High Resolution Soil Moisture with Radar and Radiometer by a Spectral Downscaling Technique <i>J. Shi, P. Guo, L. Tsang</i> 62
16:20	Monitoring Landscape Freeze/Thaw State with Microwave Remote Sensing: Characterization of the Terrestrial Carbon Cycle with NASA's Soil Moisture Active/Passive (SMAP) Mission <i>K.C. McDonald, J.S. Kimball</i> 63
16:40	Comparison of Airborne PALS Measurements with SMOS and Aquarius during SMAPVEX Field Experiment <i>A. Colliander, T. Jackson, H. McNairn, E. Njoku</i> 64
17:00	Soil Moisture Retrieval Using L-band Time-series Radar Observations Provided by Ground and Airborne Scatterometer and SAR Data <i>S.B. Kim, L. Tsang, T. Jackson, A.C. Colliander, H. McNairn, J. van Zyl</i> 65

Tuesday, October 29

Poster Session I: 15:10 - 17:40

Session Chairs: Jaan Praks and Juha Kainulainen

P1	Advanced Concept of Scatterometer METEOR-3 <i>V. Karaev, M. Kanevsky, Y. Titchenko, M. Panfilova, E. Meshkov, G. Balandina, A. Shlaferov, Y. Kuznetsov</i> 69
P2	SSPA-Based Ku Band Transmitter-Receiver Module for D3MON Radar <i>J. Lahtinen, T. Ruokokoski, J.-P. Porko, M. Vaaja, M. Toikka, M. Hallikainen</i> 70
P3	GROMOS-C, a New Ground Based 110 GHz Radiometer for Microwave Ozone Measurement Campaigns <i>S. Fernandez, A. Murk, N. Kämpfer</i> 71
P4	GMES Sentinel-1 Soil Moisture Retrieval Algorithm Independent Assessment <i>P. Snoeij, P. Imbo, T. Rabaute, N. Baghdadi, W. Wagner, F. Mattia, S. Paloscia, N. Pierdicca</i> 72
P5	Sentinel-1 Commissioning Phase Preparation <i>P. Snoeij, D. Geudtner, B. Rommen, M. Brown, I. Navas-Traver</i> 73
P6	Intra-city Urban Heat Island: A Case Study for Delhi City. <i>N. Yadav, C. Sharma</i> 74
P7	Speckle Statistics and Coherency Matrix of L Band Polarimetric SAR over Bare Soil with Rough Surfaces Using Numerical 3D Simulations of Maxwell Equations <i>K.-L. Chen, K.-S. Chen, L. Tsang, T. Hao Liao</i> . 75
P8	Airborne Radiometer Measurements of Soil Moisture in Boreal Areas <i>J. Seppänen, J. Kainulainen, M. Hallikainen</i> 76
P9	SMOS Satellite Soil Moisture Data Assimilation in the Watershed Modeling and Forecasting System in Finland <i>T. Vento, J. Jakkila, T. Rousi, B. Vehviläinen</i> 77
P10	Influence of Radio Frequency Interference on SMOS Measurements over Finland <i>J. Kainulainen, J. Seppänen, M. Hallikainen</i> 78
P11	Modelling of TanDEM-X-Measured Forest Height from Small Footprint Lidar Data <i>M.J. Soja, L.M.H. Ulander</i> 79

Wednesday, October 30

Microwave Propagation in Vegetated and Snow Covered Soils: A Session in Honor of Paolo Pampaloni

Session Chairs: Simonetta Paloscia and Roger Lang

08:20	30 Years of Research on Microwave Emission from Snow and Vegetation Covered Soils <i>S. Paloscia</i> 83
08:40	Exploiting the Effects of Snow Layering on the Retrieval of SWE from Active and Passive Microwave Measurements <i>E. Santi, S. Paloscia, P. Pampaloni, S. Pettinato, X. Chuan, M. Brogioni, G. Macelloni, E. Palchetti</i> 84
09:00	Microwave Snow Backscattering Modeling based on Three-dimensional Microstructure Reconstructed from Two-dimensional Snow Section Image <i>J. Shi, L. Tsang</i> 85
09:20	Radar Scattering Signatures of Terrestrial Snow at X and Ku Band with a Multi-layer DMRT Model combined with NMM3D Boundary Conditions <i>S. Tan, W. Chang, X. Xu, L. Tsang, J. Lemmetyinen, S. Yueh</i> 86
09:40	Modeling of Active and Passive Microwave Signatures over Grass <i>L. Dente, L. Guerriero, Z. Su, P. Ferrazzoli</i> 87

Remote Sensing of Snow

Session Chairs: Leung Tsang and Jiancheng Shi

10:30	Understanding L-band Data Acquired by SMOS over Antarctica Using in situ Measurements and Electromagnetic Modelling <i>M. Leduc-Leballeur, G. Picard, A. Mialon, E. Lefebvre, C. Rüdiger, Y. Kerr, F. Dupont, L. Arnaud, M. Fily</i> 91
10:50	Radarsat and Snow Character at Greenland Summit <i>T. Manninen, P. Lahtinen, K. Anttila, A. Riihelä</i> 92
11:10	Active and Passive Microwave Signatures of Seasonal Snow Cover: Four Years of the NOSREC Campaign <i>J. Lemmetyinen, J. Pulliainen, A. Kontu, A. Wiesmann, C. Mätzler, H. Rott, T. Nagler, K. Voglmeier, A. Meta, A. Coccia, M. Schneebeli, M. Proksch, M. Davidson, D. Schüttemeyer, M. Kern</i> 93
11:30	Comparison of Snow Water Equivalent Estimates of CMIP5 Climate Model Simulations and Satellite-based Data <i>K. Luoju, J. Pulliainen, M. Takala, J. Lemmetyinen, T. Smolander, J. Ikonen, J. Cohen, C. Derksen</i> 94
11:50	Simulations of Microwave Brightness Temperature of Snow Using HUT Snow Emission Model with SNOWPACK and in situ Measurements <i>A. Kontu, J. Vehviläinen, J. Lemmetyinen, J. Pulliainen</i> 95

Wednesday, October 30

Remote Sensing of Snow and Ice: A Session in Memory of Richard K. Moore

Session Chairs: Prasad Gogineni and Martti Hallikainen

13:10	Airborne Ultra-Wideband Microwave Radars for Snow Measurements <i>S. Gogineni, J.B. Yan, F. Rodriguez-Morales, C. Leuschen, B. Panzer, D. Gomez-Garcia, A.E. Patel, J. Paden, M.A. Aziz</i> 99
13:30	Experimental Brightness Temperature of Snow on Lake Ice <i>M. Hallikainen, M. Vaaja, J. Seppänen, A. Hakkarainen, J. Kainulainen</i> .. 100
13:50	Shortwave Broadband Black-sky Surface Albedo Estimation for Arctic Sea Ice Using Passive Microwave Radiometer Data <i>V. Laine, T. Manninen, A. Riihelä, K. Andersson</i> 101
14:10	Incidence Angle Dependence of HH/HV-polarized RADARSAT-2 SAR Backscattering over Homogeneous Ice and Open Water Regions <i>J. Karvonen</i> 102
14:30	On Estimation of Melt Pond Fraction on the Arctic Sea Ice with ENVISAT WSM Images <i>M. Mäkynen, S. Kern, L.T. Pedersen</i> 103

Remote Sensing of Forest and Vegetation

Session Chairs: Thuy Le Toan and Lars Ulander

15:20	A P-band SAR for Global Forest Biomass Measurement: the BIOMASS Mission <i>T. Le Toan</i> 107
15:40	Topographic Effects in P-band Polarimetric SAR of Boreal Forests <i>L.M.H. Ulander, G. Sandberg, M.J. Soja</i> 108
16:00	Analysis of Multitemporal Fully Polarimetric Radarsat-2 Data over Boreal Forest Zone for Land Cover Mapping <i>O. Antropov, Y. Rauste, T. Häme</i> 109
16:20	Temporal Variability of X-band Extinction Coefficient in Boreal Forest <i>J. Praks, O. Antropov, M. Hallikainen</i> 110
16:40	Multiple Scattering Effects in Radar Signatures from an Isolated Tree <i>Q. Zhao, R.H. Lang</i> 111

Wednesday, October 30

Poster Session II: 14:50 - 17:20

Session Chairs: Jaakko Seppänen and Matti Vaaja

P12	Advanced Radar Applications for Nano- and Microsatellites <i>M. van den Oever, J. Jussila, A. Kestila, P. Laurila, R. Modrzewski</i> 115
P13	Passive Microwave Emissivity Validation and Characteristic Analysis <i>L. Shi, Y. Qiu</i> 116
P14	Comparison of Microwave Radiometer Observations and Grain Size of Snow <i>L. Leppänen, A. Kontu, J. Lemmetyinen, J. Pulliainen</i> 117
P15	Correction of Ionospheric Effects on SAR Interferometry Using an Combined TEC Estimator <i>J.S. Kim, K. Papathanassiou</i> 118
P16	Precursors of Convective Activity Using Ground Based Microwave Radiometer <i>S. Das, A. Maitra</i> 119
P17	Thermal Structure of the Boundary Layer under Strongly Stable Stratification <i>I. Repina, M. Varentsov, E.N. Kadygrov, E.A. Miller</i> 120
P18	Including the Zeeman Effect in Retrievals of Stratospheric Temperature Profiles from a Ground-based Microwave Radiometer . <i>C. Straub, O. Stähli, F. Navas-Guzman, N. Kämpfer, R. Larsson, S.A. Buehler, P. Eriksson</i> 121

Thursday, October 31

Remote Sensing of Precipitation

Session Chairs: V. Chandrasekar and Francisco Navas-Guzman

08:20	Dual-polarized Microwave Signatures of Precipitation from Earth and Space Between 3 GHz to 95 GHz <i>V. Chandrasekar, D. Moiseev, L. Baldini, N. Bharadwaj, F. Junyeant, M. Le, H. Chen, R. Bechini, M. Vega</i>125
08:40	Dual-polarization Radar Observations of Hail <i>L. Nevonen, D. Moiseev, V. Chandrasekar, H. Pohjola</i>126
09:00	Linking Snowflake Microphysics and Radar Scattering Models <i>J. Leinonen, D. Moiseev, T. Nousiainen</i> 128
09:20	Comparison of the Melting Layer Model Characteristics with GPM Ground Validation Campaign Data <i>A. von Lerber, D. Moiseev, A. Heymsfield, A. Bansemer, A.-M. Harri, M.T. Hallikainen</i>129
09:40	Influence of Snowflake Aggregation on Polarimetric Radar Signatures in Snow Storms <i>S. Lautaportti, D. Moiseev, P. Saavedra, A. Battaglia, V. Chandrasekar</i>130

Remote Sensing of Precipitation and Atmosphere

Session Chairs: Animesh Maitra and V. Chandrasekar

10:30	Modelling X-band SAR Observations of Precipitating Clouds over Land and Sea Using C-band-dual Polarization Weather Radar <i>L. Baldini, N. Roberto, R. Cremonini, R. Bechini, L. Facheris, V. Chandrasekar</i> ..133
10:50	Radar and Radiometric Studies of Rain Structure at a Tropical Location <i>A. Maitra, A. Adhikari, S. Talukdar, A. Bhattacharya</i>134
11:10	Atmospheric Observations and Laboratory Measurements of a Broad-band 340 GHz Receiver System for STEAMR <i>M. Renker, A. Murk, N. Kämpfer, M. von Gruenigen, A. Emrich</i> 135
11:30	Study of Cloud Effect on the Tropospheric Temperature Retrievals <i>F. Navas-Guzman, O. Stähli, N. Kämpfer</i>136
11:50	First Continuous Middle-atmospheric Wind Profile Measurements with a Ground-based Microwave Doppler-spectro-radiometer <i>R. Rüfenacht, N. Kämpfer, A. Murk, P. Eriksson, S.A. Buehler</i> 137

GNSS Reflectometry I

The NASA Cyclone Global Navigation Satellite System (CYGNSS) Mission

Maria Paola Clarizia^(1,2), Scott Gleason⁽³⁾, Joel Johnson⁽⁴⁾, Andrew O'Brien⁽⁴⁾, Aaron Ridley⁽¹⁾, Christopher S. Ruf⁽¹⁾, Yuchan Yi⁽⁴⁾ and Valery Zavorotny⁽⁵⁾

(1) University of Michigan, Ann Arbor, MI USA

(2) National Oceanography Centre, Southampton, UK

(3) Southwest Research Institute, Boulder, CO USA

(4) The Ohio State University, Columbus, OH, USA

(5) NOAA Earth System Research Laboratory, Boulder, CO USA

The NASA Cyclone Global Navigation Satellite System (CYGNSS) is a spaceborne mission focused on tropical cyclone (TC) inner core process studies. CYGNSS attempts to resolve the principle deficiencies with current TC intensity forecasts which result from inadequate observations and modeling of the inner core. The inadequacy in observations results from two causes: 1) much of the inner core ocean surface is obscured from conventional remote sensing instruments by intense precipitation in the eye wall and inner rain bands; and 2) the rapidly evolving (genesis and intensification) stages of the TC life cycle are poorly sampled in time by conventional polar-orbiting, wide-swath surface wind imagers. CYGNSS is specifically designed to address these two limitations by combining the all-weather performance of GNSS-R bistatic radar measurements with the sampling properties of a constellation of satellites. The use of a dense constellation of micro-satellites results in spatial and temporal sampling properties that are markedly different from conventional imagers.

An overview of the mission will be presented, including the mission architecture and the current state of its execution. The expected spatial and temporal sampling properties, and the performance estimates for the CYGNSS engineering and science data products will be discussed. These are derived from modeling and simulations studies of the GNSS-R bistatic radar measurement properties, for the particular observing geometries and instrument design characteristics of the CYGNSS mission.

GEROS-ISS - GNSS Reflectometry, Radio Occultation and Scatterometry onboard the International Space Station

Jens Wickert, G. Beyerle¹, E. Cardellach², C. Förste¹, T. Gruber³, A. Helm⁴, M.P. Hess⁴, P. Hoeg⁵, N. Jakowski⁶, M. Kern⁷, O. Montenbruck⁶, A. Rius³, M. Rothacher⁸, C.K. Shum⁹, C. Zuffada¹⁰

¹German Research Center for Geosciences, Germany

²IEEC/ICE-CSIC, Institute of Space Sciences, Spain

³Technical University München, Germany

⁴Astrium GmbH, Germany

⁵Technical University of Denmark

⁶German Aerospace Center

⁷European Space Agency

⁸ETH Zürich, Switzerland

⁹Ohio State University, USA

¹⁰Jet Propulsion Laboratory, California Institute of Technology, USA

The European Space Agency Directorate of Human Space Flight and Operations released an announcement of opportunity in July 2011 in coordination with the Directorate of Earth Observation Programmes soliciting scientific experiments for the International Space Station relevant to global climate change studies. 22 Letters of intent were received from 237 science team members. After a peer-review of the received proposals and a scientific and technical evaluation, the Geros-ISS proposal was accepted to proceed to Phase A (feasibility) studies.

GEROS-ISS is a new and innovative ISS experiment primarily focussed to exploit reflected signals of opportunity from Global Navigation System Satellites (GNSS) at L-band to measure key parameters of ocean and ice surfaces which are relevant to climate change. Secondary mission goals are S.I. traceable global atmosphere and ionosphere observations using the GNSS radio occultation technique complementing other current satellite missions. Geros-ISS will pioneer the exploitation of signals from the European Satellite Navigation system Galileo for reflectometry and occultation, thereby improving the accuracy as well as the spatio-temporal resolution of the derived geophysical properties.

GEROS-ISS will contribute to the long-term S.I. (International System of Units) traceable observation of the variations of major components of the Earth System: Oceans/Hydrosphere, Cryosphere, Atmosphere/Ionosphere and solid Earth/landcover with innovative and complementary aspects compared to current Earth Observation satellite missions. Therefore the data from Geros-ISS allow for climate change related scientific studies addressing the challenges of ESA's Earth Observation strategy (SP 1304 The Changing Earth: New scientific challenges for ESA's living planet).

GEROS-ISS will mainly provide mid- and low-latitude observations on sub-mesoscale or longer oceanic variability, surface ocean currents, surface winds, wave heights and the vertical atmospheric temperature, water vapour and electron density structure for a period of at least ten years. These observations will lead to a better understanding of the climate system, e.g., of ocean barotropic variability, Rossby wave large-scale structures, eddy-current systems, fronts and coastal upwelling. Geros-ISS hereby takes advantage of the capacious infrastructure aboard the ISS, which is a unique platform for the development of further and advanced GNSS reflectometry techniques, e.g., to potentially derive additional Earth's surface parameters critical to understand anthropogenic climate change, e.g., soil moisture or mountain glacier elevation change, and other surface parameters.

We introduce and review the Geros-ISS mission idea and also overview the current status of development and research in this area with focus on the planned experiments, campaigns, technical and scientific studies to be conducted in Phase A.

PARIS In-Orbit Demonstration Mission: First End-to-End Breadboard Test Results

M. Martín-Neira⁽¹⁾, J. Benito⁽²⁾, M. Segarra⁽³⁾, J. Herrero⁽⁴⁾, A. Rius⁽⁵⁾, A. Camps⁽⁶⁾,
A. Andrés-Beivide⁽²⁾, A. Olea⁽²⁾, P. Saameño⁽²⁾, X. Ballesteros⁽³⁾, R. Vilaseca⁽³⁾,
A. Navarro⁽³⁾, J. Garriga⁽³⁾, S. Ribo⁽⁵⁾, H. Park⁽⁶⁾

⁽¹⁾European Space Agency, Noordwijk, The Netherlands; e-mail: manuel.martin-neira@esa.int

⁽²⁾EADS-CASA Espacio, Madrid, Spain

⁽³⁾MIER, Barcelona, Spain

⁽⁴⁾HV Sistemas, Guadalajara, Spain

⁽⁵⁾Institute of Space Science (IEEC-CSIC), Barcelona, Spain

⁽⁶⁾Universitat Politècnica de Catalunya - Barcelona Tech and IEEC/CRAE-UPC, Barcelona, Spain

The PARIS In-Orbit Demonstration mission [1] is under study at the European Space Agency to explore the scientific potential of GNSS signals reflected off the Earth surface. It consists of one single payload, PARIS, mounted on a small platform. This small satellite is intended to be launched as a piggy back passenger in a suitable launcher vehicle. The PARIS payload is a new instrument which tracks and receives direct and reflected GNSS signals in both polarizations through a pair of beam-forming antennas, mounted back to back. The direct and reflected signals are amplified, down-converted, digitized and cross-correlated with each other. The cross-correlation waveforms are the raw measurements from which to extract a variety of scientific information about the Earth surface and atmosphere.

The preparation of the space technology required for this instrument has started with the production of the following items: 2 RHCP up-looking antenna elements, 2 LHCP down-looking antenna elements and 2 calibration and low noise front-end electronic modules (CAL-LNA), all units working at two frequency bands, E1/L1 and E5/L5. Additional units functionally representative of the space-borne instrument have also been built using commercial off-the-shelf components to enable end-to-end testing. This equipment suite comprises: 1 beam-former to form one up-looking and one down-looking beam at E1/L1, 1 down-converter and analog-to-digital converter unit (DOCON) providing the in-phase and quadrature components of the corresponding direct and reflected signals and finally the Electrical Ground Support Equipment (EGSE). The EGSE includes the Signal Processing Unit (a correlator capable of delay-Doppler compensation, coherent and incoherent integration), the Instrument Control Unit, the Power Supply and a Spirent GNSS hardware signal simulator.

The hardware just described has been procured and assembly of all units together will start soon. The envisaged end-to-end tests comprise different test scenarios to prove the functionality and performance of the front-end electronics (excluding radiators). Three tests have been planned: (a) a static receiver at 610 km height receiving 1 static GPS satellite (with all L1 codes: C/A, P, M); (b) a dynamic receiver at the same height receiving 1 GPS satellite (this scenario is run twice: without and with beam steering); and (c) same as (b) but adding a second –interfering– GPS satellite. The results of these end-to-end tests will be presented at the conference.

References

- [1] M. Martín-Neira, S. D’Addio, C. Buck, N. Floury, R. Prieto-Cerdeira, “The PARIS Ocean Altimeter In-Orbit Demonstrator”, IEEE Transactions on Geoscience and Remote Sensing, Vol.49, No.6, June 2011.

System Performance Simulation of Spaceborne GNSS-R altimeters

Hyuk Park, Adriano Camps, Daniel Pascual, Hugo Carreno-Luengo, Alberto Alonso-Arroyo, Francisco Martin, and Raul Onrubia

Remote Sensing Laboratory, Universitat Politècnica de Catalunya (UPC) and IEEC/UPC
UC Campus Nord, building D4-100, 08034 Barcelona, Spain
e-mail: park.hyuk@tsc.upc.edu

As the phase A of the PARIS IOD [1] space-borne GNSS-R altimetry mission progressed, the importance of an accurate end-to-end (E2E) performance simulator emerged. An E2E simulator is necessary for instrument design, to predict the instrument error budget and to define specifications, and to estimate the system performances such as height accuracy, precision, and spatial resolution. Furthermore, it can be used for data processing before obtaining the real measured data. If the outputs of the simulation would have a form of L0 data, then the post processing, such as the height retrieval and additional scatterometric parameters could be pre-studied using the simulation. In summary, the system E2E simulation is a fundamental tool for any space-borne mission.

Among the very few simulators reported for space-borne GNSS-R [2-4], the P²EPS (PAU/PARIS End-to-end Performance Simulator) has implemented a very efficient and complete simulation chain, by employing the convolution algorithm in the delay-Doppler domain devised by Marchan et al. and described in [5]. P²EPS is capable of fast computations compatible with the simulation of space-borne missions, e.g., time evolution and Monte-Carlo simulations. Furthermore, as an E2E simulator, P²EPS accounts for the effects of the instrument parameters in the waveform, e.g., antenna array beamforming, receivers' frequency response, etc.

The latest upgrade version of P²EPS has improved even more the environmental and instrument effects for enhanced accuracy. First, ionospheric and tropospheric effects in the GNSS signal propagation are included. Second, more GNSS signals ranging including GPS L1 and L5, Galileo E1 and E5, can now be simulated. Third, the speckle noise commonly occurring in the microwave imaging has been improved in the waveform simulation. Finally, the tracking scheme is now cast in the time domain simulations in the P²EPS, so the tracking error impact can be evaluated and the optimum tracking method found.

P²EPS is a generic GNSS-R simulator: special attention has been paid to simulate ESA's PARIS IOD mission, but it includes as well the deconvolution of the Delay Doppler Maps for surface's wind and oil spills mapping [6,7]. The powerful simulation capabilities of the P²EPS will be demonstrated at the conference based on a realistic GNSS-R space mission.

References:

- [1] M. Martín-Neira, S. D'Addio, C. Buck, N. Floury, R. Prieto-Cerdeira, "The PARIS Ocean Altimeter In-Orbit Demonstrator", IEEE Trans. Geosci. Remote Sens., vol.49, No.6, June 2011
- [2] Hyuk Park; Marchan-Hernandez, J.F.; Rodriguez-Alvarez, N.; Valencia, E.; Ramos-Perez, I.; Bosch-Lluis, X.; Camps, A., "End-to-end simulator for Global Navigation Satellite System Reflectometry space mission," Geosci. Remote Sens. Symposium (IGARSS), 2010, pp.4294,4297, 25-30 July 2010
- [3] Alejandro Egido, Miquel Garcia-Fernandez, and Marco Caparrini, "StarGym, a GNSS-R end-to-end simulator," GNSS+R 2012, Oct. 2012.
- [4] M.P. Clarizia, C. Gommenginger, M. Di Bisceglie, C. Galdi, and M.A. Srokosz, "Simulation of L-Band Bistatic Returns From the Ocean Surface: A Facet Approach With Application to Ocean GNSS Reflectometry," IEEE Trans. Geosci. Remote Sens., vol.50, no.3, pp.960-971, March 2011
- [5] J.F. Marchan-Hernandez, A. Camps, N. Rodriguez-Alvarez, E. Valencia, X. Bosch-Lluis, and I. Ramos-Perez, "An efficient algorithm to the simulation of Delay-Doppler maps of reflected global

- navigation satellite system signals," IEEE Trans. Geosci. Remote Sens., vol. 47, no. 8, pp. 2733-2740, 2009.
- [6] Hyuk Park; Valencia, E.; Rodriguez-Alvarez, N.; Bosch-Lluis, X.; Ramos-Perez, I.; Camps, A., "New approach to sea surface wind retrieval from GNSS-R measurements," 2011 IEEE International Geoscience and Remote Sensing Symposium (IGARSS), pp.1469-1472, 24-29 July 2011
- [7] Valencia, E.; Camps, A.; Rodriguez-Alvarez, N.; Park, H.; Ramos-Perez, I., "Using GNSS-R Imaging of the Ocean Surface for Oil Slick Detection," IEEE Journal of Selected Topics in Applied Earth Observations and Remote Sensing, , vol. 6, no. 1, pp. 217-223, Feb. 2013

TIGRIS Experiment: Characterizing a Typhoon with GNSS Reflectometry

Fran Fabra⁽¹⁾ Weiqiang Li⁽²⁾ Manuel Martín-Neira⁽³⁾ Antonio Rius⁽¹⁾ Yang Dongkai⁽²⁾

⁽¹⁾ Institut d'Estudis Espacials de Catalunya (IEEC/ICE-CSIC)
Campus UAB, Fac. Ciències, Ed. C5, Bellaterra, SPAIN. e-mail: fabra@ice.csic.es

⁽²⁾ School of Electronic and Information Engineering (SEI), BeiHang University. Beijing, CHINA

⁽³⁾ European Space Agency (ESA-ESTEC)

From its conception in 1993 as a means towards sea surface altimetry [1], the GNSS-R concept (also known as PARIS) has been tested for many other remote sensing applications. Among them, this technique has been proved to infer sea surface state and then, to retrieve wind speed information (e.g. [2]). More recently, NASA started the development of CYGNSS mission [3], consisting of a constellation of 8 nanosatellites at Low Earth Orbit (LEO). Its main purpose is to obtain GNSS-R wind speed estimations while monitoring tropical cyclones, in order to improve their forecast. In this context, we present the TIGRIS experiment, a joint initiative between the European Space Agency (ESA) and the National Remote Sensing Center of China (NRSCC) to further investigate the GNSS-R concept under strong wind conditions to seek valid ancillary applications for a future PARIS IoD mission [4].

TIGRIS, which stands for "Typhoon Investigation using GNSS-R Interferometric Signals", is an experimental campaign that will be carried on during this summer in a coastal fixed-location at the East of China. By achieving a proper visibility of the ocean (North-West Pacific area), our purpose is to retrieve sea surface state before, during and after a typhoon strikes the coast. More concretely, we plan to estimate parameters like mean square slope, significant wave height and sea surface level during each particular stage of the typhoon. To do so, dedicated GNSS-R receivers from IEEC and SEI will be employed. Two different approaches will be analyzed: the standard one of cross-correlation between signals and their synthetic models (employed in CYGNSS); and the interferometric approach, where there is cross-correlation between direct and reflected signals (envisaged for PARIS IoD). In the last case, we will be able to employ additional GNSS signals, such as those transmitted from BeiDou's current constellation.

The description of the experimental setup and the preliminary results obtained will be presented.

References

- [1] M. Martín-Neira, "A passive reflectometry and interferometry system (PARIS): application to ocean altimetry," *ESA Journal*, pp. 331-355, 1993.
- [2] E. Cardellach, G. Ruffini, D. Pino, A. Rius, A. Komjathy and J. L. Garrison, "Mediterranean Balloon Experiment: ocean wind speed sensing from the stratosphere using GPS reflections," *Remote Sensing of Environment*, vol. 88, no. 3, pp. 351-362, 2003.
- [3] C. S. Ruf, S. Gleason, Z. Jelenak, S. Katzberg, A. Ridley, R. Rose, J. Scherrer and V. U. Zavorotny, "The CYGNSS nanosatellite constellation hurricane mission," *Proceedings IEEE IGARSS*, pp. 214-216, July 2012.
- [4] M. Martín-Neira, S. D'Addio, C. Buck, N. Floury and R. Prieto-Cerdeira, "The Paris Ocean Altimeter In-orbit Demonstrator," *IEEE Transactions on Geoscience and Remote Sensing*, vol. 49, no. 6, pp. 1-29, 2011.

GNSS Reflectometry II

GNSS-R experiments and simulations for soil and vegetation monitoring

Leila Guerriero⁽¹⁾, Nazzareno Pierdicca⁽²⁾, Alejandro Egido⁽³⁾, Marco Caparrini⁽³⁾,
Simonetta Paloscia⁽⁴⁾, Emanuele Santi⁽⁴⁾, Nicolas Floury⁽⁵⁾

⁽¹⁾ Tor Vergata University of Rome, DICII, Rome, Italy, guerriero@disp.uniroma2.it

⁽²⁾ La Sapienza University of Rome, DIET, Rome, Italy

⁽³⁾ STARLAB, Barcelona, Spain

⁽⁴⁾ IFAC-CNR, Sesto Fiorentino, Florence, Italy

⁽⁵⁾ ESA/ESTEC, Noordwijk, The Netherland

GNSS-Reflectometry is already recognized as a well suited technology for several Earth Observation applications, such as sea state monitoring and altimetry. Very recently, it has been observed that GNSS-R can provide a significant contribution to agricultural and forestry applications, since the use of GNSS signals as sources of opportunity allows bistatic radar measurements at L-band, which showed to be sensitive to soil moisture and vegetation parameters. This perspective has been investigated in two experimental activities funded by the European Space Agency, based on a GNSS-R sensor developed by Starlab (Barcellona): the LEiMON and GRASS campaigns. The system has polarimetric capabilities and it has been operated both on ground and on board an aircraft in Tuscany, Italy, simultaneously to ground surveys of the fundamental land bio-geophysical parameters. In the frame of the Land Monitoring with Navigation Signals (LEiMON) project [1], the GNSS-R receiver was placed on an agricultural field for a long experimental campaign (six months) during the vegetation growing season. One half of the field was cultivated with sunflower, so that different bare soil conditions and plant growing stages and biomass were experienced. The second experiment was carried out in the frame of the GNSS Reflectometry Analysis for biomaSS monitoring (GRASS) project [2]. The receiver was installed on-board an ultra-light aircraft, which acquired a large amount of data over a region with different ground covers, including forests, during two flights in different seasons, summer and autumn.

The comparison of the GNSS-R signals with LEiMON and GRASS ground truth data shows good agreement in the temporal trends and with land cover variability. The response of GNSS reflected signals shows good sensitivity to soil moisture, plant water content, and roughness, with a significant correlation coefficient. In general both LEiMON and GRASS campaigns confirmed the good prospects of GNSS-R as a remote sensing tool for land applications. Furthermore, in order to give theoretical support to the experimental findings, a GNSS-R signal simulator for bare and agricultural fields was developed within the framework of LEiMON and subsequently extended to forested targets, during GRASS. The simulator gathers the ground truth as input in order to allow comparison between predicted and measured data.

Special efforts were made in order to separate coherent from incoherent scattering components. It was determined that in flat surface situations the signal has a strong coherent components, whereas for rough surfaces and densely vegetated fields, the incoherent component becomes more important, being the predominant source of scattering. In particular, in the case of forest observation, if the coherent component is extracted, both experimental and simulated data agree that the sensitivity to biomass is significant and maintained up to 150 t/ha of dry biomass, which is beyond the monostatic radar saturation point at L-band.

[1] Egido A., M. Caparrini, G. Ruffini, S. Paloscia, E. Santi, L. Guerriero, N. Pierdicca and N. Floury, "Global Navigation Satellite Systems Reflectometry as a Remote Sensing Tool for Agriculture", *Remote Sensing*, 4, pp. 2356-2372, 2012.

[2] S. Paloscia, E. Santi, G. Fontanelli, S. Pettinato, A. Egido, M. Caparrini, E. Motte, L. Guerriero, N. Pierdicca, N. Floury, "GRASS: an experiment on the capability of airborne GNSS-R sensors in sensing soil moisture and vegetation biomass", *Proceedings of the IEEE International Geoscience and Remote Sensing Symposium*, 2013.

GNSS Reflectometry for Permittivity Retrieval of Wet Soil

Y. Pei, R. Notarpietro, P. Savi⁽¹⁾, M. Pini⁽²⁾

⁽¹⁾ Politecnico di Torino, Corso Duca degli Abruzzi 24, 10129 Torino, Italy
E-mail: Yuekun.Pei@polito.it

⁽²⁾ Istituto Superiore Mario Boella, Torino, Italy. E-mail: pini@ismb.it

Soil moisture can be retrieved using radar techniques [1] or L-band microwave radiometry [2]. Recently, Global Navigation Satellite Signal (GNSS) Reflectometry techniques have been demonstrated to be useful for many applications as sea-state retrieval [3] and soil moisture retrieval [4-6].

The Remote sensing group of Politecnico di Torino adapted a receiver developed by the Navigation Signal Analysis and Simulation group (NAVSAS) for positioning purposes, to be used for GNSS Reflectometry applications. Both direct and reflected GNSS signals were collected by this receiver mounted on an aircraft which flew over rice fields in the Vercelli area (Piedmont region, North Italy). The signals acquired by means of a commercial Left Hand Circularly polarized antenna, was processed into Delay Doppler Maps (DDMs) and Delay Waveforms exploiting a fully open loop scheme, in order to evaluate Signal to Noise Ratios (SNRs) time series. In this open loop approach, data can be acquired continuously in time (this is not possible for standard GNSS closed loop acquisition and tracking). The ground surface was considered rather smooth and the non-coherent power contribution coming from glistening zone (through rough surface scattering mechanisms) was neglected. During the flight, the signal reflected by a lake surface was also acquired in order to calibrate the bi-static radar constant. A retrieval process able to estimate dielectric constant of soil surface from evaluated SNR was applied. A good correlation between estimated dielectric constants and rice fields' flooding or dry states was obtained.

Another measurement campaign is foreseen during the forthcoming summer season. The GNSS-R receiver will be mounted onboard an Unmanned Air Vehicle, which will fly over a field non uniform from the soil moisture point of view, in order to validate the capability of GNSS-R to monitor the water content changing. Local measurements on the ground by means of a Time-Domain Reflectometry Techniques (TDR) will be also performed and the relative permittivity obtained by this method will be compared with the GNSS data.

References

- [1] F. Ulaby, *Radar measurement of soil moisture content*, IEEE Trans. Antennas propag., vol. AP-22, no.2, pp.257-265, Mar.1974.
- [2] T. J. Schmugge and T. J. Jackson, *Mapping soil moisture with microwaveradiometers*, Meteorol. Atmos. Phys., vol. 54, pp. 213–223, Jul. 1993.
- [3] A. Rius, J. M. Aparicio, E. Cardellach, M. Martín-Neira, and B. Chapron, *Sea surface state measured using GPS reflected signals*, Geophys. Res. Lett., vol. 29, no. 23, p. 2122, Dec. 2002.
- [4] D. Masters, P. Axelrad, and S. Katzberg, *Initial Results of Land-Reflected GPS Bistatic Radar Measurements in SMEX02*. Remote Sensing of Environment, Vol.92, No.4, pp. 507-520, doi:10.1016/j.rse.2004.05.016, 2004.
- [5] S.T. Gleason, *Detecting bi-statically reflected GPS signals from low earth orbit over land surfaces*, in Proc. IEEE Int. Geosci. Remote Sens. Symp., Denver, CO, Jul.31- Aug. 4, 2006, pp. 3086-3089.
- [6] M. S. Grant, S. T. Acton, and S. J. Katzberg, *Terrain moisture classification using GPS surface-reflected signals*, IEEE Geosci. Remote Sens. Lett., vol. 4, no. 1, pp. 41–45, Jan. 2007.

Normalized GNSS Interference Pattern Technique

S. Reboul ⁽¹⁾, C. Botteron ⁽²⁾, M. A. Ribot ⁽²⁾, G. Stienne ⁽¹⁾, J. Leclère ⁽²⁾,
J.B. Choquel ⁽¹⁾, M. Benjelloun ⁽¹⁾ and P.A. Farine ⁽²⁾

⁽¹⁾ Laboratoire d'Informatique, Signal et Image de la Côte d'Opale (LISIC)
Université du Littoral Côte d'Opale (ULCO), France | serge.reboul@univ-littoral.fr

⁽²⁾ Electronics and Signal Processing Laboratory (ESPLAB)
Ecole Polytechnique Fédérale de Lausanne (EPFL), Switzerland | cyril.botteron@epfl.ch

It is well known that water level and snow height can be monitored with the ground reflectometry GNSS-R approach [1, 2]. In this approach the antenna situated on a mast, receives a direct GNSS signal coming from the satellite and a nadir signal reflected by the observed surface. Assuming that the antenna position is known we can compute the position of the surface of reflection. For water level monitoring and snow determination, this approach provides precise localization and dating of the measures that allows to process spatio-temporal comparison of water level and snow cover, respectively. These parameters are very important for flood monitoring, avalanche prevention, as well as for hydroelectric companies. Furthermore the approach is noninvasive and can be easily implemented on a portable instrument and embedded in a vehicle with a mast. The Interference Pattern Technique considers the behavior of the SNR of the received GNSS signal as a function of the satellite elevation [1]. The received signal is indeed the integration by the antenna of the direct and nadir reflected GNSS signals. Due to their different phase variations, the SNR oscillates at a rate proportional to the height between the antenna and the surface of specular reflection.

Unfortunately the measurement is typically very long because it needs to process the SNR for high satellite elevation variations. We indeed need to observe a sufficient number of SNR oscillations to estimate the frequency and derive the surface height. In order to reduce the estimation time to a fraction of one period of the SNR variation, we propose to normalize the measures. The normalization consists in varying the antenna height of a value dh in order to read the minimum and maximum value of SNR for a given satellite elevation, and then in processing with these values the SNR measured for different satellite elevations. We show in this paper that the normalization allows to compute the cosine of the phase delay between the direct and reflected signals and to estimate the signal frequency on a fraction of a period. We also derive the minimum antenna variation range dh as a function of the satellite elevation. We deduce from this function the minimum time of observation as a function of the satellite elevation rate. We derive the exact evolution of the SNR as a function of the signals parameters (Doppler frequency, code delay, CN_0) of the visible satellites [3]. The proposed method is assessed on real and synthetic signals.

References

- [1] K.M. Larson, E.E. Small, E. Gutmann, A. Bilich, P. Axelrad, J. Braun, "Using GPS multipath to measure soil moisture fluctuations: initial results," *GPS Solutions*, pp. 173-177, 2008.
- [2] N. Rodriguez-Alvarez, A. Aguasca, E. Valencia, X. Bosch-Lluis, A. Camps, I. Ramos-Perez, H. Park, M. Vall-Llossera, "Snow Thickness Monitoring Using GNSS Measurements," *IEEE Geosci. Remote Sensing Lett.*, pp. 1109-1113, 2012.
- [3] A. Bourkane, S. Reboul, M. Azmani, J. Choquel, B. Amami, M. Benjelloun, "Water level monitoring using the interference pattern GNSS-R technique," *Reflectometry Using GNSS and Other Signals of Opportunity (GNSS+R), 2012 Workshop on*, pp. 1-5, 2012.

MIR: the Microwave Interferometric Reflectometer, a new airborne sensor to experiment different GNSS-R techniques

R. Onrubia, D. Pascual, A. Camps, A. Alonso-Arroyo, H. Park

Remote Sensing Laboratory, Universitat Politècnica de Catalunya (UPC) and IEEC/UPC
UPC Campus Nord, building D4-S110, 08034 Barcelona, Spain

E-mail: {onrubia, daniel.pascual, camps, alberto.alonso.arroyo, park.hyuk}@tsc.upc.edu

Global Navigation Satellite Signals (GNSS) have been used as opportunity signals for reflectometric applications (GNSS-R) since it was proposed by [1] in 1993 for a mesoscale altimeter (PARIS concept). GNSS signals are allocated at L-band, and therefore are extremely useful for some remote sensing applications, such as soil moisture retrieval, ice-layer thickness and structure, or biomass.

A new airborne sensor currently under development at UPC will be presented in this conference: the Microwave Interferometric Reflectometer (MIR). MIR will try to mimic the ESA's PARIS IoD mission payload, although it will be more flexible to help testing potential improvements over the current designs. It will use both the interferometric¹ and the conventional² GNSS-R techniques, in two bands (GPS L1 and L5 bands, and Galileo E1 and E5a bands). Despite of being interferometric, the conventional technique will also be applied to the open signals in these bands.

Two steerable hexagonal array antennas of 19-elements each will be used [2]. The up-looking one will be RHCP and will select two satellites (two beams) of interest to reduce the contributions of other satellites. The down-looking array will be LHCP and will also synthesize two beams per band (total 4 beams per array) up to $\pm 35^\circ$ with respect to the boresight. Compact and ruggedized dual band antennas have been designed and tested. Every second, the antenna elements weights will be recomputed automatically to steer the beam towards the selected satellites, according to the antenna attitude as determined by an IMU located in the ground plane.

The RF front-end are connected to the output of each antenna element and serves several functionalities: 1) to keep a low noise figure and amplify the incoming signals, 2) phase-shift each signal so as to steer the beam in the appropriate direction, and 3) compensate the phase and amplitude unbalances of the components using an external calibration signal. Due to the large amount of data generated, the beamforming will be performed in the analog domain, and only the combined output of each beamformer (8 beams: 2 antenna arrays x 2 beams/array x 2 frequency bands/beam) will be sampled synchronously using a software-defined radio.

Finally the sampled data will be processed in real-time with a FPGA using both the interferometric and the conventional GNSS-R approaches. Results of the prototypes of the different subsystems will be presented at the conference.

References:

- [1] M. Martín-Neira, "A Passive Reflectometry and Interferometry System (PARIS): Application to Ocean Altimetry," ESA Journal, Vol. 17, pp. 331-356, 1993.
- [2] R. Onrubia, "Diseño e implementación de una agrupación bibanda reconfigurable para aplicaciones GNSS-R", Master Thesis, Universitat Politècnica de Catalunya, Barcelona, July 2012; advisor: A. Camps.

¹ Direct cross-correlation between the direct and the reflected signals.

² Cross-correlation of the reflected signal against a locally-generated replica of the transmitted signal.

³Cat-2: A Novel Approach to Space-borne GNSS-R Ocean Altimetry using CubeSats

H. Carreno-Luengo, A. Camps, I. Perez-Ramos, G. Forte, R. Onrubia, R. Díez, and R. Jové
Remote Sensing Laboratory, Universitat Politècnica de Catalunya (UPC) and IEEC/UPC
UPC Campus Nord, building D4-S110, 08034 Barcelona, Spain
Tel. +34 93 4017362, Fax +34 93 4017232, E-mail: carrenyo@ieec.cat

Since the invention of the “CubeSat” concept at Stanford and CalPoly in 1999 [1], a silent revolution has been taking place in field of small satellites. Standardization and modularization have reduced manufacturing and launch costs dramatically, offering access to space “virtually” to anybody. CubeSats were originally conceived for teaching and technology demonstration. Today, the increased miniaturization of electronic and micro-electro-mechanical components allows to reduce most satellite subsystems into just one PC104 board. At the same time CubeSats have grown in size (being always multiples of 1 unit = 1 U = 10 x 10 x 10 cm³), leaving more space for scientific payloads.

UPC activities in this field initiated in 2007 with ³Cat-1: a 1 U CubeSat that includes 5 small scientific and technological experiments (atomic oxygen MEM sensor, Geiger counter, plasma effects on wireless power transfer, energy harvesting based on Peltier effect, and new solar cells). The learning curve has been slow since we have designed, manufactured and tested all the subsystems, but we are coming to the final integration.

In 2009, based on this experience and although the project proposal was not granted at that time [2], we initiated ³Cat-2: a project to launch a Global Navigation Satellite Systems-Reflectometer (GNSS-R) instrument in a nano-satellite platform to perform ocean altimetry [3]. The main payload of the ³Cat-2 is PYCARO (P(Y) & C/A Reflectometer) a dual-band conventional GNSS-reflectometer using properly tuned COTS GPS receivers [4]. Specific modifications address the improvement of the cold start Time To First Fix (TTFF), as well as the selection of the optimal tracking loop parameters etc. We expect PYCARO to perform ionospheric corrected altimetric observations, and –from the peak of the waveform- sea state and soil moisture measurements as well.

The approach used in PYCARO is different from the one used in ESA’s PARIS-IOD mission (Passive Reflectometry and Interferometry System In-Orbit Demonstrator) [5] or NASA’s CYGNSS mission (CYclone Global Navigation Satellite System) [6], which use the so-called interferometric and conventional GNSS-R techniques, but if successful, it will be much more cost-effective.

References:

- [1] S. Lee, A. Hutputasin, A. Toorian, W. Lan, and R. Munakata R, “Cubesat Design Specification”, California Polytechnic State University, 2009.
- [2] A. Camps, “PAUSAT: a concept demonstrator of enabling technologies for Earth observation nanosatellite constellations using Global Navigation Satellite Signals Reflectometry (GNSS-R)”, ERC Advanced Grant proposal, call ERC-2009-AdG_20090325, 2009 (not granted).
- [3] H. Carreno-Luengo, “Contribution to ocean altimetry using GNSS-R from small satellites”, Ph. D. Proposal, Universitat Politècnica de Catalunya-barcelona Tech, Barcelona, 2012.
- [4] H. Carreno-Luengo, A. Camps, I. Ramos-Perez, and A. Rius, “PYCARO’s instrument proof of concept”, Proceedings of the Workshop on Reflectometry using GNSS and Other Signals of Opportunity (GNSS+R 2012), Purdue University, USA, 2012
- [5] M. Martin-Neira, S. D’Addio, C. Buck, N. Floury, and R. Prieto-Cerdeira, “The PARIS ocean altimeter in-orbit demonstrator”, IEEE Transactions on Geoscience and Remote Sensing, vol. 49 (6), pp. 2209-227, 2011.
- [6] C. S. Ruf, S. Gleason, Z. Jelenak, S. Katzberg, A. Ridley, R. Rose, J. Scherrer, and V. Zavorotny, “The CYGNSS Nanosatellite constellation hurricane mission,” 2012 IEEE International Geoscience and Remote Sensing Symposium, pp. 214-206, Munich, Germany, 2012.

Sensors and Calibration

The SMOS Mission after almost 4 years into orbit: main results and achievements

Kerr Yann H ⁽¹⁾ Richaume P ⁽¹⁾ Waldteufel P ⁽²⁾ Wigneron J.-P. ⁽³⁾ Al Bitar, A. ⁽¹⁾ Cabot, F. ⁽¹⁾, Merlin, O. ⁽¹⁾, Mialon A. ⁽¹⁾, Reul, N. ⁽⁴⁾, Boutin, J. ⁽⁵⁾, Font J. ⁽⁶⁾, Mecklenburg S ⁽⁷⁾ -

⁽¹⁾ CESBIO 18 avenue E. Belin Toulouse France, yann.kerr@cesbio.cnes.fr ⁽²⁾ LATMOS Paris France

⁽³⁾ INRA EPHYSE Bordeaux France ⁽⁴⁾ IFREMER Toulon France ⁽⁵⁾ LOCEAN, IPSL Paris France ⁽⁶⁾ ICM-CSIC Barcelona Spain ⁽⁷⁾ ESA ESRIN Frascati, Italy

In early November 2012, the SMOS mission [1] celebrated 3 years in orbit. Since its launch, this mission has given many opportunities for breaking new grounds. Shortly after launch, first global maps of soil moisture [2] [3] and Salinity ever measured from space were produced. Since then, the achieved accuracy has continuously improved to match the requirements. The long term trends of surface moisture can now be closely linked to precipitation regime, and SMOS results have been successfully used in response to extreme events such as droughts and floods. SMOS has also been used to track hurricanes (both over sea and land) currents and fronts (Such as the Gulf Stream).even icebergs. Similarly several “new” products are now being made such as root zone soil moisture, dis-aggregated fields, thin sea ice and drought indices.

Some amazing results regarding river plumes or fresh water pools related to precipitation have been obtained as well as rainfall estimates improvements using SMOS data. On the theoretical point of view the SMOS data have enabled validating the interferometry concept for earth observation, and teams are still working on the reduction of spatial biases patterns. The most annoying factor for SMOS was the discovery of an important pollution by RFI in Europe and Asia. Drastic efforts have been made to reduce them with some success at least in Europe and Americas.

Currently, effort sare made on the level 4 products with the will to maximize the synergisms with other missions , mainly AMSR and the new Aquarius SAC-D mission to name only two.

This presentation will give an extensive status of the mission, emphasizing the many lessons learned and demonstrating some outstanding results and problems issues such as RFI contamination. Some perspectives on the mission and future missions will also be given.

References

- [1] Kerr, Y. H., P. Waldteufel, J. P. Wigneron, S. Delwart, F. Cabot, J. Boutin, M. J. Escorihuela, J. Font, N. Reul, C. Gruhier, S. E. Juglea, M. R. Drinkwater, A. Hahne, M. Martin-Neira and S. Mecklenburg (2010). "The SMOS mission: New tool for monitoring key elements of the global water cycle." Proceedings of the Ieee **98**(5): 666-687.
- [2] Kerr, Y. H., P. Waldteufel, J.-P. Wigneron, J.-M. Martinuzzi, J. Font and M. Berger (2001). "Soil moisture retrieval from space: The soil moisture and ocean salinity (smos) mission." IEEE Trans.Geosci.and Remote Sens. **39**(8): 1729-1735.
- [3] Kerr, Y. H., P. Waldteufel, P. Richaume, J. P. Wigneron, P. Ferrazzoli, A. Mahmoodi, A. Al Bitar, F. Cabot, C. Gruhier, S. Juglea, D. Leroux, A. Mialon and S. Delwart (2012). "The smos soil moisture retrieval algorithm " IEEE Geosci. Remote Sens. **50**(5): 1384-1403.

Performance of the Noise Injection Radiometers Onboard SMOS

Juha Kainulainen⁽¹⁾, Andreas Colliander⁽²⁾, Manuel Martin-Neira⁽³⁾, Martti Hallikainen⁽¹⁾

⁽¹⁾ Department of Radio Science and Engineering, Aalto University School of Electrical Engineering, P.O.BOX 13000, 00076 AALTO, Espoo, Finland, juha.kainulainen@aalto.fi

⁽²⁾ Jet Propulsion Laboratory, California Institute of Technology, andreas.colliander@jpl.nasa.gov

⁽³⁾ European Space and Technology Centre, European Space Agency, manuel.martin-neira@esa.int

The Soil Moisture and Ocean Salinity (SMOS) satellite has measured the L-band brightness temperature of the Earth over three years. The payload instrument MIRAS (Microwave Imaging Radiometer using Aperture Synthesis) measures two-dimensional brightness temperature maps of the L-band radiation by means of interferometry in order to obtain a reasonable angular resolution.

One key aspect in interferometric imaging is that the average brightness temperature level of each measured image is obtained from an independent measurement. In SMOS, there are three Noise Injection Radiometers (NIR units) for this purpose. Obviously, accuracy of these units, or reference radiometers, plays an important role in the performance of the whole MIRAS.

Performance of any radiometer is much characterized by thermal and temporal stability of its measurements. Especially, since the scientific mission requirements of the SMOS mission rely on averaging data from several orbits, good stability of the measurements is required. Throughout the SMOS mission the performance of the imaging system, as well as the performance of the NIR units, has been monitored with measurements of some well-behaving natural targets. Such targets have been the sky, Antarctica, and Pacific Ocean. These targets have been analyzed by Level 1 and Level 2 teams e.g. in terms of temporal stability, spatial ripple, and thermal stability of measurements.

One key result from the investigations of the three years is that there has been a clear change in thermal and electrical properties of the MIRAS hardware during the first months of the mission, and that this change has settled or at least decreased along with the mission. This change has been attributed to changes in thermal and electrical properties of the antennas. By possibly affecting to the attenuation, efficiency, matching, and antenna patterns of individual units, these changes restrict the performance of MIRAS and the NIR units.

Within the NIR units, different models have been proposed to compensate these effects. Mainly, the methods are based on relating some NIR unit parameter with the physical temperature of the antenna patch. These models have been clearly enhancing the performance of the units; however, room for further improvements still exists in this field.

In this contribution we review the front-end models of the NIR units that have been developed during the three-year life time of SMOS. We explain measurements which are used to assess the different models and the key results which yield in the development of them. Especially, we show measurements of the validation targets (sky, Antarctica and Pacific Ocean) with different NIR front-end models. From these results we conclude the current radiometric stability of the measurements of SMOS, and point out possible new ways to further improve the performance.

References

- [1] J. Kainulainen, A. Colliander, J. Closa, R. Oliva, M. Martin-Neira, G. Buenadicha, P. Rubiales Alcaine, A. Hakkarainen, M. Hallikainen, "Radiometric Performance of the SMOS Reference Radiometers – Assessment after One Year of Operation," IEEE Transactions on Geoscience and Remote Sensing, Vol. 50, No. 5, pp. 1367-1383, May 2012.

Three Frequency Precipitation Profiling Radar in Helsinki

Walter Schmidt⁽¹⁾ Kimmo Rautiainen⁽¹⁾ Ari-Matti Harri⁽¹⁾

⁽¹⁾ Finnish Meteorological Institute, Erik Palménin aukio 1, 00560 Helsinki, Finland,
walter.schmidt@fmi.fi

Precipitation profiling at the frequency bands of Ku, Ka and W bands are becoming increasingly popular in the studies of atmospheric microphysics. Ever since the introduction of Ku / Ka pair of frequencies for the Global Precipitation Measurement mission (GPM) and the success of W band in Cloudsat, the interest in precipitation profiling using these frequencies has increased. The profiling observations will also serve as ground validation instruments for several space missions such as GPM and EarthCARE [1]. In order to get better information to retrieve ice microphysics as well as to enhance sensitivity, we need to move from the standard S- and C-band weather radars to higher frequencies [2]. As was recently shown, the use of multi frequency profiling yields important additional information compared to single radar mapping [3].

During the past three years a consortium of research, academic and private industries in Finland has been developing a flexible low-cost mobile three-band radar system for precipitation profiling. The specifications and design are completed and their feasibility is being demonstrated by implementing the Ku-band part of the system. The antenna structure with antennas for Ku-, Ka- and W-band is completed. The Ku-band antenna is being integrated with the transmitter and receiver front-end electronics, the wave generation and data reception parts and the control electronics and software to fine-tune the design. Except for the front-end electronics all bands are designed in an interchangeable manner to allow the simple implementation of different wave form generation, compression and decoding schemes and their influence on the radar performance in the different bands. The waveform generation and decoding is handled by a freely programmable system allowing the usage of complex pulse compression or pulse coding schemes and their comparison during simultaneous application.

A real-time analysis software supports the data interpretation and system optimization during field tests. Via internet connection and standard data formats the collected data can be made available for operative use. The mechanical integration on a standard car trailer allows the fast deployment to different locations. The presentation shows the detailed specifications and current development status of the radar.

References

- [1] V. Chandrasekar, D. Moiseev, W. Schmidt, K. Rautiainen and A.-M Harri, "Scientific and engineering overview of the three frequency precipitation profiling radar at Helsinki" *The 9th International Symposium on Advanced Environmental Monitoring and Modeling Helsinki*, 2012.
- [2] V. Chandrasekar, H. Fukatsu and K. Mubarak, "Global mapping of attenuation at Ku- and Ka-band", *IEEE Transactions on Geoscience and Remote Sensing*, vol. 41, pp. 2166-2176, 2003
- [3] J. Leinonen, D. Moiseev, V. Chandrasekar, J. Koskinen, "Mapping Radar Reflectivity Values of Snowfall Between Frequency Bands", *IEEE Transactions on Geoscience and Remote Sensing*, vol. 49, no.8, pp. 3047-3058, 2011 doi: 10.1109/TGRS.2011.2117432

Microwave Spectroradiometric Complex for Remote Sounding of the Earth Surface

A.A. Shvetsov⁽¹⁾, V.G. Ryskin⁽¹⁾, L.M. Kukin⁽¹⁾, L.I. Fedoseev⁽¹⁾, A.M. Shchitov⁽³⁾,
V.M. Demkin^(1,2)

⁽¹⁾ Institute of Applied Physics RAS, 46, Ulyanov str., Nizhny Novgorod, 603950, Russia
Tel. +7 831 4164933, E-mail: shvetsov@appl.sci-nnov.ru

⁽²⁾ National Research University Higher School of Economics

⁽³⁾ Nizhny Novgorod Institute of Electronic Measurement "Quartz"

Novel technique of microwave sounding of a terrestrial surface which uses downward atmospheric radiation as illuminating source was proposed [1]. The method employs spectral regions that include strong emission features presenting in the millimeter wavelength range (molecular oxygen and water vapor emission lines and band). Above-mentioned technique allows simultaneously getting information concerning thermodynamic temperature, emissivity and some parameters of scattering indicatrix of effectively radiating layer of terrestrial covers. Apparatus complex including two spectroradiometers realizing that method have been developed in Institute of Applied Physics Russian Academy of Sciences.

First single side band spectroradiometer operate in the frequency range 50 – 55 GHz, that corresponds to low-frequency edge of 5-millimeter molecular oxygen band and has 8 spectral channels. It uses low noise HEMT front-end amplifier followed Shottky diode mixer.

Second one represents double polarization double side band heterodyne spectroradiometer operating in the frequency region including 2.5 mm oxygen line. It has three spectral channels, locating on the line wings.

Both spectroradiometers are equipped by the original internal calibration system [2]. It is controlled by external direct-current source and capable to provide reference noise in temperature interval from $0.6T_0$ to $2T_0$, (where T_0 - the ambient temperature) without cryogenic cooling. It realizes automatic cyclic fast calibration of the instruments and registration of atmospheric radiation signal by changing of control current. Control of calibration and data acquisition carried out by means of ADC - DAC module interfaced to the PC.

Spectroradiometers equipped teflon lens antennas with half power beam width (HPBW) equal 2.5° and 1.4° and noise temperature 1400K and 2500K, respectively.

Instrument can be used for investigation of such terrestrial cover characteristics as stratification and temperature profile, and above all for remote monitoring of snow pack.

References

- [1] A. A. Shvetsov, D. V. Korotaev, L. I. Fedoseev, "Remote sensing of the earth covers near 2.5 mm oxygen line", *Radiophysics and Quantum Electronics*, vol. 48, no 10–11, pp. 807-816, 2005.
- [2] L. I. Fedoseev, A. A. Shvetsov, A. P. Shkaev, V. M. Demkin, D. A. Karashtin, L. M. Kukin, V. G. Bozhkov, V. A. Genneberg, I. V. Petrov, A. M. Schitov, "Millimeter wavelengths region radiometers with solid-state modulator-calibrator", *18th International Crimean Conference "Microwav&Telecommunication" (CriMiCo'2008)*, Sevastopol, Crimea, Ukraine, vol. 2, pp. 878-879, 2008.

Microwave Sensor and Nanosatellite Research at Aalto University

M. Hallikainen, J. Kainulainen, J. Praks, M. Vaaja

Aalto University, Department of Radio Science and Engineering, P.O. Box 13000, 00076 Aalto, Finland
martti.hallikainen@aalto.fi

The Space Technology Group at Aalto University focuses its research activities on microwave remote sensing and nanosatellite technology. Remote sensing research includes sensor construction and application development. The Group operates the Skyvan research aircraft.

The helicopter-borne HUTSCAT scatterometer [1] operates at 5.4 and 9.8 GHz and provides data for VV, HH, VH, and HV polarizations with a range resolution of 65 cm. It is especially suitable for forest backscatter profile and height measurements.

The HUTRAD radiometer operates at six frequencies ranging from 6.9 to 94 GHz [2] including a polarimetric receiver at 36.5 GHz [3]. It was designed for accommodation onboard our Skyvan aircraft and has been used extensively for snow and ice measurements.

The L-band HUT-2D interferometric radiometer [4] employs 36 receivers in U-shaped array beneath the Skyvan fuselage. It served as a proof of concept for the SMOS radiometer. Research with HUT-2D includes SMOS Cal/Val campaigns and soil moisture and ocean salinity retrieval.

Our contributions to the ESA SMOS mission, together with Finnish industry, include preliminary design and testing of the reference radiometers (NIR) [5], their assessment after one year of operation [6], and design and testing of the flight model calibration subsystem [7].

A UHF radiometer has been constructed for tower-based measurements of soil freeze/thaw.

Two CubeSat-based nanosatellite projects are presently in progress. Aalto-1 is a student satellite [8] under construction and is scheduled for launch in 2015. The main sensors are a small spectral imager, a radiation monitor, and a deorbiting device based on the e-sail concept.

We also participate in the QB50 mission, partially funded by European Union, and are presently designing our Aalto-2 nanosatellite. It will be part of the endeavor to investigate the lower thermosphere simultaneously with about 50 other QB50 nanosatellites.

References

- [1] Hallikainen, M., Hyypä, J., Tares, T., Ahola, P., Haapanen, J., Pulliainen, J., Toikka, M., "A helicopter-borne 8-channel ranging scatterometer for remote sensing, Part I: Technical characteristics," *IEEE Trans. Geosci. Remote Sensing*, vol. 31, no. 1, pp. 161-169, 1993.
- [2] Hallikainen, M., Kempainen, M., Pihlflyckt, J., Mononen, I., Auer, T., Rautiainen, K., Lahtinen, J., Tauriainen, S., Valmu, H., HUTRAD: Airborne multifrequency microwave radiometer. *Proc. 2nd ESA Workshop on Millimetre Wave Technology and Applications*, pp. 115-120, Espoo, Finland, 27-29 May 1998.
- [3] Lahtinen, J., Pihlflyckt, J., Mononen, I., Tauriainen, S., Kempainen, M., Hallikainen, M., "Fully polarimetric microwave radiometer for remote sensing," *IEEE Trans. Geosci. Remote Sensing*, vol. 41, no. 8, pp. 1869-1878, 2003.
- [4] Rautiainen, K., Kainulainen, Auer, Pihlflyckt, J., Kettunen, J., Hallikainen, M., "Helsinki University of Technology airborne L-band synthetic aperture radiometer," *IEEE Trans. Geosci. Remote Sensing*, vol. 46, no. 3, pp. 717-726, March 2008.
- [5] Colliander, A., Ruokokoski, L., Suomela, J., Veijola, K., Kettunen, J., Kangas, V., Levander, M., Greus, H., Hallikainen, M., Lahtinen, J., "Development and calibration of SMOS reference radiometer," *IEEE Trans. Geosci. Remote Sensing*, vol. 45, no. 7, pp. 1967-1977, 2007.
- [6] Kainulainen, J., Colliander, A., Closa, J., Martin-Neira, M., Oliva, R., Buenadicha, G., Rubiales Alcaine, P., Hakkarainen, A., Hallikainen, M., "Radiometric performance of the SMOS reference radiometers – Assessment after one year of operation," *IEEE Trans. Geosci. Remote Sensing*, vol. 50, no. 5, pp. 1367-1383, 2012.
- [7] Lemmetyinen, J., Uusitalo, J., Kainulainen, J., Rautiainen, K., Fabritius, N., Levander, M., Kangas, V., Greus, H., Pihlflyckt, J., Kontu, A., Kempainen, S., Colliander, A., Hallikainen, M., Lahtinen, J., "SMOS calibration subsystem," *IEEE Trans. Geosci. Remote Sensing*, vol. 45, no. 11, pp. 3691-3700, 2007.
- [8] Kestilä, A., Tikka, T., Peitso, P., Rantanen, J., Näsälä, A., Nordling, K., Saari, H., Vainio, R., Janhunen, P., Praks, J., and Hallikainen, M., "Aalto-1 nanosatellite – Technical description and mission objectives," *Geoscientific Instrumentation, Methods, and Data Systems*, no. 2, pp. 121-130, 2013.

RFI in Remote Sensing

Detection of Spread Spectrum RFI Signals

Janne Lahtinen⁽¹⁾ Josu Uusitalo⁽¹⁾ Teemu Ruokokoski⁽¹⁾ Jukka Ruoskanen⁽²⁾

⁽¹⁾ Harp Technologies Ltd, Tekniikantie 14, 02150 Espoo, Finland, janne.lahtinen@harptechnologies.com

⁽²⁾ Defence Forces Technical Research Centre, Riihimäki, Finland, jukka.ruoskanen@mil.fi

Anthropogenic Radio Frequency Interference (RFI) is an ever-increasing problem in remote sensing microwave radiometry. Satellite data have shown that a significant amount of RFI is present in L-, C- X-, and even at Ku-bands at many locations around the world [1]-[3]. In addition, the RFI problem is getting worse [2]. Therefore, including a RFI detection and mitigation system has been set as requirement for many future radiometers, for example MetOp Second Generation mission's Microwave Imager (MWI) instrument, 18.7 GHz channels.

There are several different methods to detect and mitigate RFI, e.g., anomalous amplitude detection, kurtosis method, polarimetric method, frequency domain detection, and the combination thereof [1]. The effectiveness of these methods has been researched by several groups and systems have been developed to apply these methods to detect and mitigate RFI (see, e.g., [1], [4]).

There is a variety of potential RFI sources, varying in their frequency, waveform, and power. For example, we can expect sources operating at the radiometer band (illegally or due to shared frequency allocation), spurious signals and harmonics from lower frequency bands, or strong signals close to the radiometer band but not properly rejected by the filters of the radiometer receiver. Radars for defence and air and sea traffic control and various communication systems are potential RFI sources. The waveforms of these emitters can vary significantly. However, the systematic research on the effectiveness of different RFI detection algorithms has been concentrated on single frequency continuous wave or pulsed signals. Spread spectrum signals, widely used in various radar and communications systems, has been hardly studied.

This paper studies the effectiveness of kurtosis method, polarimetric method, and frequency sub-banding for detecting spread spectrum signals. Various signals types have been studied: (1) Frequency Hopping Spread Spectrum (FHSS) for radar, (2) Frequency Hopping Spread Spectrum (FHSS) for telecommunication, and (3) Direct Sequence Spread Spectrum (DSSS) for telecommunication. Both simulations and laboratory measurement results are presented and compared.

References

- [1] J. E. Balling, S. S. Kristensen, S. S. Søbjærg, and N. Skou, "Surveys and analysis of RFI in preparation for SMOS: Results from airborne campaigns and first impressions from satellite data," *IEEE Transactions on Geoscience and Remote Sensing*, Vol. 49, No. 12, pp. 4821-4831, December 2011.
- [2] C. L. Gentemann, F. J. Wentz, M. Brewer, K. Hilburn, and D. Smith, "Passive Microwave Remote Sensing of the Ocean: an Overview," in *Oceanography from Space, revisited* (Eds: V. Barale, J.F.R. Gower, L. Alberotanza), Springer Science+Business Media B.V., 2010.
- [3] D. McKague, J. J. Puckett, and C. Ruf, "Characterization of K-band Radio Frequency Interference from AMSR-E, WindSat and SSM/I," *2010 IEEE International Geoscience and Remote Sensing Symposium (IGARSS)*, Honolulu, USA, pp. 2492-2494, 2010.
- [4] J. Lahtinen, T. Ruokokoski, S. S. Kristensen, and N. Skou: "Intelligent Digital Back-End for Real-Time RFI Detection and Mitigation in Microwave Radiometry", *Proceedings of ARSI, ESA-ESTEC, Noordwijk*, September 2011.

Active/Passive RFI Environment at L-Band

D.M. Le Vine¹ and P. de Matthaeis²

1. NASA/Goddard Space Flight Center, Greenbelt, MD 20771
2. GESTAR/Goddard Space Flight Center, Greenbelt, MD 20771

Aquarius is an L-band radiometer/radar instrument system designed to map sea surface salinity from space [1,2]. The two instruments, radar scatterometer and radiometer, look at the same surface footprint (i.e. 3 dB ellipse) at almost the same time. The radiometer is the primary instrument for sensing sea surface salinity and the scatterometer is included to provide a correction for roughness (waves) which is a primary source of error in the retrieval of SSS. Although the primary objective is a measurement of SSS, the instrument package operates continuously, over ocean and land.

Among the novel results of this mission is a look at the L-band RFI environment for both the radiometer and scatterometer. Because of the sensitivity needed for the measurement of salinity from space, special provisions were made for detection and mitigation of man-made interference. The approach was to sample rapidly (much faster than the Nyquist rate) and to check each sample for RFI. The radiometer acquires samples every 10 ms and checks for RFI using a “glitch detector” [3]. The scatterometer also samples every 10 ms and alternates transmit-receive samples with receive-only samples which are used to determine the RFI environment. Together, the two instruments provide a global look at the RFI environment in the radiometer band at 1.4 GHz restricted for passive use only and in the radar band a 1.26 GHz where the scatterometer operates.

Large areas of Europe and Eastern Asia are contaminated with RFI for both applications (radiometer and scatterometer). A significant difference is the continental USA which is relatively free of RFI in the passive-only band (1.4 GHz) but with extensive RFI for the scatterometer at 1.26. In both cases RFI over the oceans is relatively small, but over land RFI may present an issue for future remote sensing missions such as SMAP which plan to use passive/active combinations for the retrieval of soil moisture.

1. D.M. Le Vine et al., “Aquarius: An Instrument to Monitor Sea Surface Salinity from Space,” *IEEE Trans. Geosci. Remote Sens.*, 45, pp. 2040-2050, 2007.
2. G.S.E. Lagerloef et al, “The Aquarius/SAC-D mission: Designed to meet the salinity remote sensing challenge”, *Oceanography*, Vol. 21 (#1), pp 69-81, March, 2008.
3. C. Ruf, and S. Misra, “Detection of radio-frequency interference for the Aquarius radiometer”, *IEEE Trans. Geosci Remote Sens.*, Vol. 46 (#10), 3123-3128, 2008.

SMOS, L Band and RFI: Where are we?

Yann H Kerr⁽¹⁾, Philippe Richaume⁽¹⁾, Yan Soldo⁽¹⁾, Jean Pla⁽²⁾, Roger Oliva Balager⁽³⁾, Elena Daganzo⁽⁴⁾, Sara Nieto⁽³⁾⁽²⁾

⁽¹⁾CESBIO, 18 Avenue E. Belin 31055 Toulouse cedex 9 France

⁽²⁾CNES Toulouse France; ⁽³⁾ESA ESAC Madrid Spain; ⁽⁴⁾ESA ESTEC, Noodwijk Netherlands

ESA's Soil Moisture and Ocean Salinity (SMOS) mission was launched on 2 November 2009. An overview on the objectives of the mission and its status can be found in [1]. In summary, the main scientific objectives of SMOS are to observe soil moisture over land and sea-surface salinity over oceans[1-2]. The mission also provides information for cryospheric applications. At the end of the commissioning phase in May 2010, in which the functionalities of the spacecraft, the instrument and the ground segment are tested, SMOS was declared ready for operations.

As soon as SMOS data were available the impact of radio frequency interference (RFI) became apparent over large parts of Europe, Russia, China and the Middle East. These RFI sources significantly influence the quality of the SMOS data [3]. Detecting and flagging contaminated observations remains a challenge as well as contacting national authorities to localize and eliminate point sources emitting in the protected band. Several methods were developed to locate and characterize the different interferences sources even going up to a fraction of the instrument spatial resolution. RFI were characterised as much as possible at the same time. Using this information the team addressed the national authorities to suppress those unwanted emission with some success. As of today about 45% of sources were suppressed. In parallel the flagging of corrupted measurement has made significant progress and is now done jointly with the Aquarius team.

This paper will outline the effect RFI has on SMOS data, the regulatory situation and the intended detection and mitigation of RFI contamination [4].

References

- [1] Kerr, Y. H., P. Waldteufel, J.-P. Wigneron, J.-M. Martinuzzi, J. Font and M. Berger (2001). "Soil moisture retrieval from space: The soil moisture and ocean salinity (smos) mission." IEEE Trans. Geosci. Rem. Sens. **39**(8): 1729-1735.
- [2] Kerr, Y. H., P. Waldteufel, P. Richaume, J. P. Wigneron, P. Ferrazzoli, A. Mahmoodi, A. Al Bitar, F. Cabot, C. Gruhier, S. Juglea, D. Leroux, A. Mialon and S. Delwart (2012). "The smos soil moisture retrieval algorithm " IEEE Geosci. Remote Sens. **50**(5): 1384-1403.
- [3] Kerr, Y. H., P. Waldteufel, P. Richaume, J. P. Wigneron, P. Ferrazzoli, A. Mahmoodi, A. Al Bitar, F. Cabot, C. Gruhier, S. Juglea, D. Leroux, A. Mialon and S. Delwart (2012). "The smos soil moisture retrieval algorithm " IEEE Geosci. Remote Sens. **50**(5): 1384-1403.
- [4] Oliva, R., E. Daganzo, Y. Kerr, S. Mecklenburg, S. Nieto, P. Richaume and C. Gruhier (2012). "Smos rf interference scenario: Status and actions taken to improve the rfi environment in the 1400-1427 mhz passive band." IEEE Geosci. Remote Sens. **50**(5): 1427-1439.

Protection of the 1.4 GHz passive frequency band from radio interferences

Petteri Jokela

Finnish Communications Regulatory Authority, P.O. Box 331, FI-00181 Helsinki,

petteri.jokela@ficora.fi

The frequency band 1400-1427 MHz is allocated to the Earth Exploration Satellite Service (EESS), Space Research Service (passive) and Radio Astronomy. All intentional radio transmissions are prohibited in this band; however, there is still unauthorized use of radio transmitters in this band. All countries have responsibility to assist in case there is a complaint from other country concerning a harmful interference to system operating according to the table of allocations. In practice, they should have radio monitoring capabilities to detect all transmissions originating from their country and necessary enforcement possibilities to cease those transmissions. In the European Union, member states are also obliged to do market surveillance of the radio equipment placed on the market and inhibit selling of non-compliant equipment. In spite of all preventive methods, users may get access to these radio transmitters by email orders and take them into use, quite often not even knowing to cause interferences.

There are unwanted emissions from authorized radio transmitters operating in adjacent bands. They may be out-of-band or spurious emissions from transmitters operating close to the band 1400-1427 MHz. Even if the transmitters in adjacent bands were spectrally pure, the receiver characteristics in the passive band may be a reason for interferences. This blocking phenomenon happens typically when there is a strong transmitter with small frequency separation to passive band or when there is a small geographical separation between interfering transmitter and victim receiver. Normally there are both 'unwanted' and 'blocking' phenomena simultaneously, but only the other one may be dominant and determining the possible mitigation factors.

Ultra Wide Band (UWB) devices are able to use large portion of the radio spectrum by having low spectral power density, being less than unwanted emission levels for traditional radio transmitters. It could be argued, whether UWB devices, operating also in the protected passive bands, are in contradiction with the international law. Anyway, the impact of UWB devices to passive measurements will depend on the total number of the devices in use.

The generic unwanted emission levels are mainly intended to give protection to the receivers of other active radio systems, not to passive systems. World Radio Conference (WRC-07) approved Resolution 750 intending to provide protection to passive bands by defining more stringent unwanted emission limits. Electronic Communications Committee (ECC) approved Decision ECC(11)/01 dedicated to the band 1400-1427 MHz with same limits as in Resolution 750. However, some European countries have not implemented this Decision because of difficulties to fulfill the limits with their existing radars below 1400 MHz.

Communication authorities should be more active in removing illegal transmitters operating in the band 1400-1427 MHz. Sometimes they need a formal complaint from the user of the victim system. Authorities should also verify that new installations of the active systems, especially radars, are fulfilling the unwanted emission levels before they are taken into use. In the spectrum planning of active system, a maximum frequency separation to the passive band may be considered.

Radio Frequency Interference Maps to Locate Their Sources from a Fixed Location

G. Forte, A. Camps, M. Vall-llossera

Remote Sensing Laboratory, Universitat Politècnica de Catalunya (UPC) and IEEC/UPC
UPC Campus Nord, building D4-S110, 08034 Barcelona, Spain

E-mail: giuseppe.forte@tsc.upc.edu

Radio Frequency Interference (RFI) is a serious problem in Remote Sensing, and in particular in Microwave Radiometry because of the instruments' high sensitivity and the weak level of the signals to be detected. RFI is most serious in urban areas because most of them are originated by human activity [1].

In this work the types and characteristics of the RFI detected using a new system that is being tested to make RFI maps will be presented. It uses a directive antenna mounted on an antenna azimuth/elevation positioner. The antenna output is amplified and connected to a spectrum analyzer that measures spectrograms in real-time. Spectrograms are then post-processed off-line using a RFI-detection algorithm tailored for spectrogram analysis [2]. The fraction of the band and the fraction each sub-band is interfered are then automatically computed.

The system is currently being tested in the city of Barcelona, Spain, where previous RFI surveys have shown that the reserved band from 1400 to 1427 MHz (the one used in SMOS, for example) is nearly completely contaminated [3]. The system will also be installed at the Turó de l'Home mountain peak (41° 46'35" N, 2°26'5.5"E) at about 1700 m elevation, and ~50 km NE of Barcelona city in order to obtain a wider RFI map of the surroundings.

References

- [1] M. Younis, J. Maurer, J. Fortuny-Guash, R.Shneider, W. Wiesbeck, A.J. Gasiewski, *"Interference from 24-GHz automotive radars to passive microwave earth remote sensing satellites"*, Geoscience and Remote Sensing, IEEE Transactions on vol. 42, no.7, pp.1387-1398, July 2004.
- [2] J.M. Tarongi, A. Camps, "Radio Frequency Interference Detection and Mitigation Algorithms Based on Spectrogram Analysis," Algorithms 2011,4,pp. 239-261
- [3] J.M. Tarongi, "Radio Frequency Interference in Microwave Radiometry: Statistical Analysis and Study of Techniques for Detection and Mitigation," Ph. D. Dissertation, Universitat Politècnica de Catalunya, March 6th, 2013.

Remote Sensing of Land

Towards a long-term dataset of ELBARA-II measurements in support of SMOS level-3 product and algorithm validation at the Valencia Anchor Station (MELBEX Experiment 2010-2013)

**R. Fernández-Morán⁽¹⁾, J.-P. Wigneron⁽²⁾, A. Coll Pajarón⁽¹⁾, Y. Kerr⁽³⁾, M. Miernecki⁽²⁾,
P. Salgado-Hernanz⁽¹⁾, M. Schwank⁽⁴⁾, E. Lopez-Baeza⁽¹⁾**

**(1) University of Valencia. Faculty of Physics. Dept. of Earth Physics & Thermodynamics. Climatology from Satellites Group. Calle Dr Moliner, 50, Burjassot. 46100 Valencia. Tel: 963544048, Fax: 963543385.
E-mail: Roberto.Fernandez@uv.es / Ernesto.Lopez@uv.es**

(2) INRA, UR1263 EPHYSE, F-33140 Villenave d'Ornon, Centre INRA Bordeaux Aquitaine, France

(3) CESBIO, CNES/CNRS/IRD/UPS, UMR 5126, 18 Avenue Edouard Belin, Toulouse, France

(4) Swiss Federal Research Institute WSL, Birmensdorf, Switzerland

The main activity of the *Valencia Anchor Station* (VAS) is currently now to support the validation of SMOS (*Soil Moisture and Ocean Salinity*) level 2 and 3 land products. With this aim, the *European Space Agency* (ESA) has provided the *Climatology from Satellites Group* of the University of Valencia with an ELBARA-II microwave radiometer under a loan agreement since September 2009. Since then, brightness temperature (TB) measurements have been acquired continuously, except for normal maintenance or minor repairs.

ELBARA-II is a L-band dual-polarization radiometer with two channels (1400-1418 MHz, 1409-1427 MHz). It is continuously measuring over a vineyard field (*El Renegado*, Caudete de las Fuentes, Valencia) from a 15 m platform with a constant protocol:

- sky calibration measurements
 - everyday at 23:55
 - at 150° (relative to nadir)
- angular scans
 - everyday, every hour at 0 and 30 min
 - at 30°, 35°, 40°, 45°, 50°, 55°, 60°, 65° and 70° (relative to nadir)
- fixed angle of 45°
 - everyday, every hour at 5, 10, 15, 20, 25, 40, 45 and 50 min

One of the advantages of using this site is the possibility of studying two different environmental conditions along the year. The vine cycle extends mostly between April and October and the rest of the year the area remains under bare soil conditions, adequate for the calibration of the soil model.

The measurement protocol currently running can be now considered as robust and it will be extended in time as much as possible to provide a long-term data set of ELBARA-II measurements and retrieved land products (SM and TAU). This data set can be very useful in support of SMOS scientific activities: the VAS area and, specifically the ELBARA-II site, offer good conditions to control the long-term evolution of SMOS Level 2 and Level 3 land products and interpret eventual anomalies that may obscure sensor hidden biases. For instance, the ELBARA-II TB data have been compared to those measured by SMOS (Miernecki et al., 2012). In addition soil moisture, SM and vegetation optical depth TAU were retrieved from the ELBARA-II TB data by inversion of the L-MEB model and can be compared to the level 2 and level 3 SMOS products (Wigneron et al., 2012). Furthermore, radiative transfer

properties of the vines representative for the VAS area have been investigated by means of dedicated campaigns during summer and winter (Schwank et al., 2012).

One of the advantages of the VAS site is the possibility of studying two different environmental conditions along the year. The vine cycle extends mostly between April and October and the rest of the year the area remains under bare soil conditions, in good conditions for the calibration of the soil model.

Moreover, the L-band ELBARA-II measurements provide an area-integrated estimation of SM and TAU which is more representative of the soil and vegetation conditions at field scale than ground measurements (using capacitive probes for SM and destructive measurements for TAU). For instance, Miernecki et al., (2012) and Wigneron et al. (2012) showed that very good correlations could be obtained from TB data and SM retrievals obtained from both SMOS and ELBARA-II over the 2010-2011 time period. The analysis of the quality of these correlations over a long time period can be very useful to evaluate the SMOS measurements and retrieved products (Level 2 and 3).

The present work extends these analyses over a longer period (almost 4 years) and emphasizes the need of (i) keeping a long-time record of ELBARA-II measurements (ii) enhancing as much as possible the control over other conditions, especially, soil roughness (SR), vegetation water content (VWC) and surface temperature to interpret the retrieved results obtained from both SMOS and ELBARA-II instruments.

REFERENCES

- Miernecki et al., (2012). "Analysis of roughness effects based in-situ Elbara-II and space-borne SMOS observations over the VAS (Valencia Anchor Station)". *IGARSS 2012*: 742-745
- Schwank, M., J. P. Wigneron, et al. (2012). "L-Band Radiative Properties of Vine Vegetation at the SMOS Cal/Val Site MELBEX III" *IEEE Transactions on Geoscience and Remote Sensing* 50(5): 1587-1601.
- Wigneron, J.-P., Schwank, M., López-Baeza, E., Kerr, Y., Novello, N., Millan, C., Moisy, et al. (2012). "First Evaluation of the simultaneous SMOS and ELBARA-II observations in the Mediterranean region". *Remote Sensing of Environment*, 124, 26-37.

Global Soil Frost Detection Using SMOS

Kimmo Rautiainen¹, Jouni Pulliainen¹, Juha Lemmetyinen¹, Anna Kontu¹, Cecile B. Menard¹,
Jaakko Ikonen¹, Mike Schwank², Christian Mätzler², Andreas Wiesmann²

¹Finnish Meteorological Institute, Arctic Research

²GAMMA Remote Sensing

Soil freezing and thawing, including the winter-time evolution of soil frost, are important characteristics influencing hydrological and climate processes at the regions of seasonal frost and permafrost, which include major land areas of North America and northern Eurasia. The European Space Agency's (ESA) SMOS mission (Soil Moisture and Ocean Salinity) was launched in November 2009. The payload instrument MIRAS is a radiometer using a low microwave frequency band (1.403 – 1.424 GHz) for Earth remote sensing. The output signal of the instrument is highly sensitive to changes in soil permittivity, with relatively low influence of surface vegetation. SMOS sensitivity to changes in soil permittivity and the deeper soil layer monitoring capabilities ensure new possibilities for global soil freeze/thaw cycle monitoring.

Within the frame of SMOS programme, ESA has initialized SMOS+ Innovation Permafrost, coordinated by the Finnish Meteorological Institute (FMI) with GAMMA Remote Sensing as a Swiss partner. The main objectives of the project are (1) to develop methods and algorithms for detection and monitoring of soil freezing/thawing processes using L-band passive microwave data and (2) to demonstrate the developed methods with soil frost maps derived from SMOS observations representing the whole Northern Hemisphere.

The continuous tower-based measurements in FMI Sodankylä test site in Northern Finland using the SMOS reference radiometer, ELBARA-II [1], have played a key role for our soil freezing detection algorithm development work [2]. The soil freezing affects the passive L-band observation in two clearly noticeable ways: Firstly the brightness temperature increases and tends to saturate. Secondly, the brightness temperature polarization difference decreases. These two main characteristics form the basis of the frost detection algorithm developed here. The soil frost detection algorithm, developed using ELBARA-II tower-based observations, was applied to SMOS CATDS level 3 brightness temperature data (Centre Aval de Traitement des Données SMOS). The suitability of the soil frost detection algorithm for global SMOS observations was evaluated against the Finnish Environment Institute's (SYKE) frost tube network *in situ* measurements in Finland. Using the evaluation results the algorithm parameters were tuned for SMOS data to acquire soil frost maps for the whole Northern Hemisphere. The results indicate that the event and development of soil freezing can be monitored with SMOS.

References

- [1] M. Schwank, A. Wiesmann, C. Werner, C. Mätzler, D. Weber, A. Murk, I. Voelksch and U. Wegmueller, "ELBARA II, an L-band radiometer system for soil moisture research", *Sensors*, 10, pp. 584 – 612, doi:10.3390/s100100584, 2010.
- [2] K. Rautiainen, J. Lemmetyinen, J. Pulliainen, J. Vehviläinen, M. Drusch, A. Kontu, J. Kainulainen, and J. Seppänen, "L-Band Radiometer Observations of Soil Processes in Boreal and Subarctic Environments," *IEEE Trans. Geosci. Remote Sensing*, vol. 50, pp. 1483-1497, 2012.

The Light Airborne Reflectometer for GNSS-R Observations (LARGO) instrument: Towards Soil Moisture retrievals

A. Alonso-Arroyo, G. Forte, A. Camps, H. Park, D. Pascual, R. Onrubia

Remote Sensing Laboratory, Universitat Politècnica de Catalunya (UPC) and IEEC/UPC
UPC Campus Nord, building D4-S110, 08034 Barcelona, Spain

E-mail: alberto.alonso.arroyo@tsc.upc.edu

Twenty years after its conception for mesoscale altimetry [1], the use of Global Navigation Satellite Signals Reflected (GNSS-R) is today widely accepted as a powerful tool for the retrieval of different geophysical parameters. Different parameters such as global sea mesoscale altimetry or ocean surface height, soil moisture, mean vegetation height, surface topography, sea surface roughness, ocean surface winds, or snow and ice thickness, among others (see, for example, the review paper [2]).

GNSS-R instruments are usually classified as passive sensors, but they are actually bistatic radars using the signal transmitted by the existing GNSS satellites. Therefore, GNSS-R instruments are inherently suited for ubiquitous and low-power applications.

Soil moisture is a key parameter in climatology, desertification, agriculture, forest fire prevention, etc. Today, global and routine soil moisture ~50 km maps are derived from the ESA's SMOS mission (Soil Moisture and Ocean Salinity), and at ~1 km resolution from data fusion techniques for regional applications [3]. At a more local scale, the determination of soil moisture maps is really useful for water management.

The potential of Ground-based (GB) GNSS-R observables for soil moisture determination has been already demonstrated using, for example, the Interference Pattern Technique (IPT) [4], the Interferometric Complex Field or scatterometric techniques [5]. However, the main problem faced is the area covered by a single instrument. In order to enlarge the area covered a new instrument named LARGO will be presented. LARGO operates as a scatterometer from the measurement of the peak of the waveforms of the direct and the reflected signals. It has been designed for autonomous operation and scientific research on rover or airborne platforms. The instrument will be installed in an aircraft of the University of Monash, Melbourne (Australia) in July 2013. Validation tests results from a UAV in a region close to Barcelona will be presented at the conference.

References:

- [1] Martin-Neira, M. "A Passive Reflectometry and Interferometry System (PARIS): Application to Ocean Altimetry," *ESA Journal* 17 (4), 331-355, 1993.
- [2] Jin, S. and Komjathy, A. "GNSS reflectometry and remote sensing: New objectives and results" *Advances in Space Research*, Vol. 46, 111-117, 2010.
- [3] CP34-BEC SMOS-BEC Data Distribution and Visualization Services: <http://cp34-bec.cmima.csic.es/land-datasets/>, last visited May 21st 2013.
- [4] Rodriguez-Alvarez, N.; Camps, A.; Vall-llossera, M.; Bosch-Lluis, X.; Monerris, A.; Ramos-Perez, I.; Valencia, E.; Marchan-Hernandez, J.F.; Martinez-Fernandez, J.; Baroncini-Turricchia, G.; Pérez-Gutiérrez, C.; Sanchez, N., "Land Geophysical Parameters Retrieval Using the Interference Pattern GNSS-R Technique," *Geoscience and Remote Sensing, IEEE Transactions on*, vol.49, no.1, pp.71,84, Jan. 2011
- [5] Egido, A.; Caparrini, M.; Ruffini, G.; Paloscia, S.; Santi, E.; Guerriero, L.; Pierdicca, N.; Floury, N. *Global Navigation Satellite Systems Reflectometry as a Remote Sensing Tool for Agriculture. Remote Sens.* 2012, 4, 2356-2372.

Soil Moisture Monitoring with SAR Time Series

Urs Wegmüller⁽¹⁾, Maurizio Santoro⁽¹⁾ and Charles Werner⁽¹⁾

⁽¹⁾Gamma Remote Sensing AG, CH-3073 Göligen, Switzerland
wegmuller@gamma-rs.ch - <http://www.gamma-rs.ch>

With the launch of Sentinel 1, C-band SAR time series will become available with an unprecedented spatial and temporal coverage. Its orbit repeat cycle is 12 days with one satellite and 6 days with two satellites. Furthermore, in many locations ascending and descending coverage may become available. One application that is expected to benefit strongly from Sentinel-1 is soil moisture monitoring as it requires weekly or better temporal coverage – something currently not available over large areas. In preparation for Sentinel-1, we investigated soil moisture retrieval approaches. For this, we used ERS-1 C-band data acquired during the ice phases in 1992 and 1994 in 3-day repeat orbits for its similarity (C-band, short repeat interval) with Sentinel-1.

In a first step, the SLC data are radiometrically calibrated, co-registered to a common SLC geometry, detected, and temporally filtered using an advanced multi-temporal filtering approach [1], resulting in speckle-reduced backscatter time series. Using a simple regression algorithm between the soil backscattering coefficient and the soil moisture is too simplistic to be reliable because of the strong influence of geometric parameters (soil surface roughness, local incidence angle) and vegetation cover. On the other end of the complexity scale are scatter models. A wide area application of scatter models in a retrieval concept is very challenging as many soil and vegetation parameters used are not known and cannot easily be estimated.

In the proposed retrieval concept, we built upon the hypothesis that backscatter change closely relates to moisture change as long as the other parameters (roughness, geometry, incidence angle) remain constant. High interferometric coherence is used to identify areas that are very likely not affected by geometric changes (e.g. from cultivation or erosion) and are not densely covered by vegetation. The backscatter change (in dB) over these areas is then converted to a soil moisture change value using a linear regression. Integrating backscatter change of consecutive intervals results in soil moisture change time series which can be converted to absolute soil moisture values using reference values e.g. from in-situ measurements or by using special situations such as frozen conditions that represent a very low soil moisture. The disadvantage that the spatial coverage reduces to the area that has always high coherence can be overcome by spatial interpolation of the soil moisture change estimates.

For the considered ERS-1 Ice-Phase data acquired at 3-day intervals in winter and spring, this methodology worked quite well over agricultural areas in the Netherlands. On 8 fields the result were compared to in-situ soil moisture measurements showing good correspondence. Furthermore, days with frozen conditions, judged based on temperatures measured at a nearby meteorological station, were reliably identified. Overall the method seems promising and applicable to the upcoming Sentinel-1 SAR.

References

- [1] U. Wegmüller, M. Santoro, and C. Werner, *Multi-temporal SAR data filtering for land applications*, ESA Living Planet Symposium, Edinburgh, 9-13 Sep. 2013.

Flood detection using SAR data: key radar signatures and possible ambiguities

N. Pierdicca¹, L. Pulvirenti¹, M. Chini², L. Guerriero³

¹Dept. of Information Engineering, Electronics and Telecommunications, Sapienza University of Rome, Italy. Tel. +39 06 44585411; e-mail nazzareno.pierdicca@uniroma1.it

²CRP-Gabriel Lippmann, Luxembourg

³Dept. of Computer Science, Systems and Production, Tor Vergata University of Rome, Italy

ABSTRACT

The potential of spaceborne Synthetic Aperture Radar (SAR) for flood mapping was demonstrated by several past investigations. The synoptic view, the capability to operate in almost all-weather conditions and during both day time and night time and the sensitivity of the microwave band to water are the key features that make SAR data useful for monitoring inundation events. Moreover, their high spatial resolution allows emergency managers to use very detailed flood maps.

The main electromagnetic mechanism producing a high contrast in SAR images between flooded and non-flooded areas is the specular reflection of the radar signal. Most of the impinging radiation is reflected towards the specular direction, so that very little energy is scattered back to the radar sensor and flooded areas appear dark in SAR images. However, specular reflection occurs for bare or sparsely vegetated flooded soils or even for flooded dense vegetation when the water depth is high enough to completely submerge plants. The imaging of the flooded areas is complicated by wind roughening and by vegetation emerging from water, both producing significant radar returns, thus decreasing the contrast between flooded areas and the surrounding non-flooded soil. As for wind, predicting its effect on the radar response of floodwater is complicated by the variable fetch and water depth. A typical radar signature of flooded vegetation is determined by the increase of the backscatter that may occur because of the double bounce mechanism that involves floodwater and stems or trunks, and implies that inundated vegetation may appear very bright in a SAR image. In flooded urban areas, both specular and corner reflections may occur, but layover and shadowing effects strongly complicate inundation mapping.

The timeliness requirement is generally very strict for products such as flood maps. Consequently, most of the algorithm available in the literature for flood detection search for regions of low backscatter only, generally through an analysis of the image histogram aiming at rapidly identifying a threshold separating the two populations of flooded (dark) and non-flooded pixels. From the previous discussion, it might be deduced that algorithms searching for regions of low backscatter may produce flood maps possibly affected by missed detection errors, i.e., underestimation of the flooded areas. However, even overestimation (i.e., false alarms) may occur because of: i) complex topography (or buildings, in urban areas) producing radar shadowing; ii) wet snow being a strong absorber of microwave radiation; iii) heavy precipitating clouds, which may attenuate the radar signal at high frequencies (X band). In most of these situations, the availability of an image prior the flood event may become necessary to resolve those ambiguities.

A number of case studies will be presented at the conference in order to show some methods that have been developed to deal with the aforementioned difficulties in flood mapping in the framework of an activity developed using X-band COSMO-SkyMed (CSK) images. For instance, the analysis of the CSK images of the floods occurred in Tuscany (Central Italy) on December 2009 and in Northern Italy, close to the city of Alessandria, on April, 2009 revealed the need to apply segmentation techniques to generate homogeneous flood maps in which flooded segments are strictly correlated to real objects presents in the scene. Moreover, these images turned out to be particularly useful to assess the possible added value of electromagnetic models able to simulate the radar response of flooded vegetation, once accurate information on land cover (e.g. type of vegetation and characteristics such as geometry and biomass) are available. The dataset collected in Liguria (in Northern Italy) during a storm, in November 2011, made it necessary to properly account for the effect of very thick clouds and wet snow. The analysis of the CSK acquisitions after the Japanese Tsunami in March 2011 pointed out the need to properly interpret the changes in the images that are not always related to the presence of water, including floating of debris.

Statistical Modeling and Fusion of Multifrequency PolSAR Features for Improved Rural Area Land Cover Classification

N. Gökhan Kasapoğlu and Torbjørn Eltoft

Department of Physics and Technology

University of Tromsø, Norway

{gokhan.kasapoglu, torbjorn.eltoft}@uit.no

Polarimetric synthetic aperture radar (PolSAR) measurements enable the retrieval of various physical properties of the earth based on the mechanisms producing the backscatter of the electromagnetic waves from the illuminated areas. The scattering mechanisms associated with a specific target are expected to vary with frequency and polarization. This property is useful for improving target detection and classification. For instance, over forested areas the penetration depths of electromagnetic waves at L band and C band are quite different. L band signals are capable to penetrate deeper than C signals, and therefore forested areas appear as brighter in L band than in C band in PolSAR scenes [1]. The difference in scattering property also affects the polarimetric properties of the backscatter. It is therefore expected that the statistical properties of a feature vector obtained by fusing multifrequency polarimetric features will improve target classification.

In this study PolSAR features extracted from fully polarimetric Radarsat-2 (C band) and dual polarized ALOS PALSAR (L band) data are used to make analysis of rural areas, including forests, over the Northwest of Tanzania. Bare area, cultivated land, rice field, grassland and woodland define the categories that are present in the study area [2]. For all categories and PolSAR features, the best fitted statistical model has been chosen from a library of six candidate distributions consisting of the normal, log-normal, gamma, beta, Weibull and the exponential distributions. We use the Meta-Gaussian model [3] to construct a joint multivariate distribution from the marginal distributions. Our classification experiment shows that we obtain more accurate results with a Meta-Gaussian based maximum likelihood classifier than with a conventional multivariate Gaussian maximum likelihood classifier. The Meta-Gaussian model used with the best fitted marginal distributions is able to preserve correlations properly between the PolSAR features, a property which explains the improved classification results.

References

- [1] J.S. Lee and E. Pottier, *Polarimetric radar imaging : from basics to applications*, CRC Press, Taylor & Francis Group, 2009.
- [2] N.G. Kasapoğlu, S.N. Anfinsen and T. Eltoft: Fusion of optical and multifrequency PolSAR data for forest classification, *Proc. IGARSS 2012*, Munich, Germany, pp. 3355-3358, 22-27 July, 2012.
- [3] B. Stovik, G. Stovik and R. Fjortoft, "On the combination of multisensory data using Meta-Gaussian distributions," *IEEE Trans. Geosci. Remote Sens.*, vol. 47, no. 7, pp. 2372–2379, Jul. 2009.

L-band Active/Passive Land Surface Retrievals and SMAP

SMAP Status and Calibration/Validation Activities

T. J. Jackson⁽¹⁾, E. Njoku⁽²⁾, D. Entekhabi⁽³⁾, P. O'Neill⁽⁴⁾, and A. Colliander⁽²⁾

(1) USDA Hydrology and Remote Sensing Lab, Beltsville, MD 20705 USA tom.jackson@ars.usda.gov

(2) California Institute of Technology, Jet Propulsion Lab, Pasadena, CA USA

(3) Massachusetts Institute of Technology, Cambridge, MA USA

(4) NASA Goddard Space Flight Center, Greenbelt, MD USA

The Soil Moisture Active Passive (SMAP) satellite will be launched by the National Aeronautics and Space Administration in October 2014. This satellite is the culmination of basic research and applications development over the past thirty years. During most of this period, research and development of the active and passive microwave approaches to soil moisture estimation were mainly pursued separately. Passive microwave measurements have relatively coarse resolution from space but are more sensitive to the soil moisture contribution to the observed signal. Passive microwave soil moisture retrievals are considered robust and accurate. Active microwave measurements (radar) offer much higher spatial resolution, but the signal is relatively more sensitive to surface roughness and vegetation scattering, which can make accurate soil moisture estimation from radar alone more problematic. The SMAP concept combines these two technologies to provide a suite of products. These include three L2/3 soil moisture products: active-based high resolution, passive-based low resolution, and a combined active-passive intermediate resolution. In addition, there is a SMAP L3 freeze-thaw product and two L4 products: surface and root zone soil moisture and net ecosystem exchange of carbon. Additional details on the mission can be found in [1].

Both the SMAP instrument and algorithms are advancing on schedule. The status of the mission will be presented along with a review of recent activities. SMAP will incorporate a rigorous calibration and validation program that will support algorithm refinement and provide users with information on the accuracy and reliability of its suite of products. This program engages a large number of Cal/Val partners who provide in situ observations at representative locations globally. In preparation for launch, SMAP is conducting Cal/Val rehearsals aimed at risk reduction in meeting post-launch timeline goals for calibration/validation of all data products. Results from the Phase I rehearsal will be presented.

References

[1] D. Entekhabi, E. G. Njoku, P. E. O'Neill, K. H. Kellogg, W. T. Crow, W. N. Edelstein, J. K. Entin, S. D. Goodman, T. J. Jackson, J. Johnson, J. Kimball, J. R. Piepmeier, R. D. Koster, K. C. McDonald, M. Moghaddam, M. S. Moran, R. Reichle, J. C. Shi, M. W. Spencer, and S. W. Thurman, "The soil moisture active and passive (SMAP) mission," *Proceedings of the IEEE*, vol. 98, pp. 704-716, 2010.

Estimation of High Resolution Soil Moisture with Radar and Radiometer by a Spectral Downscaling Technique

Jiancheng Shi¹, Peng Guo^{1,2}, and Leung Tsang³

1 State Key Laboratory of Remote Sensing Science, Jointly Sponsored by the Institute of Remote Sensing and Digital Earth, Chinese Academy of Science, and Beijing Normal University, jshi@irsa.as.cn

2 University of Chinese Academy of Science, Beijing, China

3 University of Washington, Seattle, U.S.

Soil moisture is a key parameter to understanding the interactions between the water, energy, and carbon cycles. Satellite-based microwave remote sensing is one of the most promising techniques to monitor global near-surface soil moisture. Soil moisture retrieval using either active or passive microwave instrument has been explored for several decades. It is understood that each instrument having its distinct advantages^[1,2]. The passive radiometric observation is sensitivity to soil moisture, even under vegetated conditions but the spatial resolution is typically low (~10s km). It is useful to address the questions that related to hydro-climatic applications. The active radar is capable of high spatial resolution (~10s m to a few km) depending on the sensor type but its measurements are highly influenced by surface roughness, vegetation canopy structure and water content. To combine the individual advantages of the passive and active approaches, the SMAP (Soil Moisture Active and Passive) was selected for development by NASA in 2008^[3]. The SMAP consists of an L-band radar (1.26GHz) and an L-band radiometer (1.41GHz) that share a single feedhorn and reflector. The soil moisture products at 10km will be obtained by combining the 40km radiometer and 3km radar measurements in a joint retrieval algorithm.

In this study, we will first demonstrate the relationship between the radar and radiometer measurements that is derived by the radiative transfer equations. With this relationship, then, a novel approach to obtain downscaling soil moisture retrievals by combining active and passive radiometer observations is presented. The algorithm is based on the spectral downscaling which combines both phase and amplitude information in Fourier domain. The principle of the spectral downscaling is the spatial field at a given resolution may be extrapolated to fine resolutions by properly modeling its spatial properties at any observable scale in the frequency domain. Using the information from radar measurements at finer resolution, a new way to estimate the Fourier phase was developed.

The PALS (Passive and Active L-band System) datasets from SMEX02 (Soil Moisture Experiment in 2002) was used to evaluate the performance of the downscaling algorithm. The PALS was mounted on a C-130 aircraft and flown over the watershed study region on June 25th, 27th, and July 1st, 2nd, 5th, 6th, and 8th, 2002 during SMEX02. The algorithm has been successfully applied to the PALS datasets. The accuracy of the downscaling soil moisture retrievals is 0.041m³/m³ (RMSE), which is very close to SMAP science requirement of 0.04 for 10km product. The results indicate that the downscaling algorithm presented in this study is a promising approach to achieving finer resolution and more accurate soil moisture retrievals from SMAP mission.

Monitoring Landscape Freeze/Thaw State with Microwave Remote Sensing: Characterization of the Terrestrial Carbon Cycle with NASA's Soil Moisture Active/Passive (SMAP) Mission

Kyle C. McDonald

Department of Earth and Atmospheric Sciences
The City College of The City University of New York
New York, NY, USA

John S. Kimball

Flathead Lake Biological Station, Division of Biological Sciences
The University of Montana
Polson, MT, USA

Satellite microwave remote sensing can be applied to characterize soil moisture and the transitioning of water between frozen and non-frozen conditions. NASA's Soil Moisture Active/Passive (SMAP) mission, currently scheduled for launch in October 2014, will use an L-band radiometer and high-resolution radar instrument to measure surface soil moisture and freeze-thaw state providing new opportunities for scientific advances and societal benefits. Major science objectives of SMAP support the understanding of processes linking terrestrial water, energy and carbon cycles, the quantification of net carbon flux and the extension of capabilities for weather and climate prediction models. The landscape transition between seasonally frozen and non-frozen conditions occurs each year over more than 50 million km² of the global biosphere, affecting hydrological and ecological processes and associated trace gas dynamics profoundly. Combined, soil moisture and its freeze/thaw state define a surface hydrospheric state that is key to linking terrestrial water and carbon cycles and a principal determinant of the terrestrial carbon cycle. SMAP mission products will include regional and global maps of landscape freeze-thaw status with a 1-3 day temporal fidelity. These products will be suitable for a range of ecological, meteorological and hydrological applications, providing improved capabilities for mapping and monitoring of the biophysical constraints to land-atmosphere CO₂ exchange, leading to improved diagnosis and attribution of a purported terrestrial carbon sink over northern land areas. This presentation reviews proposed SMAP objectives and applications addressed through the SMAP mission freeze/thaw and carbon cycle-focused datasets. A framework is described using potential SMAP data products in an integrated scheme with other satellite data sources to support assessment of global terrestrial carbon cycling.

Comparison of Airborne PALS Measurements with SMOS and Aquarius during SMAPVEX12 Field Experiment

Andreas Colliander⁽¹⁾, Thomas Jackson⁽²⁾, Heather McNairn⁽³⁾, Eni Njoku⁽¹⁾

⁽¹⁾ Jet Propulsion Laboratory, California Institute of Technology; 4800 Oak Grove Dr, Pasadena, CA 91109, USA; andreas.colliander@jpl.nasa.gov

⁽²⁾ Agricultural Research Service, United States Department of Agriculture; tom.jackson@ars.usda.gov

⁽³⁾ Research Branch, Agriculture and Agri-Food Canada; heather.mcnairn@agr.gc.ca

NASA's (National Aeronautics and Space Administration) Soil Moisture Active Passive (SMAP) Mission is scheduled for launch in October 2014. The objective of the mission is global mapping of soil moisture and freeze/thaw state. Merging of active and passive L-band observations of the mission will enable unprecedented combination of accuracy, resolution, coverage and revisit-time for soil moisture and freeze/thaw state retrieval.

For pre-launch algorithm development and validation, the SMAP project and NASA coordinated a field campaign named as SMAPVEX12 (Soil Moisture Active Passive Validation Experiment 2012) together with Agriculture and Agri-Food Canada. SMAPVEX12 took place in the vicinity of Winnipeg, Canada over a six week period in June-July, 2012. The main objective of SMAPVEX12 was acquisition of a data record that features long-time series with varying soil moisture and vegetation conditions over aerial domain of multiple parallel lines.

The coincident active and passive L-band data were acquired using the Passive Active L-band System (PALS), which is an airborne radiometer and radar developed for testing L-band retrieval algorithms. For SMAPVEX12 PALS was installed on a Twin Otter aircraft. The flight plan included flights at two altitudes. The higher altitude was used to map the whole experiment domain and the lower altitude was used to obtain measurements over a specific set of field sites. The campaign ran from June 7 until July 19. The PALS instrument conducted 17 brightness temperature and backscatter measurement flights. The airborne data acquisition was supported by extensive ground truth collection. The conditions included a wide range in both soil moisture and vegetation density.

There were seven and 16 morning overpasses by NASA's Aquarius and ESA's SMOS instruments, respectively, during the experiment. Five of the Aquarius overpasses and nine of the SMOS overpasses coincided with PALS measurements. These measurements were compared with PALS measurements. The footprints of both Aquarius and SMOS are larger than the experiment domain. However, the comparisons of the measurements have indicated strong correlation between the airborne and spaceborne acquisitions. This paper presents the comparison results. Furthermore, in order to compensate for the differences in the measurements forward modeling is used to account for the measurement geometry and landscape heterogeneity. The forward models will be adjusted utilizing the in situ measurements collected during the experiment.

Acknowledgement: This work was carried out in Jet Propulsion Laboratory, California Institute of Technology under contract with National Aeronautics and Space Administration.

Soil moisture retrieval using L-band time-series radar observations provided by ground and airborne scatterometer and SAR data

S.B. Kim⁽¹⁾, L. Tsang⁽²⁾, T. Jackson⁽³⁾, A.C. Colliander⁽¹⁾, H. McNairn⁽⁴⁾, J. van Zyl⁽¹⁾
(¹) Jet Propulsion Laboratory, California Institute of Technology, USA, (²) Univ. Washington, Washington, USA, (³) USDA ARS Hydrology and Remote Sensing Laboratory, Maryland, USA
(⁴) Agriculture and Agri-Food Canada, Canada

The Soil Moisture Active and Passive (SMAP) mission, scheduled for launch in November 2014, will offer simultaneous and collocated synthetic aperture radar (HH, VV, and HV) and radiometer (H, V, and 3rd Stokes) measurements. Using these measurements, SMAP will provide global soil moisture and the freeze/thaw state of the land surface. SMAP's conical-scanning antenna enables soil moisture products with spatial resolutions of 3 km (radar), 36 km (radiometer), and 9 km (radar-radiometer combined) at 2- to 3- day revisit frequency globally. The science requirement of the mission is to provide moisture estimates for the top 5-cm layer of soil with an absolute accuracy of 0.04 cm³/cm³ or better at a 10 km resolution for the combined product. This paper describes the radar-only component of SMAP's soil moisture retrieval, which includes the soil moisture retrieval algorithms, the results of pre-launch tests using aircraft field and simulation data, and the plans for calibration and validation of the product.

Three algorithms are under consideration and currently being tested. Two of these are the time-series inversion of radar scattering forward models "data-cubes" for 17 land cover classes [1] and the change detection algorithm [2]. Retrieval outputs of the data cube method and the change detection method were combined to produce a third algorithm (Kim/van Zyl method [3]). These algorithms were tested with field campaign data sets. The data sets include the Michigan bare surface data acquired by a ground scatterometer data, the Southern Great Plains 1999 campaign with an airborne scatterometer data, and the SMAPVEX12 campaign in Canada providing airborne synthetic aperture data. The time-series data-cube algorithm had an accuracy of 0.044 cm³/cm³ (bare surface), 0.037 to 0.86 cm³/cm³ for vegetated fields (pasture, wheat, bean, and corn) where VWC changed in time and reached 3.5 kg/m² [4]. The Kim and van Zyl method had a performance similar to that of the data cube method. The correlation between retrieval and truth were mostly comparable between the time-series data cube method and the change detection method. The data cube approach is able to systematically correct for the temporal changes in vegetation, for example, during the growth period of corn and soybean. The capability improved the data cube retrieval, leading to an enhanced retrieval compared with the results of the other methods.

A primary strategy of post-launch calibration and validation for the radar-only algorithm is to use core validation sites around the world, which the SMAP project has been coordinating. In addition, sparse-network data will be used. The details of the calibration and validation activities will be presented.

References

- [1] S. B. Kim, M. Moghaddam, L. Tsang, M. Burgin, X. Xu, and E. G. Njoku, "Models of L-band radar backscattering coefficients over the global terrain for soil moisture retrieval," *IEEE Trans. Geosci. Remote Sens.*, in press, doi: 10.1109/TGRS.2013.2250980, 2013.
- [2] V. Naeimi, K. Scipal, Z. Bartalis, S. Hasenauer, and W. Wagner, "An improved soil moisture retrieval algorithm for ERS and METOP scatterometer observations," *IEEE Trans. Geosci. Remote Sens.*, vol. 47, pp. 1999-2013, 2009.
- [3] Y. Kim and J. J. van Zyl, "A time-series approach to estimate soil moisture using polarimetric radar data," *IEEE Trans. Geosci. Remote Sens.*, vol. 47, pp. 2519-2527, 2009.
- [4] H. McNairn, T. J. Jackson, G. Wiseman, S. Belair, P. Bullock, A. Colliander, S. B. Kim, R. Magagi, M. Moghaddam, J. Adams, S. Homayouni, E. Ojo, T. Rowlandson, J. Shang, K. Goita, and M. Hosseini, "The Soil Moisture Active Passive Validation Experiment 2012 (SMAPVEX12): Pre-Launch Calibration and Validation of the SMAP Satellite," *IEEE Trans. Geosci. Remote Sens.*, submitted, 2013.

Poster Session I

ADVANCED CONCEPT OF SCATTEROMETER METEOR-3

*V.Karaev¹, M.Kanevsky¹, Yu.Titchenko¹, M.Panfilova, Eu.Meshkov¹, G.Balandina¹,
A.Shlaferov², Yu.Kuznetsov²*

(1) Institute of Applied Physics, Russian Academy of Science
46, Uljanova str., 603950, Nizhny Novgorod, Russia
e-mail: volody@hydro.appl.sci-nnov.ru

(2) Rostovskii Scientific Research Institute of Radio Communications
130, Nansena str., 344078, Rostov-na-Donu, Russia

The scatterometer is a monostatic non-nadir looking radar and wind vector information can be empirically derived from its data. Over the last two decades, scatterometers onboard satellites have provided very valuable sea surface wind field information. In addition the scatterometer data are of interest in other applications such as sea ice and permafrost detection, snow melt and rainforest deforestation.

Two concepts of scatterometer are well-known. First of all it is a scatterometer with fixed antenna system (NSCAT, ASCAST). SeaWinds is the scatterometer with rotating antenna system and pencil antenna beam.

Also the concept of scatterometer with rotating fan beam was developed [1]. However, similar scatterometer will be launched only in 2014 (RFSCAT) [2].

The concept of the future Russian scatterometer (METEOR-3) is discussed. New scatterometer will have $1^0 \times 6^0$ antenna beam and speed of rotation is significantly less than SeaWinds (5 rotations per minute). At the same time, every wind vector cell (25 km x 25 km) will observe from 4 to 10 times. It permits to improve the precision of the determination of wind direction in comparison with SeaWinds. Simultaneously two polarizations or one polarization and cross polarization can be used for measurement of radar cross sections. It improves the precision of retrieval at high wind speed, gives possibility of sea ice classification and permits to solve other tasks.

Suggested scheme of scanning was simulated and backscattered radar cross sections in each wind vector cells (25 km x 25 km) were calculated. Dependence of radar cross section on wind speed, azimuthal angle, number of views, and intensity of swell was investigated.

Comparison with SeaWinds and ASCAT scatterometers showed that new scatterometer can be more accurate. The new retrieval algorithms were developed and tested.

Acknowledgments. This work is supported by the Russian Foundation of Basic Research (grants 13-05-00852-a).

Reference

- [1] C.C. Lin, B. Rommen, J.J.W. Wilson, F. Impagnatiello and P.S. Park, "An Analysis of a Rotating, Range-Gated, Fanbeam Spaceborne Scatterometer Concept", *IEEE Trans. Geoscience and Remote Sensing*, **38**, pp. 2114-2121, 2000.
- [2] X.Dong, "Progress of development of CFOSAT scatterometer", *Proceeding of IGARSS'12*, 22-27 July 2012, pp.237-240

SSPA-Based Ku Band Transmitter-Receiver Module for D3MON Radar

Janne Lahtinen⁽¹⁾ Teemu Ruokokoski⁽¹⁾ Jukka-Pekka Porko⁽¹⁾ Matti Vaaja⁽²⁾ Martti Toikka⁽³⁾
Martti Hallikainen⁽²⁾

⁽¹⁾ Harp Technologies Ltd, Tekniikantie 14, 02150 Espoo, Finland, janne.lahtinen@harptechnologies.com

⁽²⁾ Aalto University, matti.vaaja@aalto.fi

⁽³⁾ Toikka Engineering, toikka@co.inet.fi

The measurement of moisture, temperature, clouds, precipitation, and wind with improved temporal and spatial resolution, and if possible, with reduced cost would be beneficial for a variety of purposes, such as weather forecasting, climatology, aviation, wind energy, and understanding of water cycle. To enable studies in these areas and to investigate other potential applications, a Finnish consortium of companies, universities, and research institutes is currently developing a ground-based advanced high frequency radar D3MON. The work is coordinated by the Finnish Meteorological Institute (FMI). The radar will be transportable and operate at three frequencies (Ku, Ka, and W bands). The development has been financed in public-private partnership (PPP) as part of Measurement, Monitoring, and Environmental Assessment (MMEA) activity of the Cluster for Energy and Environment (CLEEN). D3MON radar is similar in many ways to NASA D3R dual-frequency Ku/Ka radar [1], but has also significant differences.

Within the development consortium of D3MON radar, Harp Technologies is developing a Ku band (13.96 GHz) Transmitter-Receiver (T/R) module with the support of Aalto University and Toikka Engineering Ltd. To reduce cost, weight, and size, increase reliability, and prolong operational lifetime compared to traditional tube-based transmitters, the module applies Solid State Power Amplifier (SSPA) technology. Additional benefits of SSPA technology are good environmental robustness and the possibility to use more advanced waveforms for improved performance [2]. The transmit power of the D3MON Ku band T/R module will be 60 W (continuous power). Both vertical and horizontal polarizations are supported to enable fully polarimetric operation. Integrated calibration loops in both polarizations enable accurate calibration. The critical components of the module, such as the High Power Amplifier (HPA) and Power Supply Unit (PSU) are developed in-house.

In order to reduce development risk, staged development process has been selected for the Ku-band T/R module. This paper describes the concept demonstration model with 15 W transmit power. Also, measurement results of verification and performance tests are presented. In addition, the design of the full performance T/R module version with 60 W transmit power and upgraded from the concept demonstration version is presented.

References

- [1] V. Chandrasekar, M. Schwaller, M. Vega, J. Carswell, K. V. Mishra, R. Meneghini, and C. Nguyen, "Scientific and engineering overview of the NASA Dual-Frequency Dual-Polarized Doppler Radar (D3R) system for GPM Ground Validation," *2010 IEEE International Geoscience and Remote Sensing Symposium (IGARSS)*, pp. 1308-1311, 2010.
- [2] M. Vega, J. Carswell, V. Chandrasekar, M. Schwaller, and K. V. Mishra, "Realization of the NASA Dual-Frequency Dual-Polarized Doppler Radar (D3R)," *2010 IEEE International Geoscience and Remote Sensing Symposium (IGARSS)*, pp. 4815-4818, 2010.

GROMOS-C, a new ground based 110 GHz radiometer for microwave ozone measurement campaigns

Susana Fernandez ⁽¹⁾ Axel Murk ⁽¹⁾ Niklaus Kämpfer ⁽¹⁾

⁽¹⁾ Institute of Applied Physics, University of Bern

Sidlerstrasse 5, 3012 Bern, Switzerland

Contact: susana.fernandez@iap.unibe.ch, +41(0)31 631 89 59

Stratospheric ozone is of major interest as it absorbs harmful UV radiation from the sun, thus allowing life on Earth. It also influences the thermal balance of the atmosphere. Ground based microwave remote sensing is the only method that allows to measure ozone profiles up to the mesopause, 24-hours and under different weather conditions [1].

We present a new ground based microwave radiometer, called GROMOS-C (GROund based Ozone MONitoring System for Campaigns), which is designed to measure the vertical profile of ozone distribution in the middle atmosphere, by observing ozone emission spectra at a frequency of 110.836 GHz. The instrument is designed in a compact way which makes it transportable and suitable for campaign use, an advantageous feature that is lacking in present day ozone radiometers. Furthermore, it may also be used for intercomparisons between other instruments currently in operation.

GROMOS-C is a total power radiometer which uses a preamplified single sideband heterodyne receiver, and a digital Fast Fourier Transform spectrometer for the spectral analysis. Its quasi-optical system combines an ultra-gaussian feed horn in combination with ellipsoidal and flat mirrors to couple different calibration loads into the optical path. Calibration is performed with a classical hot-cold concept. However instead of using a liquid nitrogen load a new cold calibration load was specifically designed and constructed for this instrument. It is based on a wedge geometry with an optimal millimeter-wave absorber at the desired frequency which is cooled with Peltier-elements [2]. As the calibration scheme does not depend on the use of liquid nitrogen, GROMOS-C can be operated also at remote places. The radiometer concept further allows also to use a noise diode for calibration as a super-hot target. The noise is coupled into the receiver before the RF amplification stage, and calibrated periodically with the hot and cold loads. Finally, also cold sky can be used optionally as a cold reference by determining its brightness temperature with a tipping curve approach.

A description of the main characteristics of GROMOS-C and the results of the first tests and spectra measurements will be presented.

References

- [1] Michael A. Janssen, *Atmospheric Remote Sensing by Microwave Radiometry*, Wiley series in Remote Sensing, New York, 1993.
- [2] S. Fernandez, A. Murk, N. Kaempfer, "Design and characterization of a Peltier-cold calibration load for a 110 GHz radiometer", *IAP Research Report*, 2013 (<http://www.iap.unibe.ch/publications/>)

GMES Sentinel-1

Soil Moisture Retrieval Algorithm Independent Assessment

Paul Snoeij⁽¹⁾, Patrick Imbo⁽²⁾, Thierry Rabaute⁽²⁾, Nicolas Baghdadi⁽³⁾, Wolfgang Wagner⁽⁴⁾,
Francesco Mattia⁽⁵⁾, Simonetta Paloscia⁽⁶⁾, and Nazzareno Pierdicca⁽⁷⁾

⁽¹⁾ ESA/ESTEC, paul.snoeij@esa.int

⁽²⁾ CS, Patrick.Imbo@c-s.fr, thierry.rabaute@c-s.fr

⁽³⁾ Irstea, nicolas.baghdadi@teledetection.fr

⁽⁴⁾ Institute of Photogrammetry and Remote Sensing, Vienna University of Technology,
ww@ipf.tuwien.ac.at

⁽⁵⁾ CNR/ISSIA, Francesco.Mattia@cnr.it

⁽⁶⁾ CNR/IFAC, s.paloscia@ifac.cnr.it

⁽⁷⁾ Sapienza University of Rome, nazzareno.pierdicca@uniroma1.it

The objective of the Global Monitoring for Environment and Security (GMES) is to provide, on a sustained basis, reliable and timely services related to environmental and security issues in support of public policy makers' needs. GMES is an EU-led initiative, in which ESA implements the space component and the Commission manages actions for identifying and developing services, relying on both in-situ and space-borne remote sensing data. GMES will use, to the maximum extent possible, existing capacities in Member States or at European level.

The Sentinel-1 European Radar Observatory, a constellation of two polar orbiting satellites for operational SAR applications is developed by ESA as part of the GMES space component [1]. The two C-band radar satellites will provide continuous all-weather day/night imagery for user services like the marine core services, the land monitoring services and the emergency services. The land monitoring services and other GMES services require as inputs near real time biogeophysical variables at continental to global scales. One of the important water related variable is soil moisture. Spaceborne radar offers a feasible, practical, timely and cost-effective means of determining the spatial distribution of soil moisture content over large areas. SAR systems can provide the necessary information at a spatial resolution adequate for hydrological purposes.

Five algorithms have been developed for soil moisture retrieval from both the single (HH or VV) and the dual polarised (HH+HV or VV+VH) GMES Sentinel-1 interferometric wide swath image data over land using or single acquisitions or multi-temporal acquisitions. The Sentinel-1 soil moisture retrieval algorithms are designed to process operationally in near real time with a product delivery to the GMES services within 3 hours from observation in all cases, within 1 hour from observation if inside coverage of a receiving station, within 10 minutes from observation in special cases.

An independent assessment based on geophysical validation using a large database consisting of archived C-band SAR data and in-situ soil moisture and surface roughness measurements has been performed.

In this paper, the analysed retrieval algorithms shall be introduced and the experimental conditions of the assessment as well as its results will be presented. Guidelines for future activities will also be given.

References

- [1] R. Torres, Snoeij P., Geudtner D. et al., "GMES Sentinel-1 mission", *Remote Sensing of Environment*, vol. 120, pp. 9-24, May 2012.

Sentinel-1 Commissioning Phase Preparation

Paul Snoeij, Dirk Geudtner, Bjorn Rommen, Michael Brown, and Ignacio Navas-Traver
European Space Research & Technology Centre, European Space Agency (ESA), Noordwijk, The Netherlands, Paul.Snoeij@esa.int

In the framework of the EU/ESA co-funded Global Monitoring for Environment and Security (GMES) program, ESA is undertaking the development of a series of five Sentinel missions with the objective to provide routinely Earth observation data for the implementation of operational GMES and national user services. As part of the GMES space component, the Sentinel-1 mission is implemented through a constellation of two satellites (A and B units) each carrying an imaging C-band SAR instrument (5.405 GHz) providing data continuity of ERS and ENVISAT SAR types of mission [1]. In addition, the 12-day repeat orbit cycle of each Sentinel-1 satellite along with small orbital baselines will enable SAR interferometry (InSAR) coherent change detection applications such as the monitoring of surface deformations (e.g. subsidence due to permafrost melt) and cryosphere dynamics (e.g. glacier flow).

The Sentinel-1 SAR instrument supports four exclusive imaging modes providing different resolution and coverage: Interferometric Wide Swath (IW), Extra Wide Swath (EW), Stripmap (SM), and Wave (WV). All modes, except the WV mode can be operated in dual polarization. Both the IW and EW mode operate in TOPS (Terrain Observation with Progressive Scans in azimuth) mode providing large swath width of 250 km and 400 km, respectively with enhanced image performance as compared to the conventional ScanSAR mode.

The front end of the instrument is based on an active phased array antenna driven by 280 transmit/receiver modules. Thus, by switching the instrument over a multitude of different beams, progressive scanning in azimuth is possible in order to reduce the scalloping effect (TOPS) and by scanning in elevation a wide range of swath positions can be covered (up to 400 km ground range).

The most important point with respect to the in-orbit calibration of this flexible SAR system is the tight performance with an absolute radiometric accuracy of only 1 dB (3 σ) for all operational modes. Never before such a strong requirement has been defined for a satellite SAR system. Following the experience gained with ERS and ENVISAT it is necessary to have a set of precision radar transponders to act as point targets which can be automatically programmed and accessed during the Sentinel-1 commissioning phase and the remainder of the mission lifetime in order to achieve the absolute radiometric accuracy requirement.

For interferometric application of the Sentinel-1 SAR the accuracy of InSAR measurements is controlled by the orbit accuracy (ground track repeatability) and the phase stability over a data take. The phase stability over a data take is monitored by internal calibration. Ground targets with stable phase of the reflected signal can be used as references to determine the repeatability of phase measurements.

The paper provides an overview of the Sentinel-1 system characteristics including the SAR imaging modes and their key performance parameters as well as the specifics of related attitude and orbit control modes (i.e. roll steering mode and zero-Doppler steering mode). The paper will describe the different aspects of the commissioning of the Sentinel-1 constellation

References

- [1] R. Torres, Snoeij P., Geudtner D. et al., "GMES Sentinel-1 mission", *Remote Sensing of Environment*, vol. 120, pp. 9-24, May 2012.

Intra-city urban heat island: A case study for Delhi City.

Neha Yadav⁽¹⁾ Chhemendra Sharma⁽²⁾

⁽¹⁾ Radio & Atmospheric Sciences Division, CSIR-National Physical laboratory, New Delhi, India.

email: neha_evs@yahoo.co.in

⁽²⁾ Radio & Atmospheric Sciences Division, CSIR-National Physical laboratory, New Delhi, India.

email: csharma@nplindia.org

Changing land use / land cover pattern due to rapid urbanization is causing urban heat island (UHI), which in turn negatively impacts the urban environment mainly by modification of physical and chemical properties of atmosphere, increased energy consumption, production of atmospheric pollutants and compromised human health & comfort in an urbanized environment [1-4]. The objective of this study is to investigate the impact of land use pattern and important meteorological variables (wind speed and relative humidity) on urban heat island phenomenon at two sites in Delhi city. Meteorological data for Safdarjung and National Physical Laboratory (NPL) areas in New Delhi, for the period of two years of 2010 & 2011 have been used for determining the urban heat island (UHI) in conjunction with land-use data. Urban heat island intensity (UHII) has been determined as the difference in the air temperatures of Safdarjung area and NPL area. Results show that mean annual UHII in Safdarjung in 2010 and 2011 was 1.6 and 1.4 °C respectively. The magnitude of mean monthly UHII has been found to be always greater than 1°C throughout the study period. The lower mean monthly UHII has been observed in the monsoon months (June-July) as compared to the summer and winter months. A weak but negative correlation has been observed for monthly trends of wind speed and relative humidity with UHII at Safdarjung area. The highest mean (1.7°C) UHII with comparatively lower wind speed (3.6m/s) has been observed in the month of October. Conversely the month of June showed the lowest mean UHI (1.2°C) with the highest wind speed (8.2 m/s). Diurnal variation of UHII showed strongest intensity in the morning hours (0800-0900 hrs), which decreased through the daytime. The UHII showed built-up after sunset that continued during the night time. The possible cause of UHI in Safdarjung could be due to higher percentage of constructed areas, as revealed by land use/ land cover map which showed that NPL area is having much larger percentage (60.6%) of vegetated land as compared to Safdarjung area (17.9%) while built up land in Safdarjung is very large (82.1%) as compared to NPL area (39.3%). It is also evident from the NDVI results that showed maximum value for NPL area (0.24) which is higher than the NDVI range for Safdarjung area (0.14). This is because of the large fraction of area covered by vegetation in NPL area as compared to the Safdarjung area. Both NDVI and land-use pattern supports the fact that an urban area having less vegetation and more built-up area tends to show UHI.

References

- [1] Rizwan Ahmed Memon, Dennis .C. Leung, LIU Chunho, "A review on the generation, determination and mitigation of Urban Heat Island," *Journal of Environmental Sciences*, vol. 20. pp. 120-128, 2008.
- [2] Rizwan Ahmed Memon, Dennis .C. Leung, "Impacts of environmental factors on urban heating," *Journal of Environmental Sciences*, vol. 22. pp. 1903-1909, 2010.
- [3] R. Giridharan, M. Kolokotroni, "Urban heat island characteristics during winter," *Solar Energy*, vol. 83, pp. 1668-1682, 2009.
- [4] Xiao-Ling, Chen Hong-Mei Zhao, Ping-Xiang Li, Zhi-Yong Yin "remote sensing image-based analysis of the relationship between urban heat island and land use/ cover changes," *Remote Sensing of Environment*, vol.104, pp. 133-146, 2006.

Speckle Statistics and Coherency Matrix of L Band Polarimetric SAR over Bare Soil with Rough Surfaces using Numerical 3D Simulations of Maxwell equations

Kuan-Liang Chen⁽¹⁾, Kun-Shan Chen⁽¹⁾, Leung Tsang⁽²⁾ and Tien Hao Liao⁽²⁾

⁽¹⁾National Central University, Zhongli, Taiwan

⁽²⁾Department of Electrical Engineering, University of Washington, Seattle, WA 98195, USA

Abstract

Recently, we have performed simulations of random rough surface scattering using 3D numerical simulations of Maxwell Equations [1]. The numerical simulations are based on the method of Moments and dense matrix solution accelerated by the UV/PBTG/SMCG method. Surface areas used are 32 wavelength by 32 wavelengths, 16 wavelengths by 16 wavelengths and 8 wavelengths and 8 wavelengths and the rough surfaces are characterized by exponential correlation functions. Both the co-polarization and cross polarizations are calculated and the simulations results were in good agreement with experimental measurements of bare soils at L band.

In this paper, using the simulation methods, for a given rms height, correlation length, soil permittivity and for a give incident angle, we calculated the radar scattering matrix up to 1000 realizations. For each realization, the components of scattering matrix, S_{HH} , S_{VV} , S_{HV} and S_{VH} are calculated. Using the simulated scattering matrices, we calculated the coherency matrix from which the polarimetric speckle statistics (amplitude and phase difference) are estimated, followed by a comparison with Wishart distributions [2]. For fully developed speckle from the homogeneous rough surface, the results are checked and validated. The eigenvalues, entropy, anisotropy and alpha angle in coherent target decomposition are then calculated. In particular, parameters characterization for rough surface is presented. Results are compared with ground measurements and with prior polarimetric model [3,4]. We further investigated the model-based target decomposition by which the total return is decomposed into surface scattering, volume scattering, double bounce, and helix scattering components [2,5]. Issues of symmetry characteristic and negative power are discussed.

References

- [1] S. Huang, and L. Tsang, "Electromagnetic scattering of randomly rough soil surfaces based on numerical solutions of Maxwell equations in 3 dimensional simulations using a hybrid UV/PBTG/SMCG method," *IEEE Trans. Geosci. Remote Sens.*, vol. 50, pp.4025-4035, 2012
- [2] Jong-Sen Lee and Eric Pottier, *Polarimetric Radar Imaging: From Basics to Applications*, CRC Press, 2009
- [3] S. Cloude and E. Pottier, "A review of target decomposition theorems in radar polarimetry," vol.34, pp. 498-518,1996.
- [4] I. Hajnsek, , E. Pottier, and S.R. Cloude , "Inversion of Surface Parameters from Polarimetric SAR," *IEEE Trans. Geosci. Remote Sens* , vol. 41, pp.727-745,2003
- [5]Y. Yamaguchi, T. Moriyama, M. Ishido, and H. Yamada, "Four-component scattering model for polarimetric SAR image decomposition," *IEEE Trans. Geosci. Remote Sens.*, vol. 43, pp. 1699-1706, 2005.

Airborne radiometer measurements of soil moisture in boreal areas

Jaakko Seppänen⁽¹⁾ Juha Kainulainen⁽¹⁾ Martti Hallikainen⁽¹⁾

⁽¹⁾ Aalto University

Department of Radio Science and Engineering

P.O. Box 13000

FI-00076 AALTO

Finland

jaakko.seppanen@aalto.fi

The Soil Moisture and Ocean Salinity (SMOS) mission is a mission within the ESA Living Planet Program. It delivers global surface soil moisture fields at high temporal resolution which is of major relevance for weather forecasting, climate monitoring, and the global freshwater cycle. [1]

The relatively coarse surface resolution of SMOS causes the pixels to cover several different types of soil and vegetation. In order to reliably retrieve soil moisture it is vital to know the properties of all the emitters. While bogs are abundant in the boreal forest zone, there are few measurements of them at L-band.

Between 2011 and 2013 a series of airborne campaigns was conducted over the Rajamäki test area in Southern Finland. By means of this data set, the objective of this study is to present comparisons between airborne measurements and SMOS Level 2 soil moisture algorithm over different landscapes, specifically in a coniferous forest terrain.

The goal of the measurement campaigns was to collect more information of soil moisture retrieval. To model the above-surface layer of forests, satellite measurements of vegetation and in situ measurements of litter were used. Measurements of litter layer were used to model the contribution of understory layer beneath the forest canopy.

Calculations of the terrain emission are based on the L-MEB biosphere emission model [2], an essential part of the SMOS moisture algorithm, which was used to create a forward emission model, taking into account both the surface parameters and measurement parameters for each measurement.

Analysis of the data indicates, that the L-MEB model for coniferous forest can simulate the emission with decent accuracy and soil moisture retrieval is possible when dominant vegetation is dry heath forest with thin understorey. Thick canopy or understorey can mask the emission of soil completely. Bogs present a significant problem when found in in forest pixels, since their emissivity exhibits large temporal changes.

References

- [1] K. D. McMullan, M. A. Brown, M. Martin-Neira, W. Rits, S. Ekholm, J. Marti, and J. Lemanczyk, "SMOS: The payload," *IEEE Transactions on Geoscience and Remote Sensing*, vol. 46, no. 3, pp. 594–605, March 2008.
- [2] J.-P. Wigneron, Y. Kerr, P. Waldteufel, K. Saleh, M.-J. Escorihuela, P. Richaume, P. Ferrazzoli, P. de Rosnay, R. Gurney, J.-C. Calvet, J. Grant, M. Guglielmetti, B. Hornbuckle, C. Mätzler, T. Pellarin, and M. Schwank, "L-band microwave emission of the biosphere (L-MEB) model: Description and calibration against experimental data sets over crop fields," *Remote Sensing of Environment*, vol. 107, pp. 639 – 655, 2007.

SMOS satellite soil moisture data assimilation in the Watershed Modeling and Forecasting System in Finland

Tiia Vento⁽¹⁾ Juho Jakkila⁽¹⁾ Tapani Rousi⁽¹⁾ Bertel Vehviläinen⁽¹⁾

⁽¹⁾ Finnish Environment Institute, Freshwater Centre, Mechelininkatu 34a, P.O.Box 140, FI-00260 Helsinki, Finland

Email: tiia.vento@ymparisto.fi, juho.jakkila@ymparisto.fi

Estimating the state of the soil moisture storage in conceptual hydrological models is challenging but important for determining the timing and magnitude of summer and autumn floods. The Soil Moisture and Ocean Salinity (SMOS) satellite mission responds to the need of large scale soil moisture monitoring by capturing soil emission signals around the globe with L-band microwave radiometers with near real-time operational system [1]. The objective of this study is to estimate the benefits of SMOS soil moisture data assimilation in the Watershed Simulation and Forecasting System (WSFS) [2] of the Finnish Environment Institute.

A semi-distributed, conceptual HBV-based hydrological rainfall-runoff model of the WSFS provides daily water level and discharge simulations and forecasts to all watersheds in Finland and is an important tool for national flood forecasting. The soil moisture sub-model was modified to simulate soil moisture also in a 10 cm thick surface layer comparable to penetration depth of SMOS observations. Simulations with SMOS data assimilation are performed in Lapuanjoki and Aurajoki basins located in the West and Southwest of Finland. These locations were chosen for good retrieval of SMOS observations. Runoffs in Aurajoki and Lapuanjoki are usually at largest after snowmelt in spring, but heavy rains in the summer and autumn also cause frequently high discharges. Since the SMOS level 2 soil moisture data provides large scale soil moisture observations in these areas, it has the potential to improve the estimate of the state of the soil moisture storage in the WSFS.

Data assimilation of SMOS observations into the WSFS is conducted utilizing the automatic model updating procedure of the WSFS, which is based on Hooke-Jeeves optimization algorithm [3]. The procedure corrects model inputs, areal precipitation and temperature, so that the model state is consistent with water level, discharge and snowpack observations. In this study the model state corrections are made also against SMOS level 2 data. The simulations present a promising result that the satellite observations could be used as an indicator of the soil moisture storage in the WSFS after dry periods, considered one of the flaws of the current operational system.

References

- [1] Y. H. Kerr, P. Waldteufel, J. P. Wigneron, S. Delwart, F. Cabot, J. Boutin, M. J. Escorihuela, J. Font, N. Reul, C. Gruhier, S. E. Juglea, M. R. Drinkwater, A. Hahne, M. Martin-Neira and S. Mecklenburg, "The SMOS Mission: New Tool for Monitoring Key Elements of the Global Water Cycle", *Proceedings of the IEEE*, vol. 98, no. 5, pp. 666-687, 2010.
- [2] B. Vehviläinen, "The watershed simulation and forecasting system in the National Board of Waters and Environment", *Publications of the Water and Environment Research Institute, National Board of Waters and the Environment, Finland*, no. 17, 1994.
- [3] R. Hooke, and T.A. Jeeves, "Direct search" solution of numerical and statistical problems, *Journal of the Association for Computing Machinery*, vol. 8, no. 2, pp. 212-229, 1961.

Influence of Radio Frequency Interference on SMOS Measurements over Finland

J. Kainulainen, J. Seppänen, M. Hallikainen

Aalto University School of Electrical Engineering, Department of Radio Science and Engineering
P.O. BOX 13000, 00076 AALTO, Espoo, FINLAND
juha.kainulainen@aalto.fi

Radio Frequency Interference (RFI) has been a severe problem for the ESA's Soil Moisture and Ocean Salinity (SMOS, [1]) mission from the beginning of its operations in November 2009. Several activities have been invoked on many fronts to fight the problem. Cooperation between ESA and national authorities has yielded switch-offs of tens of RFI sources especially in Europe. Also, research initiatives have been launched in order to study the removal and mitigation of the influence of RFI directly in SMOS measurements. Regardless of the progress in these areas the large number of RFI sources - and their dynamics - has posed a problem over the whole life time of SMOS.

Aalto University studies these man-made 1.4 GHz RFI appearances using SMOS data, and data collected with the airborne HUT-2D L-band interferometer [2], especially over Finland. We have tested a number of RFI detection methods, e.g. [3], in order to examine the detection and influence of the RFI sources on the measurements of the two radiometer systems.

During the lifetime of SMOS two major RFI sources have been detected at the area of Finland. Aalto has pursued the detection and removal of these sources by conducting airborne measurements, and by cooperating with Finnish authorities, for the precise localization of them. Also, tools for rapid RFI detection, data quality assessment, and RFI flagging of SMOS data over Finland have been demonstrated. Such tools are provided for the use of other Finnish communities where SMOS data is used.

In this presentation we demonstrate the influence of RFI sources which affect on SMOS measurements over Finland, estimate their influence quantitatively, and present how the influence changes on the course of the SMOS mission. We also present airborne measurement results obtained with HUT-2D in order to study RFI sources at urban areas.

References

- [1] Y. Kerr, P. Waldteufel, J.-P. Wigneron, et.al., "The SMOS mission: New tool for monitoring key elements of the global water cycle," *Proc. of the IEEE*, Vol. 98, pp. 666-687, May 2010.
- [2] K. Rautiainen, J. Kainulainen, T. Auer, et.al., "Helsinki University of Technology L-band airborne synthetic aperture radiometer," *IEEE Trans. Geosci. and Remote Sens.*, Vol. 46, No. 3, pp. 717-726, Mar. 2008.
- [3] E. Anterrieu, "On the Detection and Quantification of RFI in L1a Signals Provided by SMOS," *IEEE Trans. Geosci. and Remote Sens.*, Vol. 49, No. 10, pp. 3986-3992, May 2011.

Modelling of TanDEM-X-Measured Forest Height from Small Footprint Lidar Data

Maciej J. Soja ⁽¹⁾

Lars M. H. Ulander ^(1,2)

⁽¹⁾ Chalmers University of Technology, Gothenburg, Sweden (soja@chalmers.se)

⁽²⁾ Swedish Defence Research Agency, Linköping, Sweden

TanDEM-X is a single-pass satellite-borne SAR interferometer [1]. It consists of two almost identical X-band (9.6 GHz) SAR satellites flying in a tight tandem formation. The helical shape of the orbit allows for flexible image acquisition geometry. The primary mission goal of the TanDEM-X system is to acquire a global digital elevation model (DEM). However, TanDEM-X data can also be used for forest mapping. Forest height can be mapped with TanDEM-X interferometry if a high-resolution DEM is available as ground reference. By the removal of a simulated DEM interferogram from the acquired image interferogram, a height difference map is obtained, which in forested regions gives an estimate of forest height [2].

For this work, we have produced forest height maps from TanDEM-X interferometry and lidar DEM over the boreal test site of Remningstorp, situated in southern Sweden. A processing algorithm based on [3] was developed. The general agreement of the TanDEM-X-derived forest height maps and the reference lidar maps is very good, especially for the cases with favourable baseline setup. Best mapping results were obtained with baselines giving height-of-ambiguity (HOA) values between 50 and 80 metres. Larger HOA values result in reduced height precision, which makes forest height maps noisier. Lower HOA values give better height sensitivity, but also an increased risk of phase wrapping and more pronounced baseline decorrelation. Especially in the case of mature forest with a few, tall trees, and a significant vertical scatterer distribution, phase wrapping and baseline decorrelation can cause very low coherence, which results in poor height estimates.

To address this problem, and to improve the general understanding of X-band scattering from forests, a forward model simulating TanDEM-X-derived forest height from small-footprint, high-density lidar height maps is developed. Lidar data over Remningstorp were acquired within the BioSAR 2010 campaign (pixel size 0.5 m x 0.5 m). In the model presented here, each pixel is assumed to be a scatterer. For each resolution cell, a weighted coherent sum of the contributions from all pixels is computed. The weighting factor is a number describing the degree of exposure of each pixel to the incident electric field. It is derived from the distribution of scatterers in the line-of-sight of the radar. This approach makes it possible to model the influence of gaps in forest canopy. Also, non-homogeneities in the canopy are handled. However, since the model uses deterministic forest height maps, analytical treatment of the problem is difficult. In the simplified case of constant forest height, random distribution of scatterers, and exponential attenuation profile function, the model reduces to the well-known random volume over ground model, which can be treated analytically.

References

- [1] G. Krieger, A. Moreira, H. Fiedler, I. Hajnsek, M. Werner, M. Younis, and M. Zink, "TanDEM-X: A Satellite Formation for High-Resolution SAR Interferometry", *IEEE Transactions on Geoscience and Remote Sensing*, Vol. 45, Issue 11, Nov. 2007
- [2] S. Solberg, R. Astrup, T. Gobakken, E. Naesset, and D. J. Weydahl, "Estimating Spruce and Pine Biomass with Interferometric X-Band SAR", *Remote Sensing of Environment*, Volume 114, Issue 10, October 2010, pp. 2353-2360
- [3] U. Balss, H. Breit, S. Duque, T. Fritz, and C. Rossi, "TanDEM-X Payload Ground Segment: CoSSC Generation and Interferometric Considerations", German Aerospace Center (DLR), May 2012

**Microwave Propagation in
Vegetated and Snow Covered Soils:
A Session in Honor of
Paolo Pampaloni**

30 years of research on microwave emission from snow and vegetation covered soils

Simonetta Paloscia

CNR-IFAC, Florence (Italy)

s.paloscia@ifac.cnr.it

Starting from early '80s a significant work on the characteristics of vegetation by using microwave sensors was carried out by Paolo Pampaloni and his group. The research on microwave signatures from natural surfaces was at the beginning and several experiments were started and carried out first in U.R.S.S. and US and successively in Europe. Pampaloni pioneering works on microwave remote sensing of soil moisture and vegetation biomass in agricultural areas are truly admirable and provided inspiration for future research works and developments.

The perfect preparation for measurements, the acquisition of complete measurement data sets, the foreseeing detailed analysis, and overwhelming clear conclusions of the Paolo Pampaloni's works in the early 1980s were revisited in this paper. In particular, the microwave radiometric measurements of snow, soil and vegetation features have been described, together with the models used for interpreting them. Most significant results have been shown, concerning the retrieval of soil moisture, vegetation biomass and snow water equivalent by using both ground-based and satellite data.

The first results regarded the investigation of vegetated surfaces and the effect of the structure and the biomass of different crop types on the microwave emission. A set of ground-based and airborne microwave radiometers (from Ka to L band) was built and installed on agricultural fields. The performances of microwave vegetation indexes for detecting biomass and water conditions of agricultural crops were analyzed. A simplified form of the radiative transfer model was used for modeling polarization properties of emission from soil covered with vegetation and a significant correlation between polarization and frequency indexes and biomass of corn and alfalfa was obtained.

Later on, also snow covered soils were observed and dedicated experiments with ground-based microwave radiometers were carried out. Long-term microwave and infrared radiometric measurements of snowpack were carried out with ground-based sensors, together with conventional measurements of snow-cover profiles. Adequate electromagnetic models were implemented for representing soil and snow. The comparison of model simulations with experimental data allowed one to understand some peculiar characteristics of microwave emission from the snowpack related to its physical conditions.

Microwave Propagation in Vegetated and Snow Covered Soils: A Session in Honor of Paolo Pampaloni

Exploiting the effects of snow layering on the retrieval of SWE from active and passive microwave measurements

E.Santi, S.Paloscia, P.Pampaloni, S.Pettinato, X.Chuan, M.Brogioni, G.Macelloni, E.Palchetti

IFAC-CNR, Florence (Italy)

E.Santi@ifac.cnr.it

Microwave sensors are sensitive to snow properties and are able to give information on snow depth (SD) and snow water equivalent (SWE) as demonstrated by the pioneering works of the teams of Univ. of Berne and Univ. of Kansas [1, 2]. The key frequency channels in detecting the presence of snow were found to be at Ku- and Ka- bands, and most algorithms to retrieve snow parameters by using passive sensors are based on the difference between the brightness temperature (Tb) at 19 and 37 GHz. These frequencies are not available from the present in orbit Synthetic Aperture Radars (SAR), which operate at C- or X- band where wave penetration is quite high in dry snow and very low in wet snow. However, recent investigations showed a noticeable relationship between X-band backscattering and SWE when SD is higher than about 60 cm. The case of emission from layered snow has been theoretically studied by Liang et al.[3]. In this paper, the effects of multilayer structure of snowpack on emission and backscattering have been investigated by using a physical model and experimental data collected on the Italian Alps.

The model simulates snowpack by means of a stratified medium composed by spherical ice scatterers embedded in air, overlying a rough homogeneous half-infinite medium. Volume scattering/emission from snow is computed by using a multi-layer version of the Dense Medium Radiative Transfer Theory in the Quasi Crystalline Approximation (DMRT-QCA) with sticky particles [4]. Soil contribution is simulated by using the AIEM for the co-polar components and the semi-empirical approach by Oh *et al.* for the cross-polar terms.

A huge amount of radiometric data were collected at 6.8, 10, 19, 37 GHz with ground based instruments in winter seasons from 2002 to 2009 on a site selected in NE Italy. More recently, X-band SAR images of a wide area surrounding the radiometer station were obtained from the Cosmo Skymed mission. Also snow profiles were obtained with conventional methods at convenient temporal and spatial sampling. In addition to the measured profiles, and in order to make this study as general as possible, a few “synthetic” snow profiles, representative of typical cases of dry snow cover in the Alps were realized. The parameters taken into consideration were: grain size, snow density and layer thickness. These “synthetic” profiles, that summarize the main characteristics for each period of the season, were obtained by analyzing 26 real snow profiles obtained in winter 2010-2011, when the snow depth was frequently greater than 60 cm. The performed sensitivity analysis carried out considering all the major parameters that affect emission and backscattering confirmed the high sensitivity of the model to grain size and pointed out the contribution of the layering structure of snowpack in particular to the polarized emission.

References

- [1] E. Schanda, and R. Hofer, "Microwave multispectral investigations of snow", Proc. 11th Internat. Symp. on Remote Sensing of Environment, 601-607, Ann Arbor, Mi. (1977).
- [2] F. T. Ulaby and W. H. Stiles, "The active and passive microwave response to snow parameters: Part II - Water equivalent of dry snow," *J. Geophys. Res.*, vol. 85, C2, Feb. 1980.
- [3] D. Liang, X. Xu, L. Tsang, "The Effects of Layers in Dry Snow on Its Passive Microwave Emissions Using Dense Media Radiative Transfer Theory Based on the Quasicrystalline Approximation (QCA/DMRT)," *IEEE Trans. Geosci. Remote Sensing*, 46, pp. 3663-3671, 2008.
- [4] L. Tsang, J. Pan, D. Liang, Z. X. Li, D. Cline, and Y. H. Tan, "Modeling active microwave remote sensing of snow using dense media radiative transfer (DMRT) theory with multiple scattering effects," *IEEE Trans. Geosci. Remote Sens.*, 45, no. 4, pp. 990-1004, 2007.

MICROWAVE SNOW BACKSCATTERING MODELING BASED ON THREE-DIMENSIONAL MICROSTRUCTURE RECONSTRUCTED FROM TWO-DIMENSIONAL SNOW SECTION IMAGE

Jiancheng Shi ⁽¹⁾ Leung Tsang ⁽²⁾

⁽¹⁾ Institute of Remote Sensing and Digital Earth, Chinese Academy of Sciences, Beijing, China

⁽²⁾ Department of Electrical Engineering, University of Washington, U.S

We present this paper, in honor of Dr. Paolo Pampaloni for his great contributions in microwave studies of snow, soil and vegetation. One of the key issues in the terrestrial snow microwave remote sensing is the accurate modeling of backscattering signal from snow covered terrain. In existing snow scattering models including independent scattering models, and dense media models such as QCA, QCA-CP and QCA-sticky, the snow media are modeled as discrete spheres or spheroids. However, in these models the geometric configuration of snow media is different from real snows three dimensional microstructures, moreover, due to the regular shape of spheres, the cross polarization elements of phase matrix in QCA-sticky is zero, which causes to underestimate the cross polarization backscattering.

Classical field measurement of snow particle size is a biased estimation, because its very difficult to determine proper representative grain sizes for scattering models. Snow section image is a two-dimensional plane intersecting a snow media in which features of the snow media are represented on the section as profile.

Several studies have been done to use snow section for snow scattering modeling. Shi (1993) estimated the equivalent representative grain size by stereological method based on snow section image, which is then inputted into dense media model. Zurk (1997) calculated the 3D pair distribution functions from 2D planar snow section image and then its inputted into a multi-size dense media model. However, they are all based on sphere based models, so spheres based structure were first constructed to model the scattering. Generally, dry snow is a two-phase random media with air and ice, Ding (2010) proposed a method to simulate snow microstructure by Berks (1991) level-cut method based on artificial simulated Gaussian random field, and then the scattering properties were calculated by DDA (Discrete Dipole Approximation). There are good resemblances between the simulated microstructure and real snow microstructure.

In this study, a new procedure is developed to model the backscattering of snow covered terrain based on snow section images. In order to obtain an unbiased estimation of the snow parameters, the information provided by the section image should be fully utilized. So we tried to model the snow volume backscattering from snow 3D microstructures reconstructed from 2D section image. The proposed procedure could be a direct link between field measurements and observed backscattering. The 3D structures were directly reconstructed from 2-D snow section image. The reconstruction should maintain the statistical features of 2-D images in order to make an accurate estimation of real 3D structure of snow.

Radar Scattering Signatures of Terrestrial Snow at X and Ku Band with a Multi-layer DMRT Model combined with NMM3D Boundary Conditions

Shurun Tan⁽¹⁾ Wenmo Chang⁽¹⁾ Xiaolan Xu⁽²⁾ Leung Tsang⁽¹⁾ Juha Lemmetyinen⁽³⁾ Simon Yueh⁽²⁾

⁽¹⁾ Department of Electrical Engineering, University of Washington, Seattle, WA 98195, USA

⁽²⁾ Jet Propulsion Laboratory, M/S 300-233, Pasadena, CA 91009, USA

⁽³⁾ Arctic Research Unit, Finnish Meteorological Institute, Finland

Email: srtan@uw.edu

We present this paper at this URSI Meeting in Helsinki October 2013 in honor of Professor Paolo Pampaloni who had made outstanding contributions in active and passive microwave remote sensing of snow. The two frequencies, X band and Ku band are selected for active remote sensing of terrestrial snow by two proposed satellite missions, CoReH2O of ESA, and SCLP of NASA, both equipped with dual polarization radar. The dual frequency, dual polarization configuration is useful to separate the volume scattering and surface scattering. In this paper, we study the frequency dependence and polarization dependence of snow scattering coefficient at these two frequencies for a wide range of snow conditions. Three approaches are used with various parameter configurations, (i) quasicrystalline approximation (QCA) [1] and (ii) Foldy Lax multiple scattering equations with various grain diameter and stickiness, (iii) discrete dipole approximation (DDA) of bicontinuous media model [2] with different medium statistics. The QCA scattering dependence on stickiness and bicontinuous/DDA scattering on medium statistics are also investigated. The specific surface area (SSA) and fractional volume are used to relate the parameters of the sticky spheres model and the bicontinuous model.

The extinction coefficient and phase matrix produced by bicontinuous/DDA are further put into a multi-layer dense medium radiative transfer (DMRT) equation combined with rough snow ground boundary condition. The rough surface boundary condition is derived from a Numerical Maxwell's Model in 3 Dimension (NMM3D). Interpolation is used to obtain full-directional bi-scattering coefficient of the rough surface. Multiple scattering theory is used to solve the DMRT equation set. The diffuse intensity in each snow layer is decomposed into Fourier series in the azimuth direction, and the phase matrix and rough surface boundary conditions are also transformed into harmonics. The Eigen-quadrature analysis is applied to each layer for each harmonic, and the coefficients for the eigenvectors are solved by matching boundary conditions. This quadrature solution takes into the full multiple scattering effects as well as the bistatic scattering of rough surface.

The forward model results are compared by applying the multi-layer DMRT model to the SnowSAR data. The SnowSAR data were taken from the ESA snow field measurement campaign carried out in Finland in March 2011, where detailed measurements of snow density, grain size, and temperature vertical profiles were made.

References

- [1] L. Tsang, J. Pan, D. Liang, Z. Li, D. W. Cline, and Y. Tan, "Modeling Active Microwave Remote Sensing of Snow Using Dense Media Radiative Transfer (DMRT) Theory With Multiple-Scattering Effects," *Geoscience and Remote Sensing, IEEE Transactions on*, vol. 45, no. 4, pp. 990-1004, Apr. 2007.
- [2] X. Xu, L. Tsang, S. Yueh, "Electromagnetic Models of Co/Cross-polarization of Bicontinuous/DMRT in Radar Remote Sensing of Terrestrial Snow at X- and Ku-band for CoReH2O and SCLP Applications," *Selected Topics in Applied Earth Observations and Remote Sensing, IEEE Journal of*, vol.5, no.3, pp.1024-1032, June 2012

Modeling of Active and Passive Microwave Signatures over Grass

Laura Dente⁽¹⁾ Leila Guerriero⁽²⁾ Zhongbo Su⁽¹⁾ Paolo Ferrazzoli⁽²⁾

⁽¹⁾ University of Twente, Faculty of Geo-Information Science and Earth Observation (UT-ITC),
Hengelosestraat 99, 7500 AA Enschede, The Netherlands, Email: dente@itc.nl

⁽²⁾ Tor Vergata University of Rome, Dipartimento di Ingegneria Civile e Ingegneria Informatica,
Rome, Italy

Theoretical models based on the radiative transfer approach are used to simulate backscattering and emission from various vegetation surfaces, i.e. grassland, cropland and forest. Their potential for the retrieval of biophysical parameters, such as soil moisture and vegetation biomass, is under evaluation. Among the existing models, several studies have validated the ability of the discrete scattering model developed by the Tor Vergata University of simulating both backscattering and emission from various land cover. Up to now, most direct applications of this model have focused at the field scale and have been applied to passive and active observations separately.

The main objectives of this study were to evaluate the advantage of using a unique model, i.e. the Tor Vergata model, driven by a unique set of input parameters to estimate both emissivity and backscattering coefficient and to validate these estimates with AQUA AMSR-E and Metop ASCAT observations.

The investigation was carried out for the Maqu area, located along the upstream reach of the Yellow River (in the north-eastern part of the Tibetan Plateau) at an elevation of about 3200 m, where measurements of soil moisture and soil temperature are continuously collected in several sites. The area of interest is flat and covered by homogeneous grassland with a thin litter layer over the soil surface.

The analysis consisted of two main steps: the optimization of the model inputs, which was carried out over 2009 data, and the validation of the results over 2010 data. The average of soil moisture in situ measurements and the leaf area index obtained from MODIS Terra/Aqua 8-days LAI products were used as model inputs. Moreover, the surface temperature obtained from Ka-band AMSR-E data was used to compute the brightness temperature from the modeled emissivity. This allowed us to make the comparison with the satellite data. No measurements were available for other model inputs, such as surface roughness, litter biomass and vegetation structural parameters, therefore they were optimized to obtain the best match with both ASCAT and AMSR-E observations of 2009.

The synergistic use of active and passive data was crucial at this step of the study, because it allowed us to find more realistic input values than in the case of using one kind of data only.

The optimization over 2009 data led to obtain a good agreement between model outputs and satellite signatures for the active case, with a determination coefficient (R^2) of 0.9 and a root mean square error (*rmse*) of 0.5 dB, and a slight overestimation for the passive case, with R^2 of 0.8 and *rmse* of 6.3 K for H polarization and R^2 of 0.5 and *rmse* of 5.9 K for V polarization.

The validation results with 2010 data were slightly worse than the optimization ones (R^2 of 0.8 and *rmse* of 1 dB for the active case and R^2 of 0.5 and *rmse* of 8 K for the passive case). Different sources of uncertainties affected the results, such as the coarse resolution of the satellite observations, the missing in situ measurements of several model inputs and most of all, as demonstrated by this study, the method for estimating the surface temperature.

Remote Sensing of Snow

Understanding L-band data acquired by SMOS over Antarctica using in situ measurements and electromagnetic modelling

Marion Leduc-Leballeur⁽¹⁾, Ghislain Picard⁽¹⁾, Arnaud Mialon⁽²⁾, Eric Lefebvre⁽¹⁾, Christoph Rüdiger⁽³⁾, Yann Kerr⁽²⁾, Florent Dupont^(1,4), Laurent Arnaud⁽¹⁾, Michel Fily⁽¹⁾

⁽¹⁾ LGGE (UJF-Grenoble 1, CNRS), 54 rue Molière 38041 Grenoble, France, mleduc@ujf-grenoble.fr

⁽²⁾ CESBIO (CNES, CNRS, IRD, UPS), 18 avenue Edouard Belin 31401 Toulouse, France

⁽³⁾ Department of Civil Engineering, Monash University, Melbourne, Australia

⁽⁴⁾ CARTEL, Université de Sherbrooke, Quebec, Canada

In Antarctica, remote sensing data are particularly important for the study of regional climate due to the sparse coverage of the in situ measurements. The observations of space-borne sensors are a unique mean to provide a detailed picture of the spatial and temporal variations of important climate variables.

In this context, the MIRAS radiometer on board ESA's SMOS satellite [1], with its low observation frequency (1.4 GHz), offers a great opportunity to estimate this accurate reference temperature. Indeed, as a result of the high volume scattering of the snow field produced by the snow grains at the higher frequencies, the snow emissivity is much less than unity. On the other hand, the scattering is reduced at lower frequencies such as L-band and the emissivity is close to unity when the surface reflection effect vanishes at V-polarization near the Brewster angle of $\sim 50^\circ$. As a consequence, the spatial variation of the emissivity at L-band should be smaller and more predictable than at higher microwave frequencies.

In this study, to explore those characteristics of the L-band emissivity, we jointly use the SMOS L3 daily global polarised brightness temperature product and the in-situ measurements from two ice cores up to a depth of 80 m recently performed at Dome C during the austral summer campaign of 2012-13 and we develop a multi-layer electromagnetic model based on wave approach [2]. Moreover, the estimation of the emissivity from brightness temperature requires highly accurate surface temperature, which is not available as stated in the introduction. However, for the purpose of the present analysis, we have chosen to use the surface temperature predicted by the ECMWF ERA-Interim reanalysis. The approach to derive emissivity is similar to the one presented in [3].

References

- [1] Y. H. Kerr, P. Waldteufel, J.-P. Wigneron, J. Martinuzzi, J. Font and M. Berge., "Soil moisture retrieval from space: the Soil Moisture and Ocean Salinity (SMOS) mission," *IEEE Transactions on Geoscience and Remote Sensing*, vol. 39, no 8, pp. 1729-1735, 2001.
- [2] Tsang L., Kong J. A., Ding K.-H., *Scattering of electromagnetic waves, vol 1: Theories and Application*, Wiley Interscience, 3664, 2000.
- [3] G. Picard, L. Brucker, M. Fily, H. Gallée and G. Krinner, "Modeling timeseries of microwave brightness temperature in Antarctica", *J. Glaciology*, vol. 55, no. 191, pp. 537–551, 2009.

Radarsat and snow character at Greenland Summit

Terhikki Manninen⁽¹⁾ Panu Lahtinen⁽²⁾ Kati Anttila⁽³⁾ Aku Riihelä⁽⁴⁾

⁽¹⁾Finnish Meteorological Institute, P.O. Box 503, FI-00101 Helsinki, Finland, terhikki.manninen@fmi.fi

⁽²⁾Finnish Meteorological Institute, P.O. Box 503, FI-00101 Helsinki, Finland, panu.lahtinen@fmi.fi

⁽³⁾Finnish Meteorological Institute, P.O. Box 503, FI-00101 Helsinki, Finland, kati.anttila@fmi.fi
and Finnish Geodetic Institute, Geodeetinrinne 2, kati.anttila@fgi.fi

⁽⁴⁾Finnish Meteorological Institute, P.O. Box 503, FI-00101 Helsinki, Finland, aku.riihela@fmi.fi

The RASCALS campaign [1] was carried out at the Greenland Summit camp research station during June - July 2010. The collection of surface roughness, dielectric constant and density profiles of snow were carried out concurrently with snow albedo and bidirectional reflectance distribution function (BRDF) measurements. Radarsat data were provided for a period from May to August, 2010 by ESA via the EU SOAR project, ID 6759 (ARCS). A few of them were taken during the measurement campaign. Favorable weather conditions during the campaign enabled the collection of a large dataset on Arctic snow albedo and associated quantities for use in developing and validating remote sensing algorithms for snow albedo using satellites. The surface roughness data contains about 500 individual 1 m long profiles taken in 16 days. The rms height, correlation length and autocorrelation function are determined. The dielectric constant and density of snow were obtained in 9 days for profiles of about 1 m deep with an interval of about 5 cm. Polarimetric interferometry of the Radarsat-2 quad pol fine beam images is used to study the snow surface anisotropy at Summit, Greenland. Various methods of determining the polarimetric coherence are carried out and the results are compared with the surface roughness results, which show a clear anisotropy varying with time [2, 3, 4]. In addition, surface backscattering modeling is used to check the fraction of the surface backscattering.

References

- [1] A. Riihelä, P. Lahtinen, T. Hakala, "The radiation, snow characteristics and albedo at summit (RASCALS) expedition report", Finnish Meteorological Institute Report 2011:8, 46 p., 2011.
- [2] S.R. Cloude and K.P. Papathanassiou, "Polarimetric SAR Interferometry", IEEE Transactions on Geoscience and Remote Sensing, Vol. 36, No. 5, pp.1551-1564, 1998.
- [3] I. Hajnsek, S.R. Cloude, "The Potential of InSAR for Quantitative Surface Parameter Estimation", Canadian Journal of Remote Sensing, Vol. 31, No. 1, pp 85-102, February 2005.
- [4] K.P. Papathanassiou, I. Hajnsek, T. Nagler, and H. Rott "Polarimetric SAR Interferometry for Snow Cover Parameter Estimation", Proceedings of 2nd ESA Workshop on Applications of SAR Polarimetry and Polarimetric Interferometry, POLInSAR 05, January 2005.

Active and Passive Microwave Signatures of Seasonal Snow Cover: Four Years of the NoSREx Campaign

J. Lemmetyinen⁽¹⁾, J. Pulliainen⁽¹⁾, A. Kontu⁽¹⁾, A. Wiesmann⁽¹⁾, C. Mätzler⁽²⁾, H. Rott⁽³⁾,
T. Nagler⁽³⁾, K. Voglmeier⁽³⁾, A. Meta⁽⁴⁾, A. Coccia⁽⁴⁾, M. Schneebeli⁽⁵⁾, M. Proksch⁽⁵⁾,
M. Davidson⁽⁶⁾, D. Schüttemeyer⁽⁶⁾, M. Kern⁽⁶⁾

⁽¹⁾ Finnish Meteorological Institute, Helsinki, Finland
email: juha.lemmetyinen@fmi.fi

⁽²⁾ GAMMA Remote Sensing Research and Consulting AG
Worbstr. 225, CH-3073 Grümligen, Switzerland

⁽³⁾ ENVEO IT GmbH, Innsbruck, Austria

⁽⁴⁾ MetaSensing B.V., Noordwijk, The Netherlands

⁽⁵⁾ WSL Institute for Snow and Avalanche Research (SLF), Davos, Switzerland

⁽⁶⁾ ESA-ESTEC, Noordwijk, The Netherlands

The NoSREx (Nordic Snow Radar Experiment) campaign was initiated in 2009 to aid the development of the geophysical retrieval algorithms for the proposed 7th Earth Explorer mission of the European Space Agency, CoReH2O (Cold Regions Hydrology High-resolution Observatory). The campaign provides a time-series of tower based backscatter observations at X to Ku bands, the dual frequency bands proposed for CoReH2O, as well observations using passive microwave radiometry at L to W bands. The measurements span to date four full winter seasons; together with comprehensive in situ measurements on snow, soil and atmospheric properties, the dataset provides unique possibilities for investigating the microwave signatures of snow covered terrain.

The site of NoSREx operations at the Finnish Meteorological Institute Arctic Research Centre (FMI-ARC) is a typical representative of the northern boreal forest zone, with seasonal snow cover persisting up to five months during winter. The main instrument of the campaign was the ESA *SnowScat* scatterometer, installed for the entire campaign at a fixed location. The instrument provides a consistent time series of observations, allowing to relate the backscatter signature to small scale changes in the snowpack at a high temporal resolution. During the second and third seasons of the campaign, extensive airborne data acquisitions using the ESA X/Ku band *SnowSAR* instrument were made at the site. The airborne data provide additional information on spatial variability of the backscattering signal, and allow demonstration of the CoReH2O SWE retrieval concept. The active measurements are complemented by microwave radiometry from the same site, provided by two radiometer systems, allowing to study the synergistic use of active and passive microwave instrumentation.

As a reference to microwave observations, the campaign provides routinely both manual and automated measurements of snow properties. In addition, several Intensive Observation Periods (IOPs) conducted during the experiment provide accurate information on snow cover properties by e.g. means of near-infrared photography and computer tomography of casted snow samples.

We present the main findings of the campaign, including the impact of snow structure and subnivean conditions on microwave signatures, and the feasibility of X/Ku band radar to determine key parameters of seasonal snow cover.

COMPARISON OF SNOW WATER EQUIVALENT ESTIMATES OF CMIP5 CLIMATE MODEL SIMULATIONS AND SATELLITE-BASED DATA

Kari Luojus^(1,), Jouni Pulliainen⁽¹⁾, Matias Takala⁽¹⁾, Juha Lemmetyinen⁽¹⁾, Tuomo Smolander⁽¹⁾, Jaakko Ikonen⁽¹⁾, Juval Cohen⁽¹⁾ and Chris Derksen⁽²⁾*

¹⁾ Finnish Meteorological Institute (FMI) Arctic Research, P.O.Box 503, Helsinki, Finland. (*e-mail: kari.luojus@fmi.fi)

²⁾ Climate Processes Section, Climate Research Division, Environment Canada, 4905 Dufferin Street, Toronto, Canada

ABSTRACT

The European Space Agency (ESA) GlobSnow project has produced a daily hemisphere-scale satellite-based snow water equivalent (SWE) data record spanning more than 30-years. The GlobSnow SWE record, based on methodology by Pulliainen [1] utilizes a data-assimilation based approach for the estimation of SWE which was shown to be superior to the approaches depending solely on satellite-based data [2]. The GlobSnow SWE data record is based on the time-series of measurements by two different space-borne passive radiometers (SMMR and SSM/I) measuring in the microwave region, spanning from 1980 to present day at a spatial resolution of approximately 25 km.

We briefly present the on-going efforts taking place for further enhancement of the satellite-based SWE retrieval and the way this transfers to the reliability of the long-term SWE climate record. The development of SWE retrieval are focused on application of a new HUT multi-layer snow emission model and variational snow density scheme for SWE retrieval and efforts carried out to improve the homogeneity of the long-term record of weather station-based snow depth observations that are applied within the SWE retrieval scheme.

In addition, the GlobSnow satellite-based dataset is inter-compared with climate model simulations from the CMIP5 archive. The objective of this work is to investigate the performance of the CMIP5 models in capturing the evolution of hemispheric scale snow conditions for the period of 1980 to 2012. The climate model simulations on snow cover extent, snow depth and snow water equivalent are evaluated against the GlobSnow SWE record.

The results indicate a decreasing trend in spring time hemispherical snow mass for the period of 1980 to 2012 in remote-sensing based data record. The inter-comparison of satellite-based record and climate model simulations show differences in spring time Hemispherical scale snow conditions. Similar trends of decreasing snow cover are also seen in the investigated CMIP5 models, although there is a notable variance between different models. Some of the models capture the overall hemispherical snow mass more accurately than others. In general the winter months (December, January and February) seem to be rather well captured, while the spring season, (March, April and May) appears more challenging for the climate models. Also the inter-annual variability of snow cover is higher in the observation-based record, compared with climate models.

REFERENCES

- [1] Pulliainen, J. Mapping of snow water equivalent and snow depth in boreal and sub-arctic zones by assimilating space-borne microwave radiometer data and ground-based observations. *Remote Sensing of Environment*. 101: 257-269. DOI: 10.1016/j.rse.2006.01.002.
- [2] Takala, M., Luojus, K., Pulliainen, J., Derksen, C., Lemmetyinen, J., Kärnä, J.-P., Koskinen, J., Bojkov, B., "Estimating northern hemisphere snow water equivalent for climate research through assimilation of space-borne radiometer data and ground-based measurements", *Remote Sensing of Environment*, Vol. 115, Issue 12, 15 December 2011, Pages 3517-3529, ISSN 0034-4257, DOI: 10.1016/j.rse.2011.08.014.

Simulations of microwave brightness temperature of snow using HUT snow emission model with SNOWPACK and in situ measurements

Anna Kontu, Juho Vehviläinen, Juha Lemmetyinen, Jouni Pulliainen

Finnish Meteorological Institute, Arctic Research, Sodankylä, Finland
email: anna.kontu@fmi.fi

The microwave brightness temperature of snowpack was simulated for years 2009-2013 (four winter seasons) with HUT snow emission model [1]. The aim is to find out the usability of SNOWPACK [2] modeled snow structure with HUT snow emission model, and especially to compare SNOWPACK output and manual snow measurements as input to HUT model.

We have used in situ data measured in Finnish Meteorological Institute's Arctic Research Centre (67.368 N, 26.633 E) in Sodankylä, Finland. The area is a typical representative of the northern boreal forest zone, with seasonal snow cover persisting up to five months during winter. The site is equipped with numerous automatic sensors measuring continuously e.g. snow depth, incoming and outgoing short- and longwave radiation, precipitation, and air, snow and soil temperatures. In addition, weekly manual snow pits provide time series of snow structure (layering) and profiles of visual snow grain size, temperature, density and wetness. Also available are almost continuous microwave observations with a dual-polarization radiometer manufactured by Radiometer Physics GmbH, Germany, at frequencies 10.65, 19.7, 21.0, and 36.5 GHz at 3-4 hour intervals.

The brightness temperature of snow was simulated with the multilayer version of the HUT snow emission model using two input data time series: 1) snow structure simulated with SNOWPACK from the automatic in situ measurements and 2) snow structure measured manually at the snow pits. The resulting brightness temperatures were compared to the microwave radiometer measurements.

The results indicate that the snow structure and especially snow grain size simulated by SNOWPACK is very well suited for use with HUT snow emission model. In fact, the simulation error is smaller when SNOWPACK output is used than when manual observations are used. The main reason for this is probably the high variability of grain sizes in the manual observations, mainly due to objectivity of the observations of individual persons.

References

- [1] J. Lemmetyinen, J. Pulliainen, A. Rees, A. Kontu, Y. Qiu, and C. Derksen, "Multiple-layer HUT snow emission model: Comparison with experimental data", *IEEE Trans. Geosci. Remote Sens.*, vol. 48(7), pp. 2781-2794, July 2010.
- [2] P. Bartelt and M. Lehning, "A physical SNOWPACK model for the Swiss avalanche warning Part I: numerical model", *Cold Regions Science and Technology*, vol. 35(3), pp. 123-145, November 2002.

Remote Sensing of Snow and Ice:
A Session in Memory of
Richard Moore

Airborne Ultra-Wideband Microwave Radars for Snow Measurements

S. Gogineni, J. B. Yan, F. Rodriguez-Morales, C. Leuschen, B. Panzer, D. Gomez-Garcia, A. E. Patel, J. Paden, and M. A. Aziz

Center for Remote Sensing of Ice Sheets (CReSIS), University of Kansas, Lawrence, KS 66047, USA

<pgogineni@ku.edu>

Accurate information on the thickness of snow over sea ice is needed for accurately estimating sea-ice thickness from freeboard measurements made with satellite altimeters. We designed and developed ultra-wideband radars that operate over the frequency range of 2-8 GHz and 12-18GHz, which are referred to as, respectively, the “Snow Radar” for measuring snow thickness over sea ice and mapping internal layers in polar firn, and the “Ku-band Altimeter” for high-precision surface elevation measurements. These radars operate as Frequency-Modulated Continuous Wave (FMCW) systems with a transmit power of about 200 mW. We have been operating these radars on both long-range National Aeronautics and Space Administration (NASA) aircraft and twin-engine aircraft provided by the National Science Foundation (NSF) over the last four years. We developed these radars such that data can be processed in full bandwidth mode with a range resolution of about 5 cm and sub-band mode with reduced bandwidth.

We collected a large volume of data, as a part of the NASA Operation IceBridge (OIB) over Arctic and Antarctic sea-ice, and also on the Greenland and Antarctic ice sheets. We processed these data and, with snow and firn densities, generated estimates of snow thickness over sea ice and snow accumulation over ice sheets. We are now upgrading the Snow and Ku-band radars to dual-polarized multichannel systems with beamforming capability. The dual-polarization and beamforming capability enables the measurement of radar backscattering as a function of incidence angle as well as mapping snow-air and snow-interfaces of snow-covered sea ice, and mapping internal layers in polar firn. We are planning to develop an inversion algorithm to estimate snow density/snow-water equivalent (SWE) from dual-polarized and multi-frequency backscattering measurements.

In this paper, we will present design considerations for airborne FMCW radars for measurements from fast-moving long-range aircraft and show the system impulse response function derived from simulated targets and quasi-specular returns. We will also discuss upgrades being performed to obtain dual-polarized and multi-frequency backscatter measurements as a function of incidence angle, and the algorithm being developed to estimate snow characteristics. Finally, we will discuss results obtained over Arctic and Antarctic sea ice, and ice sheets in Greenland and Antarctica. In particular, we will show the comparison between the Ku-band Altimeter data and the CryoSat-II Altimeter data, which indicates that the returns from snow-covered sea ice are dominated by signals reflected by the snow-air interface for many areas of the Antarctic. The location of dominant returns for Arctic snow-covered sea ice is highly variable depending on snow characteristics and thickness.

Experimental Brightness Temperature Behaviour of Snow on Lake Ice

Martti Hallikainen, Matti Vaaja, Jaakko Seppänen, Anssi Hakkarainen, Juha Kainulainen

Aalto University, Dept. Radio Science and Engineering, P.O. Box 13000, 00076 Aalto, Finland
martti.hallikainen@aalto.fi

Space-borne microwave radiometers provide information on terrestrial snow characteristics including the water equivalent (SWE) of dry snow. In northern regions the effect of various land-cover categories, especially boreal forests and lakes, to the brightness temperature must be accounted for in order to obtain reasonable accuracy in SWE retrieval. However, the modest spatial resolution of space-borne radiometers handicaps detailed investigation of the brightness temperature behavior of snow on lake ice with satellite data.

We have investigated the brightness temperature behavior of snow on lake ice by conducting airborne radiometer measurements over two lakes in southern Finland in 2004, 2007, 2011, 2012, and 2013. The flight path includes two lakes of different sizes and, additionally, a forested area and an open, mostly agricultural area. This allows us to compare the behavior of the brightness temperature of snow on lake ice with that of snow on ground.

The main airborne instrument is our HUTRAD system, which operates at 6.9, 10.7, 18.7, 23.8, and 36.5 GHz, providing data for both vertical and horizontal polarization at an incidence angle of 50 degrees off nadir. Some data have been collected, additionally, using our HUT-2D interferometric imaging radiometer, which operates at 1.4 GHz. The radiometers are accommodated on our Skyvan research aircraft. In-situ measurements have been made simultaneously with airborne data collection.

The encountered conditions include dry snow/ice, occasional water on top of ice, moist snow surface, and the melting season. In two occasions data were collected both in the morning and in the afternoon in order to study the effect of diurnal temperature variations during the melting season.

Our data indicate that radiometer response to the snow/ice system depends mostly on snow surface characteristics at 36.5 GHz, whereas the presence of water on top of ice dominates at 6.9 and 10.7 GHz. Brightness temperatures may vary substantially within a short distance due to the occasional presence of water at the ice/snow interface. The results for snow on lake ice are different from those for snow on ground and, additionally, the results for the larger lake were sometimes different from those for the smaller lake.

Shortwave broadband black-sky surface albedo estimation for Arctic sea ice using passive microwave radiometer data

Vesa Laine¹, Terhikki Manninen¹, Aku Riihelä¹ and Kaj Andersson²

¹Finnish Meteorological Institute, P.O. Box 503, FI-00101 Helsinki, Finland

²VTT Information Technology, P.O. Box 1200, FIN-02044 VTT, Finland

A new remote sensing method to estimate the optical broadband black-sky surface albedo using passive microwave radiometer data has been developed. In this research the AVHRR-based shortwave broadband black-sky albedos processed using the algorithms of the new surface broadband albedo CM-SAF product SAL, and the AMSR-E microwave data from the National Snow and Ice Data Center (NSIDC), Boulder, Colorado have been employed. To analyze the correspondence between AVHRR-based optical albedo and microwave brightness temperature AMSR-E frequencies of 6.9, 18.7 and 36.5 GHz have been tested by fitting a third degree polynomial curve to the SAL-albedo and the AMSR-E data points. The best correlation occurs in 6.9 GHz vertical polarization brightness temperature ($R^2 = 0.92$). To illustrate and compare the spatial variabilities of the SAL- and AMSR-E albedos of the sea ice during the melting and re-freezing period, maps of 13 weeks have been prepared of both albedos from June to August 2007. The albedo time series from AMSR-E and AVHRR data are calculated for the combined sea ice and open water cover for the Northern Hemisphere as a whole, and for six specific sea ice regions: the Arctic Ocean, the Kara and Barents Seas, the Greenland Sea, the Labrador Sea, Hudson Bay, and the Canadian Archipelago. The standard errors between the optical and passive microwave estimates varied from about 0.001 (Greenland Sea) to 0.04 (Canadian Archipelago) being 0.013 on the average in absolute units. The relative standard errors are then smaller than 5 % in most of the regions.

References

[1] V. Laine, T. Manninen, A. Riihelä, and K. Andersson, "Shortwave broadband black-sky surface albedo estimation for Arctic sea ice using passive microwave radiometer data," J. Geophys. Res. 116, D16124, doi:10.1029/2011JD015700, 2011.

Incidence angle dependence of HH/HV-polarized RADARSAT-2 SAR backscattering over homogeneous ice and open water regions

Juha Karvonen ⁽¹⁾

⁽¹⁾ Finnish Meteorological Institute (FMI), PB 503, FI-00101, Helsinki, Finland, juha.karvonen@fmi.fi

The incidence angle dependence of C-band HH-polarized SAR backscattering coefficient (σ^0) over sea ice has been studied e.g. in [1]. This has been performed using images including the same area at multiple (two or more) incidence angles. This kind of comparison requires a lot of manual work for determining the locations included in the comparison. Here we have a different approach: we just automatically locate areas with no texture in both the channels (HH/HV) based by autocorrelation thresholding, and compute the mean backscattering as a function of the incidence angle, which has been computed based on the SAR orbit parameters, for a large RADARSAT-2 ScanSAR mode SAR data set. By using a large data set, we can assume that the target types are also randomly distributed within each incidence angle bin (we have used 0.1 degrees bins or intervals in our study), and we actually get the mean incidence angle dependence over the textureless areas. These areas include both open water and level ice with no visible structures in the SAR data. The dependence at HH-channel was a linear decrease as a function of the incidence angle. This is an expected behavior according to the earlier studies over sea ice at C-band. The behavior at the HV-band, however, shows much more complex dependence, which is not linear nor uniquely decreasing. The aim of our study has been to establish a general incidence angle correction for both the channels. A straightforward linear correction can be applied to the HH channel data, and a more complex correction based on lookup tables (LUT's) is applicable for the HV channel data. At the HV band the σ^0 values are close to the instrument noise floor (around -28dB for RADARSAT-2 ScanSAR mode), and the noise floor (noise equivalent σ^0) varies along the across-track direction. The noise floor modulates the (low) HV channel signal, and for this reason at HV-band causes clearly visible stripes. These stripes complicate the visual and automated interpretation of the SAR data. According to our tests, these visible stripes at HV-channel are significantly reduced after the incidence angle correction, and the corrected data can then better be utilize both for visual interpretation and by automated SAR image analysis. We show the statistical incidence angle dependence of σ^0 for both the RADARSAT-2 dual-polarized ScanSAR wide mode channels (HH and HV). We also show examples of the incidence angle correction, based on the computed statistical dependencies. The current LUT-based HV-channel incidence angle correction is based on nearest neighbor interpolation over the whole SAR image width. An even better result would probably be achieved by using a more sophisticated interpolation technique (like spline interpolation).

References

- [1] M. Mäkynen, T. Manninen, M. Similä, J. Karvonen, M. Hallikainen, *Incidence angle dependence of the statistical properties of C-band HH-polarization backscattering signatures of the Baltic Sea ice*, IEEE Trans. on Geoscience and Remote Sensing, v. 40, n. 12, pp. 2593-2605, 2002.

On estimation of melt pond fraction on the Arctic Sea ice with ENVISAT WSM images

Marko Mäkynen⁽¹⁾ Stefan Kern⁽²⁾ Leif Toudal Pedersen⁽³⁾

⁽¹⁾ Finnish Meteorological Institute, P.O. Box 503, FI-00101 Helsinki, Finland, marko.makynen@fmi.fi

⁽²⁾ University of Hamburg, KlimaCampus Hamburg, stefan.kern@zmaw.de

⁽³⁾ Danish Meteorological Institute, ltp@dmi.dk

The accuracy microwave radiometer ice concentration (IC) retrievals is reduced during summer melting conditions by melt ponds on sea ice. Recently a method has been developed to estimate melt pond fraction (f_{mp}) with MODIS surface reflectance data. However, this method is limited by cloud cover, and thus several days of data (e.g. one week) must be typically aggregated to get a reasonable spatial coverage. In addition, automatic cloud masking of the MODIS data has typically some errors over sea ice. Current SAR methods for the f_{mp} estimation are only for smooth, thick land-fast first-year ice. They are basically linear fits between backscattering coefficient (σ°) and f_{mp} under different wind speeds.

We have studied f_{mp} estimation over the Greenland (Fram Strait) multiyear ice (MYI) with ENVISAT Wide Swath Mode (WSM) SAR images. The images were georectified to 100 m pixel size, and processed also to a daily SAR mosaic with 500 m pixel size. The incidence angle (θ_0) variation in the WSM images was compensated with empirically determined slope terms (σ° [dB] vs. θ_0). Daily f_{mp} charts with 12.5 km pixel size were available from Integrated Climate Data Center (ICDC). All datasets were acquired in summer 2009.

Relationships between σ° and f_{mp} were studied in the following ways: 1) σ° time series were extracted from the WSM images at fixed latitude-longitude grid points and one ice buoy location (ice drift tracked) to find out if significant σ° and f_{mp} changes match each other. 2) MODIS f_{mp} charts, MODIS RGB images and SAR mosaic were visually compared to see how melt ponded areas show in the SAR mosaic. 3) Temporally (daily) and spatially co-incident σ° and f_{mp} were analyzed. The σ° data were extracted using 12.5 km windows.

In the σ° time series the relationship between σ° and increase of f_{mp} (ponding period) was typically not very clear, in some cases 2-3 dB σ° increase was present. We did not find any correlation between σ° and wind speed which effects roughness of melt ponds. The pond drainage period did not show as a σ° trend. The tracking of ice drift (σ° data over same ice area) may generally improve the σ° vs. f_{mp} relationship, at least during the ponding period.

Visual analysis of the datasets suggested that during the ponding period the texture of σ° decrease and on the average the σ° level somewhat increase, whereas no monotonous σ° texture and level changes were visible during the drainage period.

Using either σ° data averaged to the same pixel size (12.5 km) as the MODIS f_{mp} data or various texture parameters calculated from the 12.5 km windows it was not possible to estimate f_{mp} . In addition, their pdfs do not differ significantly for different f_{mp} intervals, regardless of the θ_0 range. Very likely other properties of sea ice, mainly ice deformation features and mixtures of various ice types, are masking σ° variations produced by increase and decrease of f_{mp} .

Thus, we conclude that the estimation of f_{mp} from ENVISAT WSM images is not possible over drifting MYI, at least in our dataset. For studying better the relationship between σ° and f_{mp} we would need both or at least f_{mp} data at much finer resolution than here.

This study was part of the ESA Sea Ice Climate Change Initiative project which targets to provide microwave radiometer based daily IC charts from 1978 onwards for the Arctic and Antarctic with the best possible accuracy.

Remote Sensing of Forest and Vegetation

A P-band SAR for global forest biomass measurement: the BIOMASS mission

Thuy Le Toan

Centre d'Etudes Spatiales de la Biosphère (CESBIO)

CNRS, CNES, Université Paul Sabatier, Toulouse, France

With the contribution of the Biomass mission Advisory Group and the ESA Biomass team.

In May 2013, BIOMASS was selected as the ESA 7th Earth Explorer Mission. This selection is part of the user-driven process that will lead to the launch of the satellite in 2020.

The BIOMASS mission aims to determine, for the first time and in consistent manner, the distribution and temporal changes of forest biomass at a global scale. Data from the BIOMASS mission will reduce current uncertainties in the calculations of carbon stocks and fluxes associated with the terrestrial biosphere. BIOMASS will therefore advance our understanding of the carbon cycle and its role in controlling the climate.

BIOMASS is based on a single satellite carrying a P-band Synthetic Aperture Radar to provide continuous global interferometric and polarimetric radar observations of forested areas. Strong physical arguments supported the use of P-band SARs for retrieving forest biomass. However, such a mission is only possible at present, since a frequency band centred on 435 MHz has been allocated for Earth Observation, and there have been significant advances in instrument design and in development of retrieval methods.

This paper will present an overview of the mission concept, comprising the scientific requirements, the activities conducted to consolidate the mission definition and the current methods used to derive from P-band SAR data, using advanced methods combining SAR intensity, polarimetric SAR interferometry and tomography. A particular emphasis is put on the retrieval of biomass in tropical dense forests, which is a challenging task to reduce the major source of error in estimates of carbon loss by deforestation.

Topographic effects in P-band polarimetric SAR of boreal forests

Lars M.H. Ulander^(1,2) Gustaf Sandberg⁽²⁾ Maciej J. Soja⁽²⁾

⁽¹⁾ Swedish Defence Research Agency (FOI), Linköping, Sweden

⁽²⁾ Chalmers University of Technology, Gothenburg, Sweden

Forestry is a major land application of satellite remote sensing. Optical satellites are still dominating but synthetic aperture radar (SAR) is emerging with several promising concepts. One of the more promising is based on low radar frequencies to provide penetration through the canopy and scattering from the larger structural elements. The BIOMASS mission [1], which was recently selected as the European Space Agency's seventh Earth Explorer, is based on this concept. The instrument is a P-band (435 MHz) polarimetric SAR and one primary objective is to produce global maps of above-ground dry biomass on a 200 m grid with an RMSE of 20%.

Early approaches of estimating biomass from P-band SAR data often used HV-polarisation, which showed highest dynamic range and best linear regression results. However, it has been observed that single-polarisation estimates generally have limited accuracy due to effects of varying structure, ground topography and moisture conditions. For example, "double-bounce" scattering between the ground and tree structural elements becomes prominent at lower radar frequencies. This effect can be observed in multiple images from different aspect angles in topographic areas. It is strongest in high-resolution HH data where the backscatter from tree trunks on sloping ground changes significantly with aspect angle. A physical-optics model has been developed and used to predict the influence of topography on HH P-band backscatter [2].

Multiple polarisations provide significantly improved results, in particular when combined with a digital elevation model (DEM) of the ground surface. Different approaches have been used to select training and validation data. For a global mission like BIOMASS, it is important to develop estimation algorithms which can be used for broad forest classes. Training and validation data should be strictly separated, and both should be collected to represent a broad range of expected conditions (biome, structure, topography, moisture). A recent study separated training and validation data by more than 700 km. Up to four observables were used in linear regression models to estimate model parameters in one area and validate the model in the other area. A single polarization model gave a RMSE of 84%, three polarisations gave 38%, and three polarisations together with ground slope gave 24%.

In this paper, we present new results based on an airborne SAR experiment conducted in 2010. The experiment was designed to include three flight headings, i.e. 178°, 199° and 270°, in order to study the effect of topography for different aspect angles. The topography in the test area is generally small with ground elevation varying between 120 m and 145 m above sea level. However, the ground slope can locally be rather large. Results show that there is only a small difference between the SAR images for headings 178° and 199°. Significant differences occur for heading 270°, however, which clearly can be related to the ground slope effect. Perhaps most surprising is that significant topographic effects are also present in the VH-polarised data.

References

- [1] ESA, "BIOMASS, Report for Selection," *ESA SP-1324/I*, 2012.
- [2] Hallberg, B., Smith-Jonforsen, G., Ulander, L. M. H., and G. Sandberg, "A physical-optics model for double-bounce scattering from stems standing on an undulating ground surface," *IEEE Trans. Geosci. Remote Sensing*, vol. 46, no. 9, pp. 2607-2621, 2008.
- [3] M.J. Soja, G. Sandberg, G., and L.M.H. Ulander, "Regression-Based Retrieval of Boreal Forest Biomass in Sloping Terrain using P-band SAR Backscatter Intensity Data," *IEEE Trans. Geosci. Remote Sensing*, vol. 51, no. 5, pp. 2646-2665, 2013.

Analysis of Multitemporal Fully Polarimetric Radarsat-2 Data over Boreal Forest Zone for Land Cover Mapping

Oleg Antropov⁽¹⁾ Yrjö Rauste⁽¹⁾ Tuomas Häme⁽¹⁾

⁽¹⁾ VTT Technical Research Centre of Finland, P.O. Box 1000, FI-02044, Finland,
oleg.antropov@vtt.fi

The availability of timely and reliable land cover or land use information is critical for a wide range of applications. In this work, the potential of both multitemporal and fully polarimetric (PolSAR) Radarsat-2 data for land cover applications in the boreal forest zone is investigated.

The study site was selected near the town of Sodankylä in northern Finland. The centre coordinates of the study site were 67°18' N, 26°40' E. The site represents a typical sub-Arctic boreal forest zone. Dense and sparse forests cover majority of the area, with some considerable areas of peat land and open bogs also present. The test site area includes river Kitinen in the central part and lake Orajärvi in the eastern part.

SAR data used in the study is represented by time series of 12 fully polarimetric Radarsat-2 images covering the study area were acquired during February-September 2009, using 2 incidence angles. The corresponding incidence angles were 24.6 and 38.4 degrees. The radar images were pre-processed, ortho-rectified and radiometrically corrected using in-house software.

The Finnish national part of CLC 2000 land cover/use data was used in monitoring of polarimetric feature dynamics over different land cover classes. The original land cover data included 44 classes [1]. However, only 21 of these could be found on the test site itself. The resolution of the land cover data was 25 m, as well as that of the orthorectified PolSAR data. During preliminary analysis land cover/use classes were merged to 6 land cover/use super-classes, namely urban areas, sparse forest, dense forest, agriculture and field, peat-land and open bogs, and water surfaces. For detailed analysis of change of polarimetric signatures only 12 most spatially significant land cover/use classes were used, altogether representing 96 % of the total area of the study site.

One of the most important challenges for optimal use of Earth Observation data is the development of suitable and effective multi-temporal data analysis methods [2]. Issues include irregular temporal sampling, seasonal effects and imperfect registration. On the other hand, the seasonal changes occurring in the area of interest serve as a basis for expanding the spectral feature space and improving classification performance compared to a single PolSAR image acquisition. For the classification, several multi-temporal metrics and the minimum amount of SAR data acquired during one year have been analyzed to derive several basic land cover classes. High resolution aerial imagery was used for improved selection of training data and accuracy assessment of subsequent classification.

References

- [1] Härmä P., R. Teiniranta, M. Törmä, R. Repo, E. Järvenpää, and M. Kallio. 2004. "Production of CORINE2000 land cover data using calibrated LANDSAT 7 ETM satellite image mosaics and digital maps in Finland," In *Proc. International Geoscience and Remote Sensing Symposium*, vol. 4, 2703–2706, 20-24 Sep. 2004.
- [2] L. Bruzzone, P.C. Smits, and J.C. Tilton, "Foreword special issue on analysis of multitemporal remote sensing images," *IEEE Trans. Geosci. Remote Sensing*, vol. 41, no. 11, pp. 2419–2422, Nov. 2003.

Temporal variability of X-band extinction coefficient in boreal forest

Jaana Praks⁽¹⁾

Oleg Antropov⁽²⁾

Martti Hallikainen⁽¹⁾

⁽¹⁾ Department of Radio Science and Engineering,
School of Electrical Engineering, Aalto University,
P.O. Box 13000, FI-00076 AALTO, Finland
jaana.praks@aalto.fi

⁽²⁾ VTT Technical Research Centre of Finland,
P.O.Box 1000, FI-02044 VTT, Finland

Polarimetric SAR interferometry is a promising technique for forest parameter retrieval, such as forest height and forest extinction coefficient. These parameters can be further used for forest above ground biomass estimation. Naturally, emphasis is on the use of longer wavelengths, such as P-band, e.g. recently accepted BIOMASS mission of European Space Agency. However, shorter wavelengths can provide relevant information, especially in low biomass forests. Forest parameter retrieval accuracy is particularly high when additional information about the ground location is available. This was demonstrated in our previous work where airborne E-SAR interferometric images and accurate LIDAR-measured ground elevation model were used to estimate forest tree height and extinction at X-band [1]. The method was later applied also to spaceborne TanDEM-X data [2].

The key issue of forest tree height estimation under different seasonal conditions appears to be variability in forest extinction coefficient, as it influences the correction that should be made to estimated interferometric phase centre height due to penetration of radiowaves into forest canopy. In this work, we concentrate to study the extinction coefficient variability in boreal forest.

The set of TanDEM-X SAR satellite image pairs, acquired during summer and autumn 2011 over southern Finland, was combined with accurate laser measurements of terrain and canopy height in this study. Random Volume over Ground model was used as a theoretical framework to calculate estimates for forest extinction coefficient and also estimates for ground reflection contribution. Also the tree height retrieval performance was evaluated. The test site of this study is located in southern Finland close to Kirkkonummi near the Helsinki region. The interferometric image dataset gathered for the study consists of 10 TanDEM-X CoSSC scenes, with acquisition conditions covering period from fully leaved forest in summer to totally leafless deciduous forest in late autumn. Digital elevation model derived from airborne laser scanning by Finnish National Land Survey in 2008 was used as a reference data in the study.

According to our results, the spaceborne TanDEM-X CoSSC data are suitable for forest height retrieval, but as expected, the accuracy of the method is lower than in the case of airborne measurements. Our results show, that the variability in extinction is significant and depends on forest type. However, when the variability is taken into account, it is feasible to estimate tree height also from X-band single-polarization interferometric images, when accurate ground model is provided.

References

- [1] J. Praks, M. Hallikainen, O. Antropov, *LIDAR aided SAR Interferometry studies in boreal forest: scattering phase center and extinction coefficient at X- and L-band*, IEEE Trans. Geosci. Remote Sens., vol. 50, no. 10 pp. 3831-3843, February 2012.
- [2] J. Praks, M. Hallikainen, O. Antropov, D. Molina-Hurtado, *Boreal Forest Tree Height Estimation from Interferometric Tandem-X Images*, IEEE International Geoscience and Remote Sensing Symposium (IGARSS 2012), 20-27 July 2012, Munich, Germany, 2012.

Multiple Scattering Effects in Radar Signatures from an Isolated Tree

Qianyi Zhao Roger H. Lang

Department of Electrical and Computer Engineering
The George Washington University, Washington, DC, 20052
e-mail: zhao@gwu.edu, lang@gwu.edu

Radar signatures from a 5 meter high Caucasian fir tree are simulated with the aim of determining the importance of multiple scattering at 2 GHz. The fir tree has been the subject of a microwave tree scattering experiment [1] performed in June, 1996 in the anechoic chamber of the Joint Research Centre (JRC), Ispra, Italy. The radar signature of the tree in the backscattering direction has been measured in the chamber. In addition to the radar measurements, a coaxial probe reflection technique has been used to measure the dielectric constant of the tree components. The location and the size of representative portions of the tree architecture have been recorded and a vectorization technique has been employed to reconstruct the complete tree from the sampled the data.

The geometry and dielectric data for this fir tree has been used to construct an accurate model of the tree. Preliminary results from the electromagnetic tree model simulations [2] have demonstrated that double (second order multiple) scattering from branches provided 2-4 dB enhancement to the backscattering cross sections above the single scattering results. The trunk-branch interaction, however, was not considered due to computational constraints. In this work, the effects of the multiple scattering between the trunk and branches are considered. The inclusion of the fir tree trunk makes the tree simulations more realistic. We also extend our previous work to bistatic scattering to further observe the multiple scattering interactions in bistatic radar signatures.

To calculate the bistatic scattering cross sections of the tree, the Fresnel Double Scattering method [3] is employed with the effective medium theory. A numerical technique, the Discrete Dipole Approximation, is applied to find the internal electric fields in the tree trunk or branches. The characteristic parameters of the chamber and the antennas are also considered in the simulations to mimic the actual microwave tree experiment environment at the JRC. The existence and importance of the multiple scattering occurring in the L-band tree radar signatures are illustrated for both monostatic and bistatic radar configurations in this study. The tree simulations are compared to experimental results in the backscatter case.

References

- [1] R.H. Lang, R. Landry, A. Franchois, G. Nesti, and A. Sieber, "Microwave tree scattering experiment: comparison of theory and experiment," In *Proc. Int. Geosci. Remote Sens. Symp.*, vol. 5, pp. 2384-2386., 1998.
- [2] Q. Zhan and R.H. Lang, "Scattering from a fir tree: experiment and simulations," *the 13th URSI Commission F Triennial Open Symposium on Radiowave Propagation and Remote Sensing*, Ottawa, Canada, May 2013.
- [3] Q. Zhao and R.H. Lang, "Fresnel Double Scattering From Tree Branches," *IEEE Trans. Geosci. Remote Sens.*, vol. 50, no. 10, pp.3640-3647, Oct. 2012

Poster Session II

Advanced Radar Applications for Nano- and Microsatellites

Maarten van den Oever², Jaakko Jussila¹, Antti Kestila¹, Pekka Laurila¹, Rafal Modrzewski¹,

¹Department of Radio Science and Technology, Aalto University, Finland
name.surname@iceye.org

With the introduction of nanosatellites the price of space missions has drastically decreased. The lower price of nanosatellites makes it possible to set up missions that previously were not considered economically viable or not interesting enough for a separate mission.

Remote sensing missions with nanosatellites are interesting due to their low costs. However, the platform constraints pose some limitations. The small size of the nanosatellites limits the available area for the solar panels. As a result, significantly less power is available compared to conventional satellites. The small size also limits the available antenna area which is essential for radar based remote sensing. Despite these disadvantages, a radar based solution is still an interesting option due to its all-weather capabilities. In this paper feasibility of such a solution is investigated. The satellite under consideration is equipped with an X-band Synthetic Aperture Radar (SAR).

The relatively low costs of a nanosatellite system allow shorter missions to be carried out compared to regular radar satellite missions. A shorter mission makes it possible to fly lower orbits and perform drag compensation during the mission to control the orbit. Once the mission is completed the satellite burns in the Earth's atmosphere. This design strategy allows the utilisation of commercial off-the-shelf components without space qualification.

The low orbit of such a strategy has a positive impact on the power budget. Despite the low orbit the amount of required power for such a radar system is still large compared to the area of solar panels that is available. One possible solution to overcome this problem lies in the utilization of a low duty cycle.

The small size of the satellite also limits the available area for an antenna. In the conventional SAR system the length of an antenna is in direct relation with the minimum pulse repetition frequency. To avoid azimuth ambiguities the pulse repetition frequency needs to be very high for short antennas. A high pulse repetition frequency introduces another problem: it decreases the unambiguous range. A low unambiguous range causes ambiguous projections from the illuminated area to appear in the final image, thereby the usable image swath to be very narrow.

Despite the presented platform limitations the proposed system should be possible to be realized and would create possibilities for significant cost reduction. A detailed investigation is therefore desired.

Passive microwave emissivity validation and characteristic analysis

Lijuan Shi ^(1,2), Yubao Qiu ⁽¹⁾

⁽¹⁾Institute of Remote Sensing and Digital Earth, Chinese Academy of Sciences, Beijing, China
ybqiu@ceode.ac.cn; lijuan0816@gmail.com

⁽²⁾School of Geomatics, Liaoning Technical University, Fuxin, China

Surface microwave emissivity is an important parameter to describe the ground microwave radiation characteristics, and is a basis of inversion geophysical parameters with microwave remote sensing data. In this study, the half-month averaged emissivity[1-2] over different land covers were estimated using Advanced Microwave Scanning Radiometer–Earth Observing System (AMSR-E) combined with IGBP (International Geosphere-Biosphere Project labels) classification data under clear sky condition. The microwave emissivity has been compared with the estimated soil moisture and microwave vegetation indices[3] from AMSR-E, and NDVI[4] from MODIS, which aims to understand the intrinsic relationship among satellite products. The results show a high correlation between the AMSR-E microwave emissivity and other satellite products, which can validate the microwave emissivity dataset simply.

Then we analyze emissivity seasonal variation and emissivity characteristics at different frequencies, polarization over different vegetation types and desert. The results show that the emissivity of vegetation increases along with the growing frequency, and declines with the growing of frequency in the snow region. In summer, vegetation emissivity at V polarization of 89GHz is larger than 0.944. The vegetation emissivity is relatively stable and the polarization difference is low (<0.081) in summer. In the same area, for vegetation, the RMSE of emissivity summer time series is less than 0.0072. In winter, vegetation emissivity decreases in snow covered area, especially for higher frequencies. Furthermore, with vegetation density increase, the emissivity increases and emissivity polarization difference decreases. In desert area, emissivity polarization difference decrease as the frequency increases, and the polarization difference is large (0.03-0.127). The H polarization emissivity increases with increasing frequency, but the V-polarized microwave emissivity is reduced with increasing frequency because of the body scattering. The results also indicate that NDVI derived the good negative correlation with microwave emissivity polarization difference at 37GHz.

References

- [1] Yubao Qiu, Jiancheng Shi, Hallikainen M.T., Lemmetyinen J., “The AMSR-E instantaneous emissivity estimation and its correlation, frequency dependency analysis over different land cover,” *IEEE Transactions on Geoscience and Remote Sensing Symposium*, vol.2, pp.749 -752, 2008.
- [2] Shi Lijuan, Qiu Yubao, Shi Jiancheng, “Study of the Microwave Emissivity Characteristics of Vegetation over the North Hemisphere,” *Spectroscopy and Spectral Analysis*, vol.30(5), pp.31157-1162,2013.
- [3] Jiancheng Shi, T. Jackson, J. Tao, J. Du, R. Bindlish, L. Lu, K.S. Chen, “Microwave vegetation indices for short vegetation covers from satellite passive microwave sensor AMSR-E,” *Remote Sensing of Environment*, vol.112, pp.4285–4300, 2008.
- [4] Alfredo Huete, Chris Justice, Wim van Leeuwen, MODIS Vegetation Index(MOD13) Algorithm Theoretical Basis Document, April 30,1999.

Comparison of microwave radiometer observations and grain size of snow

Leena Leppänen⁽¹⁾ Anna Kontu⁽¹⁾ Juha Lemmetyinen⁽¹⁾ Jouni Pulliainen⁽¹⁾

⁽¹⁾Finnish Meteorological Institute, Arctic Research, Tähteläntie 62, 99600 Sodankylä, Finland, leena.leppanen@fmi.fi

Remote sensing observations of snow are important e.g. in monitoring climate change and hazard predictions. Extinction in snow is affected by structure of snow and generally it is described with parameter grain size in models. Among others HUT (Helsinki University of Technology) snow emission model [1,2] is sensitive to grain size and thus comparison of different grain size measurement methods is important. In this paper traditional visual grain size and optical grain size is compared to HUT snow emission model inversions of grain size from microwave radiometer observations.

Continuous microwave measurements from *in situ* measurement area are made with a tower-based microwave radiometer manufactured by Radiometer Physics GmbH, Germany. The radiometer is dual polarized and has frequency channels 10.65, 18.7, 21.0 and 36.5 GHz. Grain size is inverted with HUT snow emission model from brightness temperatures. Weekly *in situ* snowpit measurements contain visual grain size estimations, SSA (Specific Surface Area) measurements and reference measurements (e.g. temperature and density profiles). Visual grain size was estimated from macro-photographs of snow grains against 1-mm reference grid. Typical largest extent of snow grains in a layer was estimated with accuracy of 0.25 mm. Optical grain size was derived from SSA measurements made with IceCube-instrument which is a single frequency version of DUFISSS [3] instrument. Layer thickness -weighted grain size is calculated from the multilayer measurements. Experimental data were measured in Finnish Meteorological Institute, Arctic Research Centre in Sodankylä, Finland. Results of this paper are based on measurements from two winters 2011-2013.

Results show that the magnitude of visual grain size values is approximately 2.5 times the magnitude of optical grain size values. Visual grain size should have better agreement with inverted grain size from HUT snow model than optical grain size, because HUT snow model was developed by using visual grain size observations. Preliminary HUT snow emission model simulation results from visual grain size measurements fits well with brightness temperature observations.

References

- [1] J. Pulliainen, J. Grandell, and M. Hallikainen, "HUT snow emission model and its applicability to snow water equivalent retrieval," *IEEE Trans. Geosci. Remote Sens.*, vol.37(3), pp. 1378-1390, 1999.
- [2] J. Lemmetyinen, J. Pulliainen, A. Rees, A. Kontu, Y. Qiu, and C. Derksen, "Multiple layer adaptation of HUT snow emission model: comparison with experimental data," *IEEE Trans. Geosci. Remote Sens.*, vol.48(7), pp. 2781-2794, 2010.
- [3] J.-C. Gallet, F. Domine, C. Zender, and G. Picard, "Measurement of the specific surface area of snow using infrared reflectance in an integrating sphere at 1310 and 1550 nm," *The Cryosphere*, vol.3, pp. 167-182, 2009.

Correction of Ionospheric Effects on SAR Interferometry using an Combined TEC Estimator

Jun Su Kim ⁽¹⁾ Konstantinos Papathanassiou ⁽¹⁾

⁽¹⁾ Microwave and Radar Institute, German Aerospace Center (DLR), junsu.kim@dlr.de

Owing to the deep penetration into vegetation and low temporal decorrelation, the low-frequency spaceborne SAR observations are suited for global forest mapping and InSAR applications over natural terrains. For these reason, missions including JAXA's ALOS-II, NASA's DESDynI, DLR's Tandem-L (heretofore L-band) and ESA's Biomass (P-band) have been scheduled to be launched in the next years or proposed. These low-frequency missions products, however, requires compensation of the disturbing effects induced by the ionosphere. In the ionosphere the group velocity of the transmitting/receiving pulses delays, their phase(s) advances, and polarization state rotates. On the processed SAR images, shifts and blurring of focusing are introduced due to the inhomogeneity of the ionosphere. They distort intensity, as well as polarimetric, interferometric and polarimetric interferometric observation spaces.

In SAR applications, the ionosphere can be characterized using the total electron content (TEC), which is the integrated electron number density per unit volume along the direction of propagation. Most of the free electrons are distributed within a narrow altitude range allowing the application of thin-layer model at a fixed altitude. The ionosphere is a 2-D scalar field of TEC [1], [2].

We propose a concept integrating the detections of the ionospheric disturbing effects. In accordance, a novel generic correction schema enabling the use of the combined (and improved) estimates of the 2-D TEC field (or the associated differential TEC field in the interferometric case) is also proposed and assesses by means of the interferometric coherence [3].

As a special case, a combined 2-D differential TEC field estimator based on the differential Faraday rotation measurements and the relative azimuth shifts is presented. A linear inverse problem relating both independent observations to the differential TEC estimation is established. Geophysical knowledge, e.g. the anisotropic nature of the TEC distribution, has been incorporated as a priori information in the "combined" (differential) TEC estimator. In addition the method to estimate the ionospheric altitude from SAR data is also presented.

The performance of the proposed approach is tested using ALOS quad-pol interferometric data sets over Alaska. The achieved estimates are characterized by an improved performance: While the Faraday rotation-based estimator suffers from the random deviation pattern of TEC after conversion, the proposed combined estimator is effectively free of such artifacts.

References

- [1] F. Meyer and J. Nicoll, "Prediction, detection, and correction of Faraday rotation in full-polarimetric L-band SAR data", *IEEE Trans. Geoscience and Remote Sensing*, vol. 46, no. 10, October 2008.
- [2] X. Pi, A. Freeman, B. Champman, P. Rosen, and Z. Li, "Imaging ionospheric inhomogeneities using spaceborne synthetic aperture radar", *Journal of Geophysical Research*, vol. 116, A04303, 2001.
- [3] J. S. Kim, K. Papathanassiou, S. Quegan, and N. Rogers, "Estimation and correction of scintillation effects on spaceborne P-band SAR images", *Proc. of IGARSS 2012*, pp. 5101-5104, 23-27. July 2012.

Precursors of Convective Activity Using Ground Based Microwave Radiometer

Saurabh Das⁽¹⁾ and Animesh Maitra⁽²⁾

Institute of Radio Physics and Electronics, University of Calcutta

92 A. P. C. Road, Kolkata-700009, India

Email: ⁽¹⁾das.saurabh01@gmail.com; ⁽²⁾animesh.maitra@gmail.com

High convective activity in tropical region is mostly responsible for thunderstorm clouds and precipitation. It is one of the major natural threats to aviation industry as well as economy. Nowcasting of such atmospheric phenomena is one of the important applications of microwave remote sensing using both ground based and space based instrument. At Kolkata, a tropical location in India, several thunderstorms occurs every year which cause severe devastation of property and human life. In this study, we use a multi-frequency microwave radiometer, RPG-HATPRO, operating at this location to identify the possible signature of these convective activities.

We observe that the brightness temperature of water vapor line increases rapidly before the heavy rain. However, an increase in brightness temperature is only indicative of the increase in water vapor, which is not always associated with the convective rain [1]. Since the convective activity is generated from the planetary boundary layer, a look into the stability of this layer is very important. Boundary layer wind profile is important for that purpose. We attempted to generate the stability profile of boundary layer using the brightness temperatures of these microwave frequencies of the radiometer. The microwave signature of the boundary layer scan indicates sharp change before heavy rain. The brightness temperature of ~58 GHz frequency is found to be most effective in identification of the turbulence in the boundary layer. The result indicates that the microwave radiometer can be useful to identify the convective activity without wind profiler. Further, the methodology can be used in monitoring the convective activity in larger scale using satellite based radiometry.

[1] M. Akkiseti, M Rajeevan, M Venkat Ratnam, J. N. Bhate, C.V. Naidu, "Nowcasting severe convective activity over South-east India using ground-based microwave radiometer observations", *J. Geophys. Res.*, doi:10.1029/2012JD018174, in press., 2012

Thermal structure of the boundary layer under strongly stable stratification

Irina Repina⁽¹⁾, Mikhail Varentsov⁽²⁾, Evgeny N. Kadyrov⁽³⁾, Evgeny Al. Miller⁽³⁾

⁽¹⁾ A. M. Obukhov Institute of Atmosphere Physics, Air-Sea Interaction Lab., repina@ifaran.ru

⁽²⁾ Department of Meteorology and Climatology, Faculty of Geography,
Lomonosov Moscow State University

⁽³⁾ Central Aerological Observatory, Microwave Remote Sensing Lab., 3 Pervomayskaya str.,
Dolgoprudny, Moscow region, 141700 Russia

This work covers the results of observations at White Sea Biological Station of Lomonosov Moscow State University in the end of January – beginning of February 2012. The station is located at the shore in the northern part of White Sea at the Arctic Circle. The weather during observations was formed by anticyclone; air temperature was extremely low and reached -35°C . Our observations included measurements of the vertical structure and turbulent regime of the boundary layer. The measuring complex, including acoustic anemometer, temperature profiler MTP-5 and automatic weather station (AWS), was set up at the station at the sea-level, and another one AWS was set up at the top of the closely-located hill with the height of 100 m. Obtained data allowed us to investigate of the diurnal variation of the air temperature at different heights, detect the inversions and analyze their features and genesis. For more confidence comparison between remote measurements by temperature profiler and contact measurements by two AWS was made, it shown high correspondence with correlation coefficient of 0.96. The dependencies between vertical temperature gradients and characteristics of the surface layer were also investigated.

Analysis of the vertical temperature profiles showed the existence of permanent and powerful inversion during the period of observations. The difference between the surface and zero-gradient level reached the value of 21.3°C , which is close to powerful Antarctic inversions [1]. Temporal variation of the vertical temperature gradients for the period from 30th of January to 2nd of February is shown in Fig. 1. The maximum value of $8^{\circ}\text{C}/100\text{ m}$ was observed in the layer 50-100 m. In the lowest layer 0 - 50 m nocturnal destruction of the inversion under the influence of surface was observed. Synoptic analysis showed that inversion was formed by radiation cooling, advection of the cold air from Siberia in lower troposphere and advection of warmer air from Atlantic in middle troposphere. Such inversions are unusual for European part of Russia, and this work is the first attempt of their detailed investigation by temperature profiler.

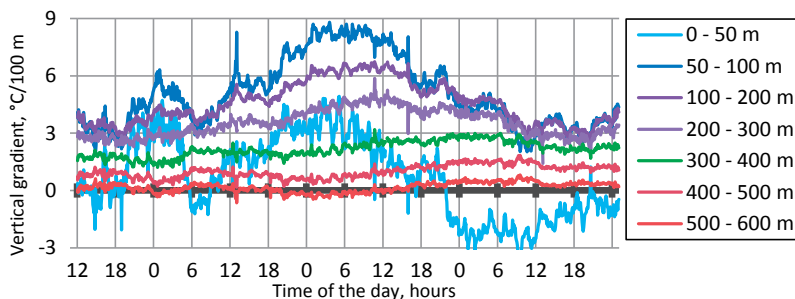


Fig. 1. Variation of the vertical temperature gradient dT/dz during the observations

References

- [1] S. Argentini, I. Pietroni, G. Mastrantonio, A. Viola and S. Zilitinchevich, *Characteristics of the Night and Day Time Atmospheric Boundary Layer at Dome C, Antarctica*. EAS Publications Series, 25, pp 49-55, 2007.

Including the Zeeman effect in retrievals of stratospheric temperature profiles from a ground-based microwave radiometer

C. Straub ⁽¹⁾, O. Stähli ⁽¹⁾, F. Navas-Guzman ⁽¹⁾, N. Kämpfer ⁽¹⁾,
R. Larsson ⁽²⁾, S.A. Buehler ⁽²⁾, P. Eriksson ⁽³⁾

⁽¹⁾ Institute for Applied Physics, University of Bern, Switzerland, corinne.straub@iap.unibe.ch

⁽²⁾ Department of Computer Science, Electrical and Space Engineering, LTU, Kiruna, Sweden

⁽³⁾ Department of Earth and Space Sciences, Chalmers University of Technology, Gothenburg, Sweden

The cooling of the stratosphere is an indicator for climate change as it provides evidence of natural and anthropogenic climate forcing just like surface warming ([1] and references therein). However, our understanding of the observed stratospheric temperature trend and our ability to test simulations of the stratospheric response to emissions of greenhouse gases and ozone depleting substances remains limited. Stratospheric long term data sets are sparse and obtained trends differ from one another [1]. Therefore it is important that in the future such datasets are generated.

Ground-based microwave radiometers are able to provide long term measurements at stratospheric altitudes as these passive instruments are characterized by long operational lifetimes. Thus, long term global datasets can be generated, which are crucial for climate research.

TEMPERA is a newly developed ground-based microwave radiometer designed, built and operated at the University of Bern. The instrument and the retrieval of temperature profiles has been described in detail in [2]. TEMPERA is measuring two pressure broadened oxygen lines at 52.5 GHz and 53.1 GHz, respectively in order to determine stratospheric temperature profiles. The retrieved profiles of TEMPERA cover an altitude range of approximately 20 to 45 km with a vertical resolution in the order of 15 km. The lower limit is given by the instrumental baseline and the bandwidth of the measured spectrum. The upper limit is given by the fact that above 50 km the oxygen lines are split by the Zeeman effect in the terrestrial magnetic field.

This presentation investigates the potential to extend the upper limit of temperature profiles from ground-based microwave radiometers beyond 50 km by including the Zeeman effect in the forward model of the retrieval. The inversions of the O₂ spectra to retrieve temperature profiles are performed using the optimal estimation method implemented in the Qpack software package. The forward model is provided by the Atmospheric Radiative Transfer Simulator (ARTS) [3]. For the retrievals presented here we use v2.1 of ARTS which treats the Zeeman effect as described in [4].

References

- [1] D. Thompson, D. Seidel, W. Randel, C.-Z. Zou, A. Butler, C. Mears, A. Osso, C. Long, and R. Lin, “The mystery of recent stratospheric temperature trends,” *Nature*, vol. 491, pp. 692–697, 2012.
- [2] O. Stähli, A. Murk, N. Kämpfer, C. Mätzler, and P. Eriksson, “Microwave radiometer to retrieve temperature profiles from the surface to the stratopause,” pp. 2857–2905, 2013.
- [3] P. Eriksson, S. Buehler, C. Davis, C. Emde, and O. Lemke, “ARTS, the atmospheric radiative transfer simulator, version 2,” *Journal of Quantitative Spectroscopy and Radiative Transfer*, vol. 112, no. 10, pp. 1551–1558, 2011.
- [4] R. Larsson, S. Buehler, P. Eriksson, and J. Mendrok, “A treatment of the Zeeman effect using Stokes formalism and its implementation in the Atmospheric Radiative Transfer Simulator ARTS.”

Remote Sensing of Precipitation

Dual-polarized Microwave Signatures of Precipitation from Earth and Space Between 3 GHz to 95 GHz

V. Chandrasekar^(1,2), D. Moisseev⁽²⁾, L. Baldini⁽³⁾, N. Bharadwaj⁽⁴⁾, F. Junyeant⁽¹⁾, M. Le⁽¹⁾,
H. Chen⁽¹⁾, R. Bechini⁽¹⁾, M. Vega⁽⁵⁾

⁽¹⁾ Colorado State University, 1373, campus Delivery, Fort Collins, CO 80523-1373,
Chandra@engr.colostate.edu

⁽²⁾ University of Helsinki, Helsinki, Finland

⁽³⁾ Institute of Atmospheric Sciences and Climate, Rome, Italy

⁽⁴⁾ ARM Climate Research Facility, Pacific Northwest National Laboratory

⁽⁵⁾ NASA Goddard Space Flight Center

Backscatter and propagation signatures due to hydrometeors along the propagation path, either in earth space propagation links, or radar to target volumes has been studied for a long time specially since the beginnings of radar. However the interest in these propagation properties have seen renewed interest, especially due to innovative use of dual-polarized propagation properties. Since the advent of dual-polarization radars, the dual-polarization propagation properties have become very important. In addition, the innovative uses of dual-polarization propagation properties to mitigate attenuation effects have led to the building of weather radars at attenuating frequencies such as X band. The specific attenuation in precipitation is basically the manifestation of the extinction cross section of the precipitation particles in the path weighted by the size distribution. The specific differential phase between the two linear polarization states is the difference in forward scatter amplitudes, weighted by the size distribution. The attenuation due to rain can be corrected for by measuring the differential propagation phase. In addition the differential propagation properties are weighted closer to the volume of precipitation particles than the backscatter effects such as reflectivity. Therefore the propagation phase measurements are better suited for remote sensing applications.

Thus the dual polarized signatures precipitation have become active area of research. Many radars are being built to remotely sense precipitation from the lower S band frequencies such as 3 GHz, to the mm wave range such as 35 GHz. Though it is useful to observe differential propagation phase, it is a challenging measurement. The differential propagation phase is a path integrated quantity and any observation of the characteristics at a small range is estimated as range derivatives that makes it noisy.

This paper presents challenges and advantages of dual-polarization propagation measurements through precipitation from 3 to 95 GHz. Observations made at several frequency bands in between such as S, C, X, Ku and Ka will be presented. The impact of attenuation on the choice of polarization state will also be discussed. Subsequently differential propagation properties of multi-frequency systems will be shown for potential use in space borne observations of precipitation

Dual-polarization Radar Observations of Hail

L. Nevvonen⁽¹⁾, D. Moiseev⁽²⁾, V. Chandrasekar^(1,2,3), H. Pohjola⁽⁴⁾

⁽¹⁾Finnish Meteorological Institute, PO BOX 503, 00101 Helsinki, Finland, ljubov.nevvonen@fmi.fi

⁽²⁾University of Helsinki, P.O. BOX 64 00014 Helsinki, Finland, dimitri.moiseev@helsinki.fi

⁽³⁾Colorado State University, 1062 Campus Delivery Fort Collins CO 80523-1062, U.S.A,
Chandra@engr.colostate.edu

⁽⁴⁾Vaisala Oyj, Vanha Nurmijärventie 21, 01670, Vantaa, Finland, heikki.pohjola@vaisala.com

Applications of dual-polarization radar measurements include rainfall measurement, hail detection, and identification of hydrometeor types. Compared to the previous conventional radar generation, dual-polarization radars can provide much more detailed information especially with respect to hydrometeor characteristic: size, shape, orientation, and dielectric strength (phase and density).

Hail is a form of precipitation that occurs when updrafts in thunderstorms carry raindrops upward into extremely cold areas of the atmosphere where they freeze into ice. Hail falls when the thunderstorm's updraft can no longer support the weight of the ice or the updraft weakens. Even relatively small hail can shred plants to ribbons in a matter of minutes. Vehicles, buildings roofs, houses, and vegetation are the other targets most commonly damaged by hail. Hail has been known to cause injury to humans, and occasionally has been fatal.

Validation of hail detection is a challenging task. Studies employing radar at S-band frequencies have typically found that hail is characterized by high reflectivity ($Z > 50$ dBZ) and near zero differential reflectivity ($-1 < Zdr < 1$ dB) at and just above the ground (Bringi et al. 1984, Illingworth et al. 1986, Bringi et al. 1986, Aydin et al. 1990, Herzegh and Jameson 1992, Hubbert et al. 1998). Values of RhoHV for hail at S-band (Balakrishnan and Zrnica 1990) and C-band (Tabary et al. 2010) have been found to be below 0.95. Radar hail signatures in C-band weather radars are ambiguous. In several studies (Vivekanandan et al., 1990), it was reported that Zdr values of rain-hail mixtures could be higher than 5 dB. This result is contrasting with S-band radar observations where differential reflectivity values close to 0 dB are expected.

Many studies have demonstrated that dual-polarization weather radars are effective tool for hail detection. In this topic will be conducted studies for the classification of hydrometeors based on such polarimetric variables as Differential Reflectivity (Zdr) and Correlation Coefficient (RhoHV). Zdr is a measure of the decibel (dB) reflectivity difference between horizontal (Zh) and vertical (Zv) polarizations (Bringi and Chandrasekar 2001 p. 381). Therefore, Zdr is helpful in estimating the oblateness of a hydrometeor. The more oblate the particle the larger Zdr is. RhoHV Correlation coefficient measures the consistency of the H and V returned power and phase for each pulse. This “cross correlation” looks at how the power and phase of one channel compares to the other channel. If the consistency is high, changes with one channel are similar to changes with the other.

Unfortunately, due to a high spatial and temporal variability of hailstorms, it is very difficult to provide sufficient ground-truth observations to validate these measurements. Furthermore, for the same reason, performance of current hydrometeor classification algorithms is very rarely quantified in terms of such metrics as for example probability of hail detection. In this study we will use a unique dataset collected in the framework of the Helsinki Testbed to address the above-mentioned problems.

For this study, observations of hail storms by University of Helsinki C-band weather radar Kumpula will be compared to the WXT 510 weather transmitter measurements, Probability-Of-Hail (POH) and against reports published in Flickr, YouTube and others social media reports. Those observations were typically taken during late spring several cases are from October and

December. Retrieved hail climatology is similar to one reported by Saltikoff et al. (2010), with an exception of the most active month. Saltikoff et al. reports July as the most active month. Most hailstones are observed in the afternoon, 14:00–16:00 local time. The hail “season” extends from May to early September with maximum occurrences in June, July and August. This means that hail is most frequently observed when the convective energy available for storm growth is at its diurnal or seasonal peak.

The Helsinki Testbed was established in 2005 jointly by the Finnish Meteorological Institute (FMI) and Vaisala. The Testbed instrumental setup includes more than 60 Vaisala WXT 510 weather transmitters (ground and tower based) and 12 FMI AWS stations were installed in the Helsinki Metropolitan area.

The comparison of radar observation, the WXT hail reports and the Probability-Of- Hail show a good agreement between those observations. For the observed high intensity hail cases in about 50 % of the time radar hydrometeor classification was reporting graupel. In those cases Z_h varied between 40 and 64 dBZ, Z_{dr} varied between 3 and 4.5 dB, Rho_{HV} varied between 0.94 - 0.98, KDP 4-5 deg /km in one case -5 deg/km. . On the other hand, radars often do not show any hail signatures. This study shows that hail at C-band is typically characterized by high $Z > 50$ dBZ, high Z_{dr} and low Rho_{HV} .

Linking Snowflake Microphysics and Radar Scattering Models

J. Leinonen⁽¹⁾ D. Moisseev⁽²⁾ T. Nousiainen⁽³⁾

⁽¹⁾ Finnish Meteorological Institute, P.O.Box 503, 00101 Helsinki, jussi.leinonen@fmi.fi

⁽²⁾ University of Helsinki, dmitri.moisseev@helsinki.fi

⁽³⁾ University of Helsinki, timo.nousiainen@helsinki.fi

Millimeter-wavelength precipitation radars are commonly used for cloud observations. Recently, they have been increasingly applied also for observations of falling snow, either as standalone instruments or as part of a multi-frequency radar configuration. These radars have a low detection threshold, and attenuation is weaker in snowfall than it is in rain, alleviating the usual problem with using short-wavelength radar to observe precipitation. However, quantitative retrieval of snowfall rate from the observations is difficult because of the variety of density, shape and structure exhibited by snowflakes. Evidence from previous studies suggests that homogeneous spheroidal particle models, which are commonly used to model backscattering from precipitation particles, cannot always consistently capture the backscattering properties of snowflakes for multiple wavelengths.

The Rayleigh-Gans scattering approximation (RGA) has been shown to be quite accurate for modeling microwave scattering from aggregate snowflakes. Although RGA is an approximation where some error is inevitable, it has the advantage of being mathematically simple, and thus it allows one to examine the scattering properties analytically. We found that the ice in aggregate snowflakes is, on average, distributed around the center of mass according to the normal distribution. However, at large particle sizes, using the normal distribution as a model of the "average particle" gives backscattering cross sections that are drastically different from those directly computed using the RGA or the discrete dipole approximation (DDA) for model aggregate snowflakes. Similar behavior is seen with spheroids. The RGA and DDA, on the other hand, are in relatively good mutual agreement. This suggests that the reason for the failure of spheroids as models of large particles is mainly due to the internal inhomogeneities of the snowflakes rather than the internal electromagnetic interactions that are modeled by the DDA but ignored by the RGA.

To investigate this problem, we used a simple conceptual model of an aggregate snowflake consisting of a finite number of constituent particles to derive an analytical expression for the average backscattering cross section given by the RGA. This expression can explain the behavior of the backscattering cross section up to particle sizes of at least 10 times the radar wavelength. The difference between this description and average-particle models (e.g. spheroids) is seen to result from second-order statistical effects that are caused by the presence of discrete crystals within the aggregate. The average-particle model emerges from the new model as a low-frequency approximation, explaining why spheroids are useful as models of scatterers that are sufficiently small compared to the wavelength, but fail at larger sizes.

Comparison of the melting layer model characteristics with GPM ground validation campaign data

von Lerber A.⁽¹⁾, D.Moisseev⁽²⁾, A. Heymsfield⁽³⁾, A. Bansemer⁽³⁾, A.-M. Harri⁽¹⁾, M.T. Hallikainen⁽⁴⁾

⁽¹⁾ Finnish Meteorological Institute, Earth Observation, P.O.Box 503, 00101 Helsinki, Finland.
email: annakaisa.von.lerber@fmi.fi, ari-matti.harri@fmi.fi

⁽²⁾ University of Helsinki, dmitri.moisseev@helsinki.fi

⁽³⁾ National Center for Atmospheric Research, heyms1@ucar.edu, bansemer@ucar.edu

⁽⁴⁾ Aalto University, martti.hallikainen@aalto.fi

Two international co-operation ground validation campaigns were recently organized to study and improve the satellite precipitation estimates in detecting light rain and snowfall: 2010 Light Precipitation Validation Experiment (LPVEx) in Finland [1] and 2012 GPM Cold-season Precipitation Experiment (GCPEX) in Canada [2]. The field projects are connected to the launch of the core observatory satellite of the Global Precipitation Mission scheduled for 2014 [3]. During the campaigns data sets of microphysical parameters and observations with W-band cloud radar were gathered with the airborne instrumentation relative to ground-based radar data. The aircraft flew spiral ascents/descents in the melting layer providing data of particle size distribution, area ratio, the 2D-shadow images of the particles, humidity and temperature profile above, inside and under the melting layer. These quantities reveal the stages of melting as a function of height and, together with the melting layer model, the computed reflectivity factor and the reflectivity-weighted fall velocity as a function of melted mass fraction can be compared with the measured values.

Several melting layer models have been developed with different assumptions and approximations of the modeled parameters such as e.g. snow fall velocity, snow density, and their dependence of melted mass fraction [4-6]. In this study we have examined the different solutions with respect to measured values and characterized their influence. We show e.g. that the sub-saturated conditions do have a significant effect on the onset of melting and, therefore, on the width and the location of the maximum reflectivity factor of the melting layer. Hence this should be considered in the modeling and 100% relative humidity should not be assumed as is done in many of the modeling solutions. We have also studied the effect of chosen mass-dimensional relation [7].

References

- [1] Light Precipitation Validation Experiment (LPVEx), website: <http://lpvex.atmos.colostate.edu/>
- [2] GPM Cold –season Precipitation Experiment (GCPEX) website: <http://pmm.nasa.gov/node/485>
- [3] Global Precipitation Mission, website: http://www.nasa.gov/mission_pages/GPM/overview/index.html
- [4] T. Yokoyama and H. Tanaka, “Microphysical Processes of Melting Snowflakes Detected by Two-Wavelength Radar. Part I. Principle of Measurement Based on Model Calculation,” *Journal of the Meteorological Society of Japan*, vol. 62, no. 4, pp. 650–666, 1984.
- [5] W. Szyrmer and I. Zawadzki, “Modeling of the Melting Layer. Part I: Dynamics and Microphysics,” *Journal of the Atmospheric Sciences*, vol. 56, pp. 3573–3592, October 1999.
- [6] S.K. Mitra, O.Vohl, M.Ahr and H.R. Pruppacher, “A Wind Tunnel and Theoretical Study of the Melting Behavior of Atmospheric Ice particles. IV: Experiment and Theory for Snow Flakes”, *Journal of the Atmospheric Sciences*, vol. 47, no.5, pp. 584-591, 1990.
- [7] A.J. Heymsfield, C. Schmitt, A. Bansemer, C.H. Twohy, “Improved Representation of Ice Particle Masses Based on Observations in Natural Clouds”, *Journal of the Atmospheric Sciences*, vol.67, nr. 10, pp. 3303-3318, 2010.

Influence of Snowflake Aggregation on Polarimetric Radar Signatures in Snow Storms

Susanna Lautaportti ⁽¹⁾, Dmitri Moiseev ⁽¹⁾, Pablo Saavedra ⁽²⁾, Alessandro Battaglia ⁽³⁾, V. Chandrasekar ^(1,4,5)

⁽¹⁾University of Helsinki, P.O. Box 48, FIN-00014 Helsinki, Finland, susanna.lautaportti@helsinki.fi

⁽²⁾University of Bonn, pablosaa@uni-bonn.de

⁽³⁾University of Leicester, ab474@leicester.ac.uk

⁽⁴⁾Colorado State University, chandra@engr.colostate.edu

⁽⁵⁾Finnish Meteorological Institute

Radar observations of high differential reflectivity (Zdr) bands and specific differential phase (Kdp) bands in winter storms and ice clouds have been reported in a number of published studies [1, 2]. The observed Zdr values vary from 1 to 8 dB. Just below these bands Zdr values smaller than 1 dB are observed. The Kdp maximum is typically reached 100-200 meters below the Zdr maximum, in the area of low Zdr values. The bands typically occur at altitudes where temperatures are approximately -15°C. There are also several reports of the bands occurring at warmer temperatures, around -4°C.

The main explanation of these high Zdr and Kdp bands is that they are caused by scattering of radio waves from ice crystals rapidly growing in a high humidity environment. During the Light Precipitation Validation Experiment (LPVEx) that took place in Helsinki in fall 2010 we have collected a large number of observations of winter storms with such bands. During the LPVEx campaign we collected coincident radar and microwave radiometer measurements. The passive microwave radiometer, ADMIRARI (ADvanced MICrowave Radiometer for Rain Identification), was provided by the University of Bonn for the experiment. Based on its multi frequency observations a liquid water path (LWP) data was retrieved.

During the LPVEx we classified more than 40 distinct snowfall events. In this study we are focusing on 5 of these events which are dated between November 2010 and January 2011. During LPVEx campaign the LWP values reached up to 500g/m². The 5 events were selected to have a maximum LWP value of approximately 200g/m² to avoid riming. Our preliminary analysis indicates that there is some liquid water present when the high Zdr and Kdp bands are visible.

The goal of this study is to understand the origin of the Zdr and Kdp bands, to see whether the amount of liquid water affects the strength of these bands and if the bands can be linked to the increase of the radar reflectivity values below these bands.

References

- [1] R. J. Hogan, P. R. Field, A. J. Illingworth, R. J. Cotton and T. W. Choularton, "Properties of embedded convection in warm-frontal mixed-phase cloud from aircraft and polarimetric radar," *Quart. J. Roy. Meteor. Soc.*, vol. 128, pp. 451-476, January 2002
- [2] P. C. Kennedy and S. A. Rutledge, "S-band dual-polarization radar observations of winter storms," *J. Appl. Meteor.*, vol. 50, pp. 844-858, April 2011

Remote Sensing of Precipitation and Atmosphere

Modelling X-band SAR observations of precipitating clouds over land and sea using C-band-dual polarization weather radar

Luca Baldini⁽¹⁾, N. Roberto⁽¹⁾, R. Cremonini^(2,4), R. Bechini^(2,5), L. Facheris⁽³⁾, V. Chandrasekar^(5,6)

⁽¹⁾ CNR – Istituto di Scienze dell'Atmosfera e del Clima, Roma, Italy, l.baldini@isac.cnr.it

⁽²⁾ ARPA Piemonte, Torino, Italy, ⁽³⁾ Università di Firenze, Italy

⁽⁴⁾ Dept. of Physics, University of Helsinki, Finland, ⁽⁵⁾ Colorado State University, Fort Collins, CO,

⁽⁶⁾ Finnish Meteorological Institute, Helsinki, Finland

Data collected by weather radars, typically at S, C and X-band frequencies, and in particular those with dual-polarization capabilities are frequently used to investigate observations of precipitation events collected by satellite borne instruments, such as real or synthetic aperture radars operating at different frequencies. Satellite borne SAR aims at providing surface characteristics for different applications in “all weather” conditions. However, precipitation affects SAR images depending on the employed wavelength, and results in attenuation of surface backscattering, additional backscattering from sampled precipitation, geometric and radiometric distortion. At the 9.6 GHz frequency (X band) of the Italian Space Agency Cosmo Sky Med (CSK®) constellation (and by other SARs currently in orbit), attenuation induced by intense precipitation can be significant, masking features of the observed surface. Over land, attenuation prevails over increased backscattering due to precipitation sampled by radar beam, often negligible with respect to terrain backscattering, also influenced by the terrain wetting. Coincident dual polarization radar measurements allow to estimate X band specific attenuations at the frequency and incidence angle of SAR [1][2]. A classification of hydrometeors obtained from weather radar polarimetric signature of precipitation can be used to select the proper algorithms for specific attenuation [3]. Over the sea precipitation induces also changes in the sea NRCS that can be treated by resorting to rainfall fields retrieved by weater radar and a proper modelling [4][5]. Precipitation cases collected in 2 years by the CSK satellites over terrain and sea are analyzed through a model applied to simultaneous observations collected by C-band dual-pol weather radars in Italy. Being C-band attenuated by precipitation, a proper processing of weather radar data must be adopted. The Bric della Croce radar (Turin, Italy) manged by Arpa Piemonte (the environmental protection agency of the Piedmont region) and the Polar 55 C (Rome, Italy) of the National Research Council of Italy (CNR), are used in this study.

References

- [1] Fritz, J.P.; Chandrasekar, A fully polarimetric characterization of the impact of precipitation on short wavelength Synthetic Aperture Radar, IEEE Trans. Geosci. Remote Sensing, 50 , 2037-2048, 2011.
- [2] Baldini L., Roberto N., Gorgucci E., Fritz J, V. Chandrasekar, Analysis of dual polarization images of precipitating clouds collected by the Cosmo Skymed constellation, Atmos. Research (in press), 2013.
- [3] Chandrasekar V., R. Keränen, S. Lim, D. Moisseev, Recent advances in classification of observations from dual polarization weather radars, Atmos. Research, 119, 97–11 , 2013.
- [4] F. Capolino, L. Facheris, D. Giuli, F. Sottili, E.m. models for evaluating rain perturbation on the NRCS of the sea surface observed near nadir, IEE Proc. Radar, Sonar and Navigation, 145, 226-232, 1998.
- [5] N. Roberto, L. Baldini, L. Facheris, Chandrasekar V., Modelling COSMO-SkyMed measurements in precipitation over the sea using simultaneous weather radar observations, Atmos. Research (submitted), 2013.

Radar and Radiometric Studies of Rain Structure at a Tropical Location

Animesh Maitra[#], Arpita Adhikari, Shomitaksha Talukdar and Aniruddha Bhattacharya

S. K. Mitra Centre for Research in Space Environment

Institute of Radio Physics and Electronics, University of Calcutta

Kolkata, India

Email: [#]animesh.maitra@gmail.com

The rain structures, both in horizontal and vertical direction, vary in a complex manner and play an important role in determining the types of rain at tropical locations. The type of rain can change from event to event and even within a single event. In this paper, the experimental observations, pertaining to the year 2012, have been utilized to investigate the features of convective and stratiform rain in terms of radar reflectivity, liquid water content and rain drop size distribution. The radar reflectivity and rain drop size distribution data have been obtained using an FM-CW radar operating at 24.1 GHz. For liquid water content multi-frequency radiometric observations are utilized. Both the instruments operate at the same location of Kolkata (22°34' N, 88°29' E) situated in the tropical region.

An FM-CW Micro Rain Radar (MRR) is compact vertically pointed radar that is capable to measure the vertical profile of rain drop size distribution (DSD) using Doppler principle. MRR transmits 24.1 GHz signal vertically into the atmosphere and some part of the signal is scattered back. As the Doppler shift depends on the velocity of the rain drops and size, the back scatter signal contains the information of DSD. The vertical profile of DSD, in turn gives information on rain, rain rate and radar reflectivity.

The multi-frequency radiometer (RPG-HATPRO) measures brightness temperatures at 14 different frequency channels spreading over two frequency bands having frequency ranges of 22.24-31.40 GHz and 50-59 GHz. An IR-radiometer in combination with the radiometric observations provides cloud base height and liquid water profile of atmosphere.

Vertical profiles of rain microstructures, such as, mean drop size, rain rate, and liquid water content have been studied for two different types of rain, namely, stratiform and convective. In the case of a convective system, a profile of liquid water showing high liquid water density is indicated beyond 6 km height before the occurrence of rain. MRR observations show high radar reflectivity throughout a height range which is associated with large rain drops. On the other hand, for stratiform rain, small drops are more abundantly found and a bright band, caused by the melting layer, at a height around 4-5 km is observed. The height profile of DSD indicates much larger variation of drop sizes for stratiform rain compared to the convective type. Also, the liquid water content profile, in the case of stratiform event, is limited to a height of 5 km. Thus, a combination of radiometric and MRR observations provides very useful microwave signatures for studying the different types of rain events and estimating the meteorological parameters associated with rain events at a tropical location.

Atmospheric Observations and Laboratory Measurements of a broadband 340 GHz Receiver System for STEAMR

Matthias Renker⁽¹⁾, Axel Murk⁽¹⁾, Niklaus Kaempfer⁽¹⁾, Michael von Gruenigen⁽¹⁾, A. Emrich⁽²⁾

⁽¹⁾ Institute for Applied Physics, University of Bern, 3012 Bern, Switzerland
Email: matthias.renker@iap.unibe.ch

⁽²⁾ OMNISYS INSTRUMENTS
August Barks gata 6B, SE-421 32 Vaestra Froelunda, SWEDEN

STEAMR is a radiometric multibeam limb-sounder for the proposed ESA Earth Explorer Mission PREMIER [1]. Each of its fourteen double sideband receivers covers two frequency bands at 324-336 and 343.25-355.25 GHz. The very wide bandwidth is resolved by digital autocorrelation spectrometers with 6.6GHz bandwidth. The sideband ratio of the mixers and the transfer characteristics of the spectrometers need to be known with a relative accuracy better 0.1% to meet the science requirements of PREMIER. In this paper we present laboratory measurements of STEAMR receiver prototypes, as well as first atmospheric observations from the High Altitude Research Stations Jungfraujoch and Gornergrat in the Swiss Alps in the winters 2012 and 2013.

The radiometer test-bed accommodates a subharmonic double sideband Schottky diode mixer with integrated low noise amplifier [2], a local oscillator consisting of an active multiplier chain driven by a microwave synthesizer tunable from 13.6 to 14.5 GHz, and two complex autocorrelation spectrometer covering a bandwidth of 6.6 GHz with a spectral resolution of 25.88 MHz. The autocorrelation spectrometers have an individually tunable center frequency ranging from 8-12 GHz. With this flexibility in spectral coverage it is possible to observe the complete frequency range from 324 to 355 GHz with different observations. The optical path consists of a high gain feedhorn illuminating a fixed elliptical reflector and a flat rotating reflector controlled by a servomotor to choose between view-angles and hot and cold calibration loads. The setup for the laboratory tests includes high resolution sweeps with a narrow band synthesizer to determine the frequency response of the spectrometer and a Martin-Puplett Interferometer to determine the frequency dependent sideband response of the mixer.

This contribution focuses on the spectral line observations made during the atmospheric measurement campaigns. They are compared with forward model calculations based on the ARTS2 radiative transfer model [3] and ECMWF weather data. The results of the laboratory measurements of sideband and channel response are included in the instrumental model of the simulations. From the differences between the observed and simulated spectra the authors will draw conclusions on artifacts and nonlinearities of the receiver chain and back-ends.

References

- [1] PREMIER: Process Exploration through Measurements of Infrared and Millimetre-wave Emitted Radiation. http://esamultimedia.esa.int/docs/EarthObservation/SP1324-3_PREMIERr.pdf
- [2] Peter J. Sobis, Niklas Wadefalk, Anders Emrich, and Jan Stake, *A Broadband, Low Noise, Integrated 340 GHz Schottky Diode Receiver*, IEEE Microwave and Wireless Components Letters, VOL. 22, NO. 7, JULY 2012
- [3] P. Eriksson, S.A. Buehler, C.P. Davis, C. Emde, O. Lemke, *ARTS, The Atmospheric Radiative Transfer Simulator, Version 2*, Journal of Quantitative Spectroscopy & Radiative Transfer, 112 (2011), 1551-1558.

Study of cloud effect on the tropospheric temperature retrievals

F. Navas-Guzman ⁽¹⁾, O. Stähli ⁽¹⁾ and N. Kämpfer⁽¹⁾

⁽¹⁾ Institute for Applied Physics, University of Bern, Switzerland, francisco.navas@iap.unibe.ch

The importance of the knowledge of the temperature structure in the atmosphere has been widely recognized. Temperature is a key parameter for dynamical, chemical and radiative processes in the atmosphere. Different techniques allow to measure atmospheric temperature profiles as radiosonde, FTIR, LIDAR or satellite and ground-based microwave radiometers. The main advantage of microwave radiometers against other instruments is a high temporal resolution with a reasonable good spatial resolution. Moreover, the measurement at a fixed location allows to observe local atmospheric dynamics over a long time period.

TEMPERA is a new ground-based radiometer which measures in a frequency range from 51-57 GHz radiation emitted by the atmosphere using a filterbank with 4 channels. By adjusting the local oscillator (LO) frequency with a synthesizer we actually measure at 12 frequencies. For every measured zenith angle the LO frequency is changed three times.

The instrument is able to monitor temperature structures from ground to the upper stratosphere [1] with a gap in the upper troposphere. The system has been operated at the Institute of Applied Physics, University of Bern (Switzerland) since July 2011. It is important to note that this is the first ground-based microwave radiometer that allows to obtain temperature profiles in the troposphere and stratosphere at the same time.

Although many studies have addressed obtaining temperature profiles under all-weather conditions in the troposphere from microwave radiometer measurements, so far the consideration of clouds in temperature retrievals is sparse. Most of the studies found important discrepancies when temperature profiles from microwave radiometers and radiosondes are compared under cloudy conditions [1].

In this study the temperature retrievals have been done with the optimal estimation method by using the QPack2/ARTS2 software [2, 3]. The main goal of this work has been to consider liquid water information in this software in order to study its effect on the temperature profiles. In order to characterize the clouds several instruments have been used such as information from a co-located ceilometer to obtain information about the location of the cloud base. Liquid water content was obtained from the radiometer TROWARA. A direct comparison of the temperature profiles obtained from TEMPERA and those measured from radiosondes in Payerne (40 km West of Bern) have allowed to study the improvements in the retrievals.

References

- [1] O. Stähli, A. Murk, N. Kämpfer, C. Mätzler, and P. Eriksson, “Microwave radiometer to retrieve temperature profiles from the surface to the stratopause,” *Atmospheric Measurement Techniques Discussions*, vol. 6, no. 2, pp. 2857–2905, 2013.
- [2] P. Eriksson, C. Jiménez, and S. A. Buehler, “Qpack, a general tool for instrument simulation and retrieval work,” *Journal of Quantitative Spectroscopy and Radiative Transfer*, vol. 91, no. 1, pp. 47 – 64, 2005.
- [3] P. Eriksson, S. Buehler, C. Davis, C. Emde, and O. Lemke, “Arts, the atmospheric radiative transfer simulator, version 2,” *Journal of Quantitative Spectroscopy and Radiative Transfer*, vol. 112, no. 10, pp. 1551 – 1558, 2011.

First continuous middle-atmospheric wind profile measurements with a ground-based microwave Doppler-spectro-radiometer

Rolf Rüfenacht ⁽¹⁾, Niklaus Kämpfer ⁽¹⁾, Axel Murk ⁽¹⁾, Patrick Eriksson ⁽²⁾, Stefan A. Buehler ⁽³⁾

⁽¹⁾ Institute of Applied Physics, University of Bern, Switzerland. Contact: rolf.ruefenacht@iap.unibe.ch

⁽²⁾ Department of Earth and Space Sciences, Chalmers University of Technology, Gothenburg, Sweden

⁽³⁾ Department of Computer Science, Electrical and Space Engineering, Luleå University of Technology, Kiruna, Sweden

Today, the wind data for the upper stratosphere and lower mesosphere are commonly extrapolated using models or calculated from measurements of the temperature field, but no continuously running application for direct wind measurements existed so far. Aiming to contribute to the closing of this data gap the Institute of Applied Physics of the University of Bern built a ground-based 142 GHz Doppler-spectro-radiometer with the acronym WIRA (WInd RAdiometer) specifically designed for the measurement of middle-atmospheric wind. WIRA is in operational use since September 2010.

The instrument uses a passive heterodyne receiver together with a digital Fourier transform spectrometer for the data acquisition. The optics enables WIRA to scan a wide range of azimuth angles including the directions east, west, north, and south for zonal and meridional wind measurements. The design of the radiometer is fairly compact and its calibration does not rely on liquid nitrogen what makes it transportable and suitable for campaign use. WIRA is conceived in a way that it can be operated remotely and does hardly require any maintenance. By a technical upgrade in autumn 2012 with the inclusion of an RF amplifier and a sideband-selecting filter the signal to noise ratio could be drastically increased.

A first time series of middle-atmospheric zonal wind profiles obtained with a non-OEM retrieval approach revealed good agreement with ECMWF on average [1]. In the meanwhile a wind retrieval based on the optimal estimation technique (OEM) has been set up using an upgraded version of the ARTS/QPACK radiative transfer and inversion model [2].

Time series of middle-atmospheric wind from measurement campaigns of 7 to 11 months duration at mid and high latitude sites (Bern, 46°57' N, 7°26' E; Sodankylä, 67°22' N, 26°38' E; Observatoire de Haute-Provence, 43°56' N, 5°43' E) have already been obtained. In September 2013 WIRA will be moved to Observatoire du Maïdo (21°04' S, 55°23' E) to study the dynamics of the tropical middle atmosphere. Since the instrumental upgrade in 2012 the meridional component is permanently measured along with the zonal wind to get a full picture of the horizontal wind field.

At the conference, the main results from the measurement campaigns will be presented along with the measurement technique and the instrument properties.

References

- [1] Rüfenacht, R., Kämpfer, N., and Murk, A. (2012). First middle-atmospheric zonal wind profile measurements with a new ground-based microwave Doppler-spectro-radiometer. *Atmos. Meas. Tech.*, 5(11):2647–2659.
- [2] Eriksson, P., Buehler, S., Davis, C., Emde, C., and Lemke, O. (2011). ARTS, the atmospheric radiative transfer simulator, version 2. *J. Quant. Spectrosc. Radiat. Transfer*, 112(10):1551 – 1558.

Author Index

- Adhikari, 134
Al Bitar, 35
Alonso-Arroyo, 22, 30, 54
Andersson, 101
Andres-Beivide, 21
Antropov, 109, 110
Anttila, 92
Arnaud, 91
Aziz, 99
- Baghdadi, 72
Balager, 45
Balandina, 69
Baldini, 125, 133
Ballesteros, 21
Bansemer, 129
Battaglia, 130
Bechini, 125, 133
Benito, 21
Benjelloun, 29
Beyerle, 20
Bharadwaj, 125
Bhattacharya, 134
Botteron, 29
Boutin, 35
Brogioni, 84
Brown, 73
Buehler, 121, 137
- Cabot, 35
Camps, 21, 22, 30, 31, 47, 54
Caparrini, 27
Cardellach, 20
Carreno-Luengo, 22, 31
Chandrasekar, 125, 126, 130, 133
Chang, 86
Chen, 75, 125
Chini, 56
Choquel, 29
Chuan, 84
Clarizia, 19
- Coccia, 93
Cohen, 94
Coll, 51
Colliander, 36, 61, 64, 65
Cremonini, 133
- Daganzo, 45
Das, 119
Davidson, 93
de Matthaeis, 44
Demkin, 38
Dente, 87
Derksen, 94
Diez, 31
Dongkai, 24
Dupont, 91
- Egido, 27
Eltoft, 57
Emrich, 135
Entekhabi, 61
Eriksson, 121, 137
- Fabra, 24
Facheris, 133
Farine, 29
Fedoseev, 38
Fernandez, 71
Fernández-Morán, 51
Ferrazzoli, 87
Fily, 91
Floury, 27
Font, 35
Forte, 31, 47, 54
Forste, 20
- Garriga, 21
Geudtner, 73
Gleason, 19
Gogineni, 99
Gomez-Garcia, 99

Gruber, 20
 Guerriero, 27, 56, 87
 Guo, 62
 Gokhan, 57

 Hakkarainen, 100
 Hallikainen, 36, 39, 70, 76, 78, 100, 110, 129
 Hao, 75
 Harri, 37, 129
 Helm, 20
 Herrero, 21
 Hess, 20
 Heymsfield, 129
 Hoeg, 20
 Häme, 109

 Ikonen, 53, 94
 Imbo, 72

 Jackson, 61, 64, 65
 Jakkila, 77
 Jakowski, 20
 Johnson, 19
 Jokela, 46
 Jove, 31
 Junyeant, 125
 Jussila, 115

 Kadygrov, 120
 Kainulainen, 36, 39, 76, 78, 100
 Kanevsky, 69
 Karaev, 69
 Karvonen, 102
 Kasapoglu, 57
 Kern, 20, 93, 103
 Kerr, 35, 45, 51, 91
 Kestilä, 115
 Kim, 65, 118
 Kimball, 63
 Kontu, 53, 93, 95, 117
 Kukin, 38
 Kuznetcov, 69
 Kämpfer, 71, 121, 135, 136, 37

 Lahtinen, 43, 70, 92
 Laine, 101
 Lang, 111
 Larsson, 121

 Laurila, 115
 Lautaportti, 130
 Le, 125
 Le Toan, 107
 Le Vine, 44
 Leclere, 29
 Leduc-Leballeur, 91
 Lefebvre, 91
 Leinonen, 128
 Lemmetyinen, 53, 86, 93, 94, 95, 117
 Leppänen, 117
 Leuschen, 99
 Li, 24
 Liao, 75
 Lopez-Baeza, 51
 Luoju, 94

 Macelloni, 84
 Maitra, 119, 134
 Manninen, 92, 101
 Martin, 22
 Martín-Neira, 21, 24, 36
 Mattia, 72
 McDonald, 63
 McNairn, 64, 65
 Mecklenburg, 35
 Menard, 53
 Merlin, 35
 Meshkov, 69
 Meta, 93
 Mialon, 35, 91
 Mierniecki, 51
 Miller, 120
 Modrzewski, 115
 Moisseev, 125, 126, 128, 129, 130
 Montenbruck, 20
 Murk, 71, 135, 137
 Mäkynen, 103
 Mätzler, 53, 93

 Nagler, 93
 Navarro, 21
 Navas-Guzman, 121, 136
 Navas-Traver, 73
 Nevvonen, 126
 Nieto, 45
 Njoku, 61, 64
 Notarpietro, 28

Nousiainen, 128
 O'Brien, 19
 O'Neill, 61
 Olea, 21
 Oliva, 45
 Onrubia, 22, 30, 31, 54

 Paden, 99
 Pajaron, 51
 Palchetti, 84
 Paloscia, 27, 72, 83, 84
 Pampaloni, 84
 Panfilova, 69
 Panzer, 99
 Papathanassiou, 118
 Park, 21, 22, 30, 54
 Pascual, 22, 30, 54
 Patel, 99
 Pedersen, 103
 Pei, 28
 Perez-Ramos, 31
 Pettinato, 84
 Picard, 91
 Pierdicca, 27, 56, 72
 Pini, 28
 Pla, 45
 Pohjola, 126
 Porko, 70
 Praks, 39, 110
 Proksch, 93
 Pulliainen, 53, 93, 94, 95, 117
 Pulvirenti, 56

 Qiu, 116

 Rabaute, 72
 Rauste, 109
 Rautiainen, 37, 53
 Reboul, 29
 Renker, 135
 Repina, 120
 Reul, 35
 Ribo, 21
 Ribot, 29
 Richaume, 35, 45
 Ridley, 19
 Riihelä, 92, 101
 Rius, 20, 21, 24

 Roberto, 133
 Rodriguez-Morales, 99
 Rommen, 73
 Rothacher, 20
 Rott, 93
 Rousi, 77
 Ruf, 19
 Ruokokoski, 43, 70
 Ruoskanen, 43
 Ryskin, 38
 Rüdiger, 91
 Rüfenacht, 137

 Saameno, 21
 Saavedra, 130
 Salgado-Hernanz, 51
 Sandberg, 108
 Santi, 27, 84
 Santoro, 55
 Savi, 28
 Schmidt, 37
 Schneebeli, 93
 Schwank, 51, 53
 Schüttemeyer, 93
 Segarra, 21
 Seppänen, 76, 78, 100
 Sharma, 74
 Shchitov, 38
 Shi, 62, 85, 116
 Shlaferov, 69
 Shum, 20
 Shvetsov, 38
 Smolander, 94
 Snoeij, 72, 73
 Soja, 79, 108
 Soldo, 45
 Stienne, 29
 Straub, 121
 Stähli, 121, 136
 Su, 87

 Takala, 94
 Talukdar, 134
 Tan, 86
 Titchenko, 69
 Toikka, 70
 Tsang, 62, 65, 75, 85, 86

 Ulander, 79, 108

Uusitalo, 43

Vaaja, 39, 70, 100
Vall-Ilossera, 47
van den Oever, 115
van Zyl, 65
Varentsov, 120
Vega, 125
Vehviläinen, 77, 95
Vento, 77
Vilaseca, 21
Voglmeier, 93
von Gruenigen, 135
von Lerber, 129

Wagner, 72
Waldteufel, 35
Wegmüller, 55
Werner, 55
Wickert, 20
Wiesmann, 53, 93
Wigner, 35, 51

Xu, 86

Yadav, 74
Yan, 99
Yi, 19
Yueh, 86

Zavorotny, 19
Zhao, 111
Zuffada, 20



ISBN 978-952-60-5400-1
ISBN 978-952-60-5399-8 (pdf)
ISSN-L 1799-4896
ISSN 1799-4896
ISSN 1799-490X (pdf)

Aalto University
School of Electrical Engineering
Department of Radio Science and Engineering
www.aalto.fi

**BUSINESS +
ECONOMY**

**ART +
DESIGN +
ARCHITECTURE**

**SCIENCE +
TECHNOLOGY**

CROSSOVER

**DOCTORAL
DISSERTATIONS**